CRANFIELD UNIVERSITY

Giovanni Piscopo

Preliminary Aerothermal Design of Axial Compressors

School of Engineering

Part Time Master by Research
Academic Year: 2011 - 2013

Supervisors: Dr. P. Zachos & Prof. P. Pilidis
January 2013

CRANFIELD UNIVERSITY

School of Engineering

Part Time Master by Research

Academic Year 2011 - 2013

Giovanni Piscopo

Preliminary Aerothermal Design of Axial Compressors

Supervisors: Dr. P. Zachos & Prof. P. Pilidis
January 2013

The research work disclosed in this publication is partially funded by the Strategic Educational Pathways Scholarship Scheme (Malta). The scholarship is part-financed by the European Union – European Social Fund under Programme II – Cohesion Policy 2007-2013.

This thesis is submitted in partial fulfilment of the requirements for the degree of Masters by Research

Dedicated to my wife Diane

This dissertation documents a compressor preliminary design study conducted by the author in fulfilment of his MSc thesis requirements. The compressor is intended for a new development engine within the 20Klbf thrust category, planned to be used on a short-haul aircraft, namely the ERJ-190.

A market research suggests that there exists a definite opportunity for a commercially profitable engine within this thrust class. Furthermore, the proposed new engine is projected to outperform current production engines on critical issues such as fuel efficiency and operability.

By and large, the objectives of this work have been achieved and a compressor design and layout is suggested, which matched or exceeded all the initial requirements. The quality of the results from this study are thought to be of sufficient detail to allow a further, more detailed development study to resolve some subtle pending issues. It is expected that, some compressor stages may have to be altered slightly during detailed design to augment their performance and ease of manufacture and assembly.

Throughout this study, the importance of the compressor design figure of merits, pertaining to a short haul engine, has been outlined and their interaction on the design process is well documented. Furthermore, some rather unorthodox objectives such as compressor performance retention and reliability have been discussed. The author approached these subjects in an innovative way due to the limited non-proprietary knowledge available on these issues, especially considering their implications within preliminary design.

Furthermore, the author developed and tested a new preliminary turbomachinery design code, named Turbodev, which can be used as an aid in future compressor design endeveours. Turbodev can handle most types of compressor layouts and generates an overall aerodynamic assessment of the turbomachinery performance.

In conclusion; this documentation and the associated literature review aim to provide the reader with an overview of the work done and yield a better understanding of the decisions that face any design bureau when developing a new or modified engine component.

KEYWORDS: short-haul, compressor layout, figure of merits, Turbodev, compressor reliability, performance retention.

I would like to express my most sincere gratitude to my supervisor, Dr. Pavlos Zachos, for his continuous encouragement and guidance throughout this research project.

Thanks are also due to my co-supervisor Prof. Pericles Pilidis for his useful suggestions and for the interest shown in this project.

Moreover, I would like to thank my family together with my wife Diane, for the encouragement and moral support given throughout this course.

a	Distance of the point of maximum camber from leading edge of blade or a constant depending on blade profile
α	Absolute flow angle measured from the axial direction
α'	Blade angle measured from the axial direction
β_1	Relative inlet flow angle measured from the axial direction
β_2	Relative outlet flow angle measured from the axial direction
BPR	Bypass ratio, assumed to be at sea level static unless stated otherwise
c	Blade chord length
C_d	Propelling nozzle coefficient of discharge
C_p	Gas specific heat at constant pressure
C_v	Gas specific heat at constant volume
C_x	Propelling nozzle thrust coefficient
CFD	Computation fluid dynamics
D_{eq}	Lieblein's equivalent diffusion factor
D_{loc}	Local diffusion factor
DF	Lieblein's diffusion factor
$\overline{D_m}$	Compressor mean diameter (average of inlet and outlet mean diameters)
$\overline{D_{m,1}}$	Compressor inlet mean diameter
EEE	Energy Efficient Engine
FADEC	Full authority digital engine control
FPR/FPR_{bypass}	Fan pressure ratio, assumed to be bypass stream pressure ratio unless stated otherwise
FPR_{core}	Fan pressure ratio of core stream
FOM	Figure of merit
GE	General Electric Co.
h	Static enthalpy or blade height
H	Total enthalpy
HP	High-pressure
HPC	High-pressure compressor
HPT	High-pressure turbine
i	Blade incidence
i*	Blade incidence at design condition

$\mathbf{i_o^*}$	Blade incidence at design condition for $t_b/c=0.1$
Δi	Magnitude of the amount by which the actual incidence exceeds that for Lieblein's minimum loss
IAE	International Aero Engines Corporation
ICAO	International Civil Aviation Organisation
IDG	Integrated drive generator
IP	Intermediate-pressure
IPC	Intermediate-pressure compressor
ISA	International Standard Atmosphere
$\mathbf{K_{sh}}$	Blade shape parameter
$\mathbf{K_{t,i}}$	Design incidence angle thickness correction factor
$\mathbf{K_1}$, $\mathbf{K_2}$	Constants to be determined
L	Characteristic length
$\mathbf{L_c}$	Compressor length
LE	Blade leading edge
LCV	Lower heating value of fuel
LP	Low-pressure
LPC	Low-pressure compressor
LPT	Low-pressure turbine
M	Mach number
m	Camber angle slope parameter
$\dot{m}$	Mass flow
$\mathbf{M_{crit}}$	Critical value of inlet Mach number at which suction surface velocity first attains sonic conditions
$\dot{m}_f$	Fuel flow
$\mathbf{M_1}$	Blade relative inlet Mach number
N	Shape parameter or constant depending on boundary layer type or compressor number of stages
$\mathbf{N_{row}}$	Blade row number
NGV	Nozzle guide vane
$\mathbf{\eta_B}$	Blade row efficiency
$\mathbf{\eta_{comb}}$	Combustion efficiency
$\mathbf{\eta_{comp}}$	Compressor polytropic efficiency
$\mathbf{\eta_{fan}}$	Fan polytropic efficiency

η_{mech}	Mechanical efficiency
η_{p}	Propulsive efficiency or stage polytropic efficiency
η_{th}	Thermal efficiency
η_{turb}	Turbine polytropic efficiency
$\Delta\eta_{leakage}$	Reduction in blade row efficiency due to tip clearance
OPR	Overall pressure ratio, assumed to be at sea level static unless stated otherwise
P	Static gas pressure
Pc	Gas critical pressure
P_o	Total gas pressure
PR	Pressure ratio
P&W	Pratt & Whitney Co.
ΔP	Blade row static pressure loss
ΔP_0	Blade row total pressure loss
ΔP_{th}	Stage theoretical pressure rise
$\dot{Q}$	Heat input per unit time within system
R	Gas constant, assumed constant (287.05J/KgK) for air and combustion products
Re	Reynolds's number, assumed to be based on momentum thickness unless stated otherwise
RR	Rolls Royce plc
r_{tip}	Blade tip radius
s	Blade pitch
SI	Système international unit standard
Sfc	Specific fuel consumption
sfc_{cruise}	Specific fuel consumption at cruise condition
sfc_{ssl}	Specific fuel consumption at sea level static
T	Static gas temperature
t_b	Blade maximum thickness
t_b/c	Blade thickness to chord ratio
T_c	Gas critical temperature
T_{cruise}	Thrust at initial cruise altitude
T_o	Total gas temperature
T_{ssl}	Thrust at sea level static

TE	Blade trailing edge
TIT	Turbine inlet temperature (in front of first rotor row), assumed to be takeoff limiting temperature unless stated otherwise
TIT_{cruise}	Turbine inlet temperature for cruise
TOC	Top of climb
ΔT_{0s}	Stage temperature rise or drop
U	Blade speed
U_c	Blade tip leakage parameter
USD	United States Dollar
V	Flight velocity or mean velocity of fluid relative to solid surface
V_a	Axial velocity component
V_w	Tangential velocity component
V_j	Jet velocity
VIGV	Variable inlet guide vane
VSV	Variable stator vane
VTOL	Vertical takeoff or landing
V_1	Absolute flow velocity into blade row or component
V_2	Absolute flow velocity out from blade row or component
W_c	Compressor estimated weight
W_{max}	Blade suction surface peak velocity
W_1	Relative flow velocity into blade row or component
W_2	Relative flow velocity out from blade row or component
$\bar{w}$	Loss coefficient
$\dot{W}$	Work input per unit time within system or stage
$\dot{W}_{net}$	Gas generator net power output
ΔW_Θ	Magnitude of change in tangential velocity through the blade row
X	Distance along the direction of flow
Z	Number of blades in a row or compressibility error of real gas from ideal properties
σ	Blade solidity (blade chord/pitch)
ρ	Gas density
γ	Ratio of gas specific heat at constant pressure and volume

μ	Gas Viscosity
Θ	Blade camber angle or boundary layer momentum thickness
ξ	Blade stagger
δ	Flow deviation
δ_c	Tip clearance
Λ	Stage reaction or work done factor
Ψ	Stage loading
Ψ_{mean}	Compressor mean stage loading
φ	Flow coefficient

Chapter

1

Introduction

1.1
- Gas Turbine overview
- A brief history

1.2
- Aircraft type and mission requirement
- The Flight profile

1.3
- Engine development time and cost
- Sales forecast and competitive engines

1.4
- Compressor importance for engine sfc
- Compressor layout

1.1 Gas turbine overview

The gas turbine engine has now been in use for just over half a century, yet in this time it has, to some extent, revolutionised our way of life. In fact, few people in the world today can claim that their life has been unaffected by this technology; be it from air or sea transport, gas-line pressurisation or electricity generation it has permeated into the core needs of today's civilised society.

The gas turbine engine is considered to be conceptually easy to understand. Frank Whittle, who successfully ran the world's first gas turbine in 1937, remarked to former Rolls Royce (RR) director Ernest Hives that the key to his success was the simplicity of his machine [1]. This statement may however be hard to appreciate today considering the complexity of modern engines, each having thousands of functioning parts, all working seamlessly together to produce work.

This gas turbine, as illustrated in Figure 1.1, can be segregated in three major parts. The compressor section, as the name implies, compresses the working fluid which is usually air to a higher pressure. This then passes through the combustor, where it is heated to a higher temperature, and is then finally expanded in the turbine, or in case of aircraft engines, propelling nozzle to produce work. This report focuses on the compressor section of the engine, however the close relationship between this and the turbine cannot be neglected hence the latter will also be mentioned extensively within this documentation. On the other hand, the combustor will be treated as sort of a 'black box' yielding the required change in air temperature and composition yet all technical aspects relating to it will not be mentioned to unless they have a direct influence on either the compressor or turbine sections.

As this dissertation concerns aircraft engines, the term 'work' will from henceforward be referred to as 'thrust'. Also, even though the engine thrust magnitude is sometimes quoted in pounds (lbf) within this report, most units will conform to *système international* standard, more commonly referred to as SI. This may seem a bit misleading; however, engine thrust measurements are almost always referred to as pounds of thrust rather than the more scientific term of Newtons.

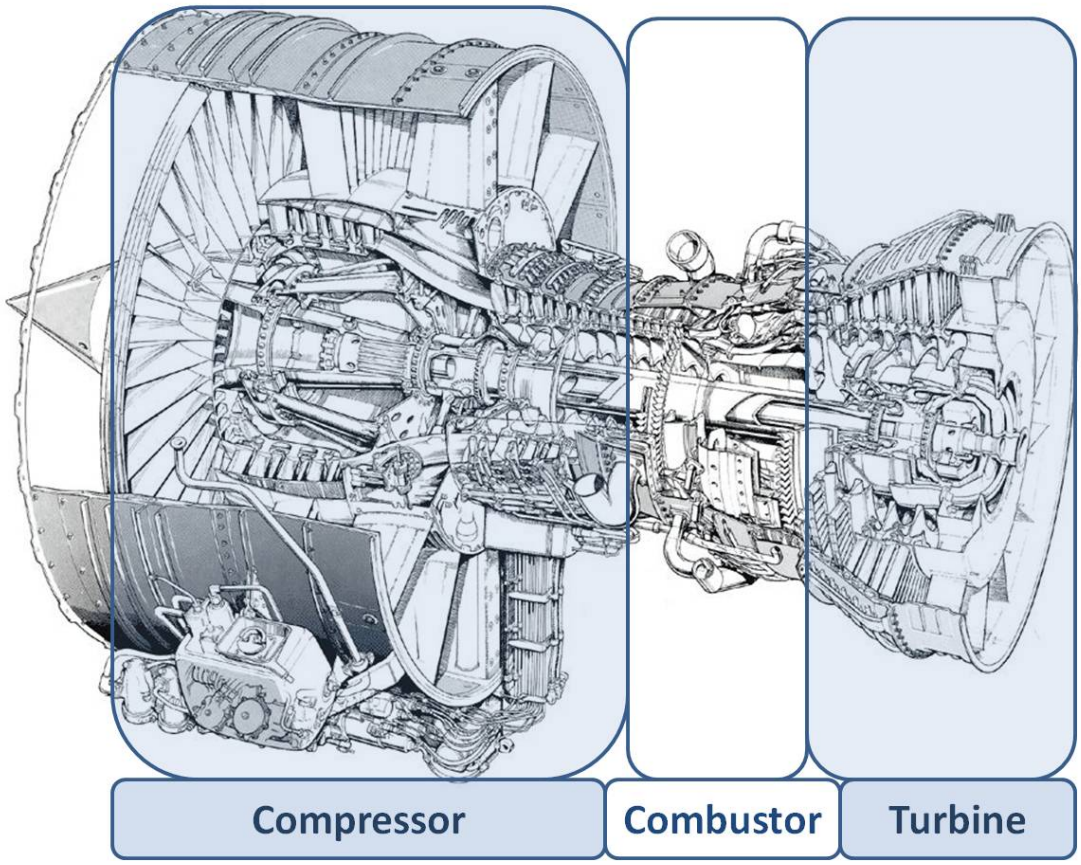

Figure 1.1: The gas turbine engine, a CFM56-5A

1.1.1 A brief history

As mentioned in Section 1.1 above, the gas turbine engine first ran in England in 1937 under the directorship of Whittle. Despite this engine's superiority in almost all aspects over the conventional piston engine, this technology found a lot of resistance from others at the time. This was mostly due to the fact that established scientists and engineers found it difficult to comprehend how a young RAF officer had invented such a radical new powerplant.

The Germans, not far behind the British at the time, embraced much more this new power source and were the first to take it to the air in their Heinkel He178 in 1939. Later, after the war had ended, Hans Pabst von Ohain, the inventor of the HeS3B which powered this aircraft, remarked that if the allied *"experts had the vision to back Whittle, World War II would probably never have happened"* [2]*;* such was the importance of this new invention.

Things did not change much in the immediate post-war era. The gas turbine kept on being developed for military endeavours and then adapted later for civilian use. The first engine specifically designed for a civilian marked was the Pratt & Whitney JT8D in the early 1960s. This was a significant powerplant not only because 12,000 were eventually sold but also because it started utilising a bypass jet to improve the powerplant's efficiency [2]. Even though this was a new concept for a commercial engine, Whittle, with remarkable foresight, had proposed it as a means to better the efficiency almost two decades earlier. These types of engines are known as bypass jets or more commonly nowadays as turbofans. Turbofans compress additional air to that required by the core engine, or gas generator as is normally referred to, and then discharge it at a slightly higher velocity. This, as shown later, radically improves the propulsive efficiency of the engine.

Today's engines have far greater bypass ratio $\left({}^{bypass\ air}/_{core\ air}\right)$ compared to the earlier generation. The BR710, commissioned in 1996, has a bypass ratio (BPR) of 4 giving a static thrust at sea level of 14.8Klbf which is comparable to that of the JT8D-11. However, the latter had a very conservative BPR of 1.05 [3]. This, together with other technological advancements, led to an improvement in engine efficiency of 33% over a span of thirty years.

1.2 Aircraft type and mission requirement

Few customers in the world today have the financial resources to sponsor a new development engine specifically catered to their needs; maybe a notable exception is the military. As regards to aviation, what usually happens is that after an airframe manufacturer such as Boeing or Airbus decides to go ahead with a new aircraft project, or a modification to an existing airframe, the engine manufactures develop engines specifically tailored to that variant. Hence, to pursue an engine development study, such as is the case of this report, an airframe type should preferably be specified. This in turn defines the engine's constraints and the order of merits given to the different requirements.

The relative importance of different requirements varies between engine types mainly because of the aircraft's mission. Engines intended for short-haul aircraft such as the BAe146, whose cruise sector is normally less than one hour, are more biased towards ease of maintenance and reduced weight compared to engines tailored for longer range aircraft. This reasoning may explain the bad reputation inherited by the ALF502R, the engine which powers this aircraft and is considered by many engineers as too complex and troublesome for an aircraft accumulating a lot of sectors.

The aircraft assumed for this study is a twin-engine, short-haul aircraft, similar to the ERJ-190 which requires engines within the 20Klbf thrust category. Incidentally, the scope for reducing emissions from aircraft engines by the use of such short-haul aircraft far outweighs any possible technical gain realistically achievable in the near future. This, as discussed in [4], can be explained as follows; for a long range flight, much of the aircraft initial weight is fuel hence the payload is only a small fraction of the aircraft's takeoff weight. On the converse, a greater percentage of the aircraft's weight is payload for a shorter flight. Now, the former would have to burn a significant portion of its fuel just to carry the large initial fuel load, whereas in the latter case only a small portion of fuel burned is used to carry the additional fuel weight. Cumpsty [5], suggests that if an 8100nm (15,000km) journey is split into three equal sectors the reduction in fuel burn will be of the order of around 40%. This is very significant considering the projected achievement in efficiency from technological advancements alone is only around a percentage point per year.

1.2.1 The flight profile

Each engine operates best at one specified condition. This operating point, or design point, is chosen in accordance with the intended flight profile of the recipient aircraft. Operation at other thrust requirements is referred to as off-design operation and yields an efficiency penalty compared to design point operation.

Because of the importance in minimizing fuel consumption the design point is often chosen as the condition at which the aircraft intends to spend most time. This is normally cruise, even for a short-haul aircraft such as that assumed for this study.

The assumed flight profile is thought to be similar to that used for the CFM56-5 which is customized to a similar type of aircraft albeit at a slightly higher thrust rating. Also, the design point is taken to be at the initial cruise portion of the flight.

Power	Altitude (ft)	Mach no.	Time interval (min)
Take-off	0	.35	1.39
End take-off	1500	.40	
Climb		.61/.85	20
Cruise	30000	.85	20
Descent		.85/.61	14
Approach	5000	.3	5
Thrust reverse	0	.2	0.26

Table 1.1: CFM56-5 flight profile; data obtained from [6]

Note

i. *The only differences between the CFM56 flight profile and that assumed for this study is that the present aircraft will cruise at an altitude of 36,000ft (11,000m) and at a Mach number of 0.8 instead of 30,000ft and Mach 0.85 respectively. This choice of cruise speed and altitude is thought to be representative of modern flight trajectories at long range cruise. This speed is slightly faster than maximum range cruise, or that for minimum fuel consumption, and is used to shorten the flight time with a marginal sacrifice of efficiency.*

1.3 Engine development time and expense

The development of a new engine is a huge endeavour by any measure. It must be emphasized that the financial investment required even for a medium-sized turbofan prohibits any new company from undertaking such a project. Hence, such engines are only developed by well established corporations or multi-nationals. Such is the expense required for a new turbofan development program that the Economist of 18th September 1999 reported that the GE90 had cost General Electric (GE) an average of 1million USD per day for 4½ years totalling 1.6billion USD [5]. Also, the design and development phase may take anywhere from 3 to 7 years [7], hence the return on investment merits also serious consideration.

The trend nowadays is for new projects to be split between different companies. In fact, even engines which are thought of as being from a single manufacturer, such as the GE90 mentioned above, are in reality a mixed venture. General Electric (GE) actually only has a 59% stake in the GE90 [8]. The globalisation of new projects is such that in the case of the RR Trent 900 development programme, the expenses were shared between ten different multi-nationals amongst which were Honeywell from the US and Avio of Italy [9].

To combat the huge development costs of these projects, the engine is often modified to fit other similar aircraft types. This allows the engine to be sold at a more competitive price. The Trent engine mentioned above has been adapted to produce a thrust range of between 55Klbf and 110Klbf. This is partly due to the three spool layout flexibility which permits the same basic engine to be used anywhere from the A340 to the B777 which have vastly different engine thrust requirements. A spool is a compressor and turbine section with the adjoining shaft. Most engines nowadays have at least two spools, meaning that the required pressure ratio is split between two or more compressor and turbine sections in series. This, as explained later, improves the off-design performance.

1.3.1 Sales forecast and competitive engines

Because of the huge capital investment required for the research and development phase of a new or modified engine, the manufacturer must be reasonably sure that there exists a realistic market which may yield the required return. One typical delivery forecast has been prepared by Rolls Royce in 2007 [10]. Table 1.2 shows projected aircraft sales by sector for the next two decades as presented in the latter report.

Sector	Units
Business jets	63,816
Regional aircraft	14,427
Mainline aircraft	51,126
Freighters	2,244

Table 1.2: Forecast aircraft sales 2007-2026; data obtained from [10]

Furthermore, the RR's report also states that the number of engines required within the 20Klbf category should exceed 20,000 units, valued at 69billion USD. Also, a number of new regional aircraft that are currently in production or in final phases of development will require engines within this category. Most notable of which are the Sukhoi Superjet 100 and Bombardier CSeries. Therefore, the market for such an engine is considered potentially very lucrative.

However, no matter how good an engine is, no manufacturer will ever expect to monopolise the market. Hence a feasibility study for a new endeavour should also factor in other competitive engines within the same thrust rating. It is important to note that even though an engine might be more efficient than a competitive unit it might still fair badly in the market. This is because even though the fuel operating cost is a very significant factor for an operator, it is not the only engine related expense. Ease of maintenance and manufacturer guarantee also play a very significant role; not to mention the close relationship a manufacturer may have with a client which will, more often than not, bias the final decision of the customer.

Table 1.3 lists some current production engines within the examined thrust category. It must be emphasised that these are not the only engines available however they should give an indication of what the benchmark in performance is for this class.

It should also be noted that the specific fuel consumption (sfc) is a measure of the engine's efficiency. This gives an indication of the fuel flow required per each Newton of thrust produced; hence a low value is desirable. Also, the values of both sfc and thrust in Table 1.3 are quoted at sea level static (sfc_{ssl}).

Engine	Thrust (Klbf)	Weight (kg)	Sfc_{ssl} ($x10^{-5}$ [kg/s]/N)
CFM56-7B18	18.5	2366	0.99
BR715-55	19.9	2062	1.05
CF34-10E5	18.5	1724	1.08

Table 1.3: Representative engines within the 20Klbf thrust class; data obtained from [3]

1.4 Compressor importance for engine sfc

Engine efficiency, or lack of, affects performance in two ways. Inefficiency not only causes a reduction in output thrust but also reduces cycle pressure ratio as the compressor exit temperature is limited by available materials' capabilities [11]. These two contribute towards a higher turbine inlet temperature, and thus fuel flow, to maintain the required thrust and may even necessitate the use of a bigger core and thus engine size.

Compressor efficiency is a very important criterion for overall engine performance since it consumes 55-60% of the power generated by the engine [12]. Furthermore, as discussed in Section 1.3 above, the required cycle pressure ratio is normally achieved through the use of two or more compression units mounted in series, each driven by a separate turbine. The outer and inner compressors are called the low-pressure (LP) and high-pressure (HP) compressor (LPC and HPC) respectively. If there is an additional spool in between these two, this is then referred to as the intermediate-pressure (IP) compressor (IPC).

Figure 1.2 shows a two-spool layout. Note how the first stage of the LPC is a much larger blade row, called a fan. The fan is a specialised compressor stage, used to compress the bypass air.

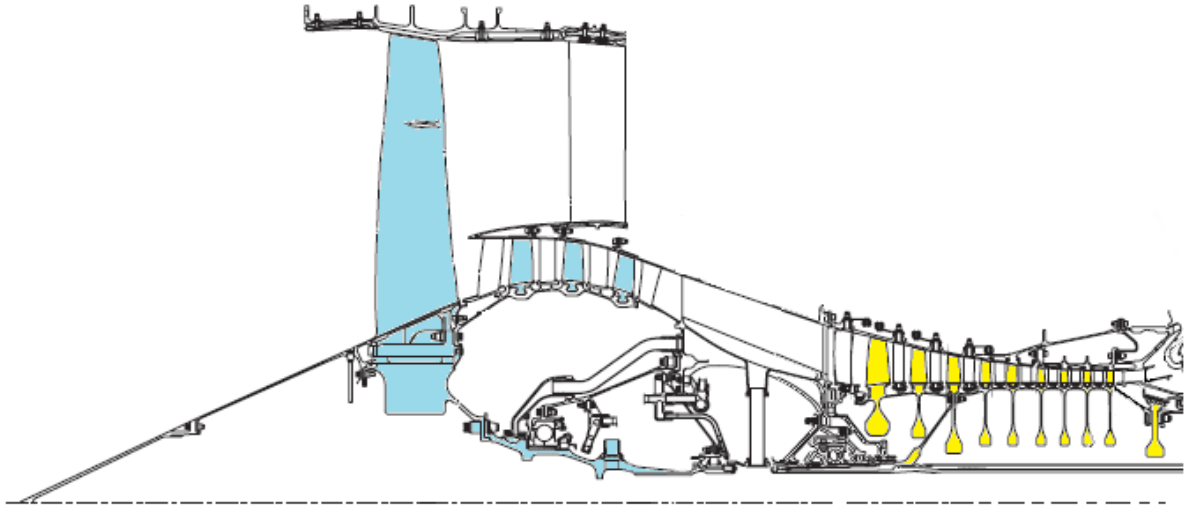

Figure 1.2: Compression section of CFM56-5A, modified from [13]

Amongst the two or more compression units, the HPC has the largest influence on thrust and air mass flow through the core [5]. Moreover, the HPC's layout optimisation is regarded as one of the key requirements dictating, to a large extent, whether or not an engine design will be successful. A 1% reduction in HPC efficiency translates into a 0.5-1.1% sfc penalty [14], [5].

1.4.1 Compressor layout

With regards to the importance of the HPC towards engine sfc and operability, the aim of this study was to determine the optimum compression layout for the 20Klbf engine discussed above. The engine parameters pertaining to this engine are outlined in Chapter 4.

The required pressure, as dictated by cycle analysis, is achieved through the use of a number of stages on each compression spool. A stage is the term given to a couple of adjacent rotor and stator blade rows. It is obviously beneficial to minimize the total number of stages as this would have a dramatic effect on the compressor's weight; however, there is a limit, as described in the literature review, on how much a stage can impart energy to a moving airstream. Beyond this limit, the compressor will behave badly and may even go into what is called surge. Surge is the complete breakdown of flow within the compression system, followed by a total or partial reversal of the airstream. This phenomenon is further described in Section 3.4.5.

Normal practice nowadays is to place some compression stages on the fan rotor, as illustrated in Figure 1.2, and then the rest on a separate spool. The compression stages on the LPC behind the fan blade row are sometimes referred to as booster stages.

The fan blades are restricted to rotate at a relatively low speed because of compressibility problems associated with the blade tips. Hence, because of this limitation, the booster stages are considered to be relatively inefficient since they are constrained to rotate at this slow speed. This suggests that the designer may try to minimize the number of booster stages and place as many blade rows as possible on the HP spool which may rotate much faster than the corresponding LP spool.

The maximum number of compression stages within the HP spool may be dictated by the turbine requirements. Like the compressor, the available expansion ratio within turbine has to be split between a number of stages. However, the permissible work extracted per stage within the turbine is much greater than that correspondingly put in the compressor. This is because the accelerating flow within the turbine is much more tolerant to separation than the diffusing flow of compressors. In fact, a single stage turbine can give four times the work transfer than is possible by a well designed single stage transonic fan [15].

Most production engines within this category employ a single stage HP turbine (HPT). Hence, the use of booster stages is inevitable since the work extracted by this turbine stage is insufficient to power the whole compressor. One notable exception, albeit at a slightly higher rating, is the IAE V2500-A1 which has a two-stage HPT. The design intent of this design characteristic was not so much as to minimize the use of booster stages but rather to off-load the HPT and thus achieve higher efficiency. In fact, this engine has a cruise sfc (sfc_{cruise}) of $1.63x10^{-5}$ (kg/s)/N, compared with that of the competitive CFM56-5B's $1.7x10^{-5}$ (kg/s)/N). CFM's president Laviec owes this difference to the latter's use of a more highly loaded single-stage HPT [2].

The use of a two-stage HPT may not necessarily result in a heavier engine. A notable case was that of the RR Avon which in 1949 was re-designed with a two-stage HPT which actually reduced the overall engine weight [2]. The increased HPT weight may be offset by the downstream LP turbine (LPT) may then require fewer stages to power the smaller LPC. Thus, if designed properly, a two-stage HPT, driving a larger HPC may result in a lighter engine compression unit and a more efficient turbine.

In addition, there are other arguments as to what is the optimum HPT design. Since most HPT stages nowadays are cooled by compressor delivery air, so as to support higher turbine inlet temperatures (TITs), the choice of a single-stage or a two-stage HPT may bear a significant impact on the amount of cooling air required. Minimizing the amount of bleed air from the compressor improves noticeably the engine efficiency.

Furthermore, even if the HPT is designed to power a large compressor, the resulting HPC may not perform as predicted. This is because, the use of many compression stages on a single spool unit may perform very inefficiently at off-design operation hence requiring

extensive use of variable stator vanes (VSVs) or bleed ports as described in the following chapter. These may negate the performance benefit realised at the design point. This consideration is particularly relevant for the present study as short-haul aircraft spend a considerable amount of time at other than cruise condition, as evidenced by Table 1.1 above.

This dissertation aims to outline the designer's choices and constraints when evaluating the design of the engine's compression system. This section introduced the reader to the intricate nature of how the fundamental design decisions influence, to a great extent, the engine's overall efficiency, weight and operability.

Chapter

2

Thesis overview

2.1

- Work statement
- Thesis layout

2.1 Work statement

In accordance with the arguments raised in the previous chapter, the aim of this thesis can be summarised as follows.

A compressor comparative design assessment for a short haul engine

The aim is to document a compressor development exercise, under the prism of different figures of merit, and ultimately propose an apt design layout for a short haul engine intended for use on a 100 to 150 seat regional jet.

The objectives required for achieving this aim are,

1. The definition of the boundary conditions which will specify the engine working environment.
2. Document and prioritise the required compressor figure of merits pertaining to this aircraft mission.
3. Enumeration of all the possible candidate compressor configurations which may be suitable this engine.
4. Utilise any suitable means to assess these layouts.
5. Finally, specify the preferred layout and gauge the overall suitability and also, any limitations related to this design.

2.1.1 Thesis layout

This thesis is structured in a manner that satisfies the above requirements. The previous chapter introduced the reader to the overall task definition and also documented a market research study which highlighted the need for such an engine.

The following chapter will expose the reader to the required engineering concepts for understanding the work disclosed in the subsequent chapters of this thesis. The literature review will also outline all the correlations and nomenclature which will be used throughout this dissertation.

Moreover, Chapter 4 will define the compressor boundary conditions and will thus set the component working environment. Any assumptions pertaining to the geometry constraints or adjoining modules' performance are justified and suitably referenced.

Chapter 5 is one of the more important chapters detailing the methodology used for satisfying the aforementioned tasks. A total of sixteen different layouts are enumerated and the procedure adopted towards specifying the most promising design is established. Also, the compressor figure of merits are discussed and prioritised. Furthermore, a new turbomachinery preliminary design tool is documented. This tool, was successfully tested, and used extensively throughout this work to aid the author in analysing the different designs.

Finally, the concluding chapter highlights the overall achievements of this work and highlights the aerodynamic and mechanical qualities of the chosen design.

INTENTIONALLY LEFT BLANK

Chapter 3

Literature review

3.1
- Chapter layout

3.2
- The gas turbine engine
  - Thrust and efficiency
  - Main engine parameters
  - TIT and OPR
  - BPR and FPR
  - Engine diameter considerations
  - Engine design process

3.3
- The working fluid
  - Total and static thermodynamic conditions

3.4
- The compression module
  - Flow description
  - Annulus blockage
  - Stage work input
  - High speed flow
  - Compressor stall and surge
  - The compressor characteristic
  - Compressor dimensional analysis

3.5
- Blade nomenclature
  - Incidence selection and theoretical optima
  - Blade stagger and camber
  - Blade thickness and profile shapes
  - Flow deviation

3.6
- Blade loading
  - Vortex flow

3.7
- Stage loading and design point efficiency
  - Efficiency terminology
  - Loss generation and efficiency prediction

3.8
- A general turbine overview
  - Turbine loading and efficiency potential

3.9
- Method of analysis and general assumptions

3.1 Chapter layout

The literature review will introduce all the necessary engineering concepts required for understanding the arguments raised in the subsequent chapters. A general overview of the gas turbine engine and the associated development process is presented.

This is followed by an introduction of generic compressor theory in Section 3.4. Each segment builds on the one before, increasing in complexity and depth of knowledge as the chapter progresses. Section 3.5 then outlines the terminology related to blade nomenclature and the correlations pertaining to blade turning and optimum design methodology.

Thereafter the concept of blade loading is introduced in the ensuing section. This is one of the more critical parameters affecting the overall performance of the compressor. The influence of the latter on compressor efficiency is discussed, in some detail within Section 3.7.

Some basic theory related to turbine design is outlined towards the end of the chapter. This knowledge is included because it is thought useful due the latter's influence on compressor design and performance. The information presented regarding turbine design is much more superficial in nature, when compared to the previous sections, and is only intended as an aid for understanding the compressor design constraints imposed by this module.

Finally, the concluding literature documents some of the more fundamental flow assumptions which are used throughout this work.

3.2 The gas turbine engine

This section will give a brief overview of the main engine variables. These are decided upon during preliminary design in accordance to the mission profile the engine is expected to perform. The selected mission profile for this study has been outlined in Section 1.2.1 of Chapter 1.

Furthermore, the ideal engine design process is also well explained with particular emphasis on compressor design.

3.2.1 Thrust and efficiency

The engine design thrust and sfc are amongst the most important specifications in any aero-engine design study. The ability of an engine to deliver the required thrust at the given sfc is crucial for its success.

The required thrust, as stipulated by the aircraft manufacturer, is the maximum thrust the aircraft will require throughout its flight envelope. As indicated in Figure 3.1 below, the thrust lapse, due to inlet momentum drag, of a moderate to high BPR engine is quite significant. Hence, the engine is normally sized to deliver a TOC thrust which will enable the aircraft to achieve a further rate of climb of 300ft/min, or 1.5m/s, as is usually stipulated by the airworthiness authorities. Once this thrust benchmark is satisfied, the single-engine takeoff thrust requirement and field performance are normally adhered to automatically.

The specification of efficiency for an aero-engine is different to that of a stationary industrial powerplant. The term ‘sfc’ rather than the more common expression of thermal efficiency is used in such a case.

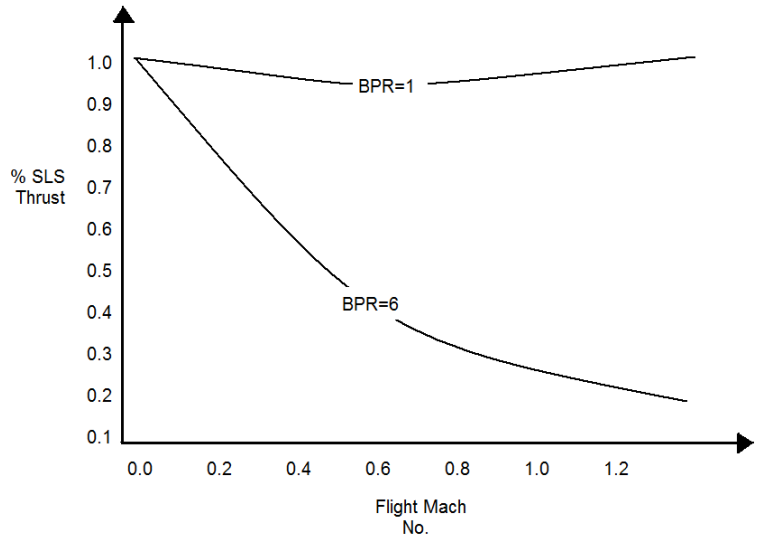

Figure 3.1: Thrust lapse with Mach number, modified from [16]

The thermal efficiency (η_{th}) of any powerplant, including an aero-engine, relates the work output to the work input. The work output for a turbofan is the net gas power generated ($\dot{W}_{net}$) and the work input is associated with the fuel flow ($\dot{m}_f$) and the calorific value of the fuel (LCV).

$$\eta_{th} = \frac{\dot{W}_{net}}{\dot{m}_f LCV} \qquad \textit{(equation 3.1)}$$

The thermal efficiency of an aero-engine describes the engine's ability to generate work. However, for such engines, the propulsive efficiency (η_p) is further used to describe the efficiency with which this work is used to create thrust. η_p is a parameter which relates the flight (V) and jet (V_j) velocities as illustrated in Equation 3.2.

$$\eta_p = \frac{2V}{V+V_j} \qquad \textit{(equation 3.2)}$$

It is apparent, from the above equation, that for a high η_p, one must design an engine which has a jet velocity only marginally higher than the flight velocity. However, such an engine would yield very low thrust. Hence, as illustrated in Figure 1.2, modern engines employ a considerable amount of bypass air to accelerate, only slightly, a large airflow thus satisfying the thrust requirement with maximum efficiency.

Now, since the bypass air has to be accelerated by a fan, the resulting thermal efficiency of the gas turbine is worsened somewhat by the introduction of the fan and driving turbine inefficiencies; however, the significant improvement in propulsive efficiency overcomes this slight deficiency. Some authors, such as Philpot [17], favour the introduction of a further efficiency term, called transfer efficiency, to cater specifically for this fact, thus leaving the original n_{th} unaffected. However, the former philosophy is used in this report due mainly to its more widespread use.

Finally, the engine's overall efficiency (η_o) is a factor of both the η_{th} and η_p. An improvement in either one results in a better η_o and hence sfc as illustrated by Equation 3.4.

$$\eta_o = \eta_{th}\eta_p \qquad \textit{(equation 3.3)}$$

$$\eta_o = \frac{1}{sfc}\frac{V}{LCV} \qquad \textit{(equation 3.4)}$$

3.2.2 Main engine parameters

For virtually any commercial engine produced today there are two pre-eminent requirements which must be satisfied: minimum direct operating cost and long overhaul life. What might not seem intuitively obvious is that, from a commercial point of view, what is actually required is an engine which has a low direct operating cost and not necessarily best fuel consumption. Even though fuel is a significant part of any operator's expenditure it is by no means the only engine related cost. So much so that, on short to medium-haul missions, fuel tends to account for only 25% of the airline's operating costs [18].

Also, an engine which has a good overall efficiency may not necessarily have the lowest fuel burn for the assumed flight profile. This is because a fuel efficient engine may be much heavier than a slightly less efficient one. Thus, more fuel may be consumed during the flight when compared to the lighter engine because the extra weight offsets the better fuel efficiency. This is further explained in Section 3.2.4 with the use of the range factor.

A similar scenario is experienced on the B777-200 between the GE 90-85B and the RR Trent 892-17. The former has an sfc_{cruise} of 1.47×10^{-5} (kg/s)/N whilst the Trent only attains

$1.58x10^{-5}$ (kg/s)/N [3]. However, the GE90 weighs 7074kg whilst the Trent is over a tonne lighter. Data acquired from the airlines confirms that, on most routes, the RR engine is more economical than the GE engine even though the latter has a better fuel efficiency [5].

Any engine design study aims to maximise the performance of the above requirements by optimising the core engine parameters around three operating conditions [17].

1. maximum thrust at normal cruise flight, normally referred to as top of climb (TOC),
2. normal cruise thrust, usually 70-80% of the latter,
3. maximum required thrust for a sea-level takeoff on a hot day.

For this study, condition (2) was chosen for defining the engine parameters. Once this design point is chosen the designer has to establish the engine's four fundamental variables.

1. Turbine inlet temperature (TIT)
2. Overall pressure ratio (OPR)
3. Bypass ratio (BPR)
4. Fan pressure ratio (FPR)

3.2.3 TIT and OPR

The selection of TIT and OPR go hand in hand since an increase in one will more often than not necessitate an increase in the other. This is evidenced by Figure 3.2 below, which depicts the variation of these parameters over the last half a century.

The TIT defines the technology level of the engine. The primary objective of increasing the TIT is to allow for higher thrust from a given engine size. Due to improvements in materials science and blade cooling techniques, the allowable TIT has steadily increased by 10^{o}K per year over the last few decades and there is every hope that this trend will continue [19]. Unfortunately however, the life of the turbine blades is halved by each 15^{o} rise in temperature, hence newer technologies are always being sought to suppress creep, thermal fatigue and oxidation which are the primary mechanisms that limit blade life.

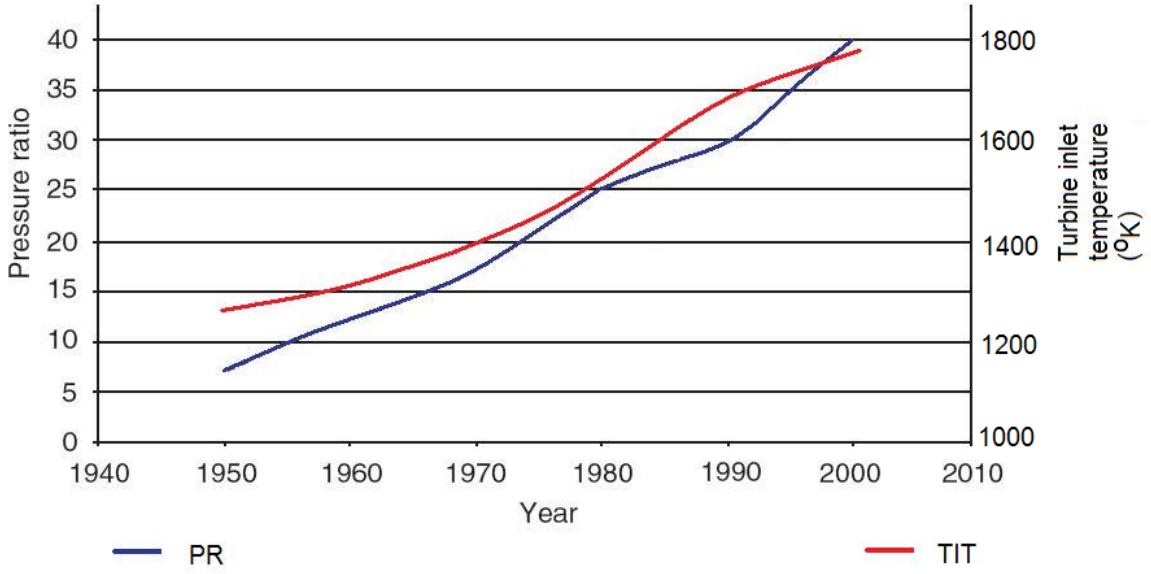

Figure 3.2: Trend of OPR and TIT, modified from [12]

When considering that engines today, such as the Trent 900, are designed to operate with a takeoff TIT of 1900°K [1], it can be appreciated how much progress has been achieved towards increasing this limit in view of the fact that engineers in the early 1940s were facing huge technical difficulties with a mere 1200°K when testing their BMW003 [8].

The TIT which is usually quoted in literature, including this dissertation, is assumed to be the takeoff limiting temperature, unless stated otherwise. The cruise temperature (TIT_{cruise}) is normally around 150° cooler [20]. This is a welcome relief considering that the turbine blade materials melt at 1450°K; thus, because of this fact, extensive cooling is usually required to keep the blade strength at acceptable levels.

Furthermore, even though the available technology may allow very high temperatures, the engine design may specify lower TITs. The incentives for low TIT may be either to lower cost or to allow room for further future growth of the basic design. Such was the case of the Lycoming LF507 [21].

Once the TIT is specified, the OPR is then chosen with the intent of maximising either efficiency or specific thrust. Specific thrust is the amount of thrust produced by the engine per unit air flow through the core and is a measure of the engine size and weight. A high value is obviously beneficial [6]. However, the optimisation for specific thrust will

necessitate a lower OPR than if the engine were designed for minimum sfc, hence, a compromise is usually inevitable. For the case study examined in this report, the requirement of high specific thrust will bear more weight on the final decision than if the engine were designed for a longer-range aircraft.

Moreover, there are further incentives for keeping the OPR as low as possible. A low pressure-ratio compressor will have a wider operating range, i.e. mass flow range from choke to stall, and therefore will be less susceptible to dirt, foreign object damage or vane angle settings [12]. Also, a low pressure ratio engine may require less exotic materials for the last compressor stage and first stage turbine, which are both effectively at compressor delivery temperature. This temperature, which also depends on ambient total temperature and compressor efficiency, may also act as a constraint for the highest permissible OPR considering it is nowadays approaching 930^{o}K [1], [22].

On the other hand, the greatest motivation for increasing OPR is the valuable effect this has on improving cycle efficiency. In addition, high compressor delivery pressures may aid combustor design. Lefebvre [23] notes that increasing the combustor inlet pressure improves combustion stability by widening the stable operating range of the flame and also reduces the ignition energy required thus easing igniter design.

These considerations have naturally led to different decisions being taken for different designs. The RR Trent 900 which powers the A380 has been optimised towards minimum sfc and thus has a high TIT of 1870^{o}K [1] and an OPR of 41. Conversely, the RB211-535E4 which is one of the options on the medium range B757-200 and Tu-204 has a TIT and OPR of 1500^{o}K and 25.8 respectively [3]. The latter's choice of low OPR was further influenced by the desire to keep the turbine cooling flow rate low, thus simplifying the design of the turbine and secondary air system [20]. Finally, the CF34-3A which is used on the short-haul Canadair Regional Jet has a TIT of 1477^{o}K together with an equally low OPR of 21 [3].

3.2.4 BPR and FPR

Once the TIT and OPR are specified, the energy available to provide work within the turbine is set. It is then up to the designer how to best utilise this energy to obtain thrust. As outlined in Section 1.4, the thrust is normally generated by two streams of air, the bypass air compressed by the fan, and the core air, passing through the turbines and the downstream propelling nozzle. The purpose of the bypass air is to improve the engine's propulsive efficiency and thus sfc.

The BPR for a given engine may be specified with the use of the range factor [7].

$$Range\ factor = \frac{weight\ of\ fuel\ used + engine}{engine\ thrust - pod\ drag} \qquad (equation\ 3.5)$$

A low value of range factor is obviously desirable.

Increasing BPR improves sfc and hence reduces the fuel used but also increases the engine's weight per unit thrust produced; thus, the range factor depends greatly on the assumed flight profile. An increase in BPR also leads to significant noise reduction benefits; however, this also causes the engine's frontal area for a given thrust to increase. Additionally, the number of LPT stages increases rapidly when the BPR is increased beyond 5 [7].

These considerations have led to engines which are optimised towards minimum sfc, such as the Trent 900 outlined above, to have a BPR of between 6-10 whereas short-haul engines have a much lower BPR of around 3-6 [7]. Figure 3.3 depicts how for a 1000km journey at a cruise speed of M0.8, a BPR or around 5 is considered to be about the optimum.

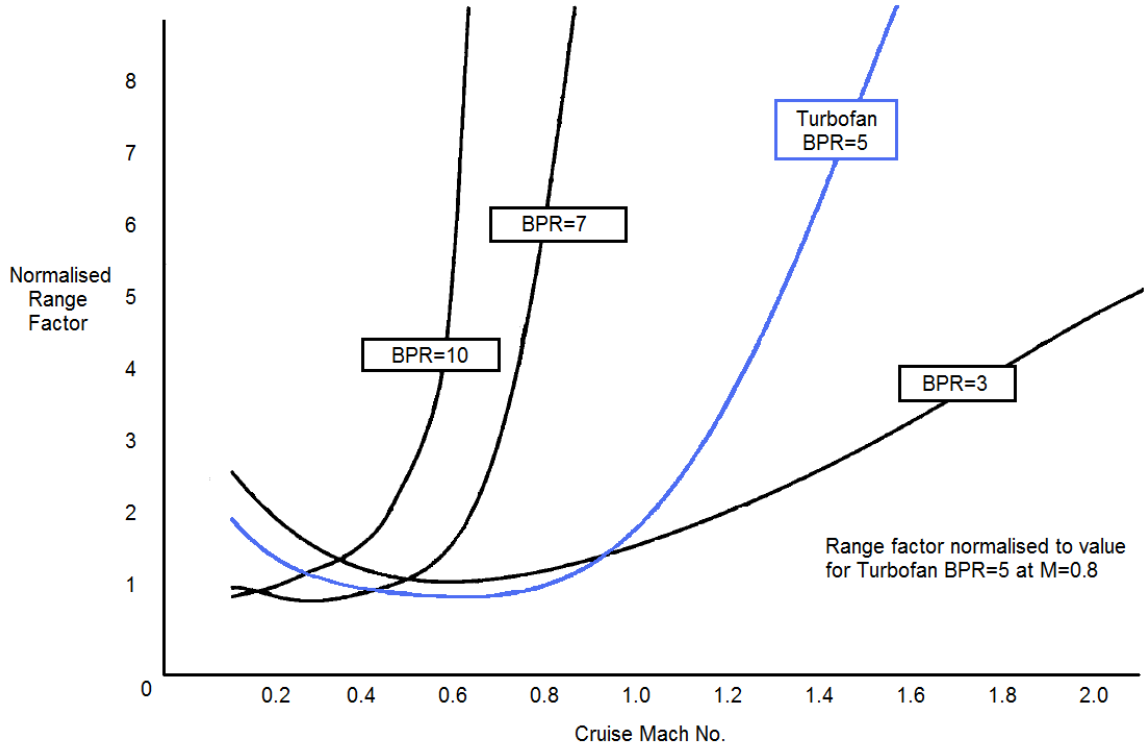

Figure 3.3: Range factor vs. Mach no. for a range of 1000km

When the BPR is set, the FPR specifies the work split between the cold (bypass) and hot (core) streams. Theoretically, the FPR depends on the efficiencies of the fan and LPT. Since the efficiencies of these components are normally in the range of 85-90%, the optimum FPR yields the following approximate jet velocity ratio:

$$Core\ jet\ velocity = 1.2 x bypass\ jet\ velocity \qquad \textit{(equation 3.6)}$$

3.2.5 Engine diameter considerations

It might initially seem that the designer has quite some flexibility in designing a 'clean sheet' engine, however in reality, his choices are severely restricted by technological and feasibility constraints. Even though, as shown above, it is theoretically beneficial to increase the BPR and hence η_p, in reality there are some other considerations that need to be taken into account.

Current technology levels restrict the minimum core size for a given thrust level. This minimum, even though it decreases gradually because of higher allowable TITs, still acts as a constraint which needs to be adhered to. Thus, choosing a large BPR effectively implies increasing the engine's outer diameter. However, there are some incentives or even restrictions for keeping this below a certain maximum.

One such constraint is due to the engine's operating environment. Civil engines have, in recent times, been attached below the wing of the aircraft for a variety of reasons, not least because of ease of maintenance and noise considerations within the cabin. Hence, for such an arrangement, keeping the engine's outer diameter small requires a shorter and lighter undercarriage and thus aircraft weight.

However, this is not the only incentive for keeping the outer diameter as small as possible. When designing the Trent 900 for the A380, RR chose to limit the diameter to 2.95m even though this aircraft could accept a slightly larger engine. The reason for this had less to do with the aircraft weight than ease of maintenance for the airlines. This constraint was chosen to enable the engine to be transported as a complete unit within the B747 freighter, which some of RR clients use to transfer cargo between different locations.

A further constraint on the engine's outer diameter is due to the aerodynamics of the fan. The fan tip section approaches the airflow at around M1.5. Increasing beyond this limit penalises the efficiency of the fan and hence affects noticeably the engine's sfc. Therefore, to enlarge the engine's diameter, may necessitate a slower rotating fan, which in turn dictates an increase in the number of LPT stages to maintain the turbine efficiency at an acceptable level. This addition to engine's length and weight may, in some cases, more than offset the beneficial improvement of η_p.

It is sometimes suggested to install a reduction gearbox on the fan shaft. This effectively decouples the fan and turbine speeds, hence the aerodynamic loading can be optimised for both [24]. However, this option, in addition to adding weight and complexity to the engine may also prove problematic. For a 20Klbf engine, the fan shaft will have to transfer around 7MW of power from the LPT to the fan at cruise speed. Thus, a gearbox of 99% efficiency would dissipate around 100hp/70KW into the oil system. This extra heat addition within the scavenge oil may then prove somewhat problematic to cool using conventional methods.

3.2.6 Engine design process

The design process overviewed in this section is described as being a series of distinctly demarcated phases. However, it must be appreciated that this is more of an ideal representation, as there is no such absolute procedure for the design of an aero-engine and the exact steps involved will depend to a large extent on the organisational structure of the company. Also, the process described hereunder is more representative of a new powerplant development process since an engine modification study will require much less analysis.

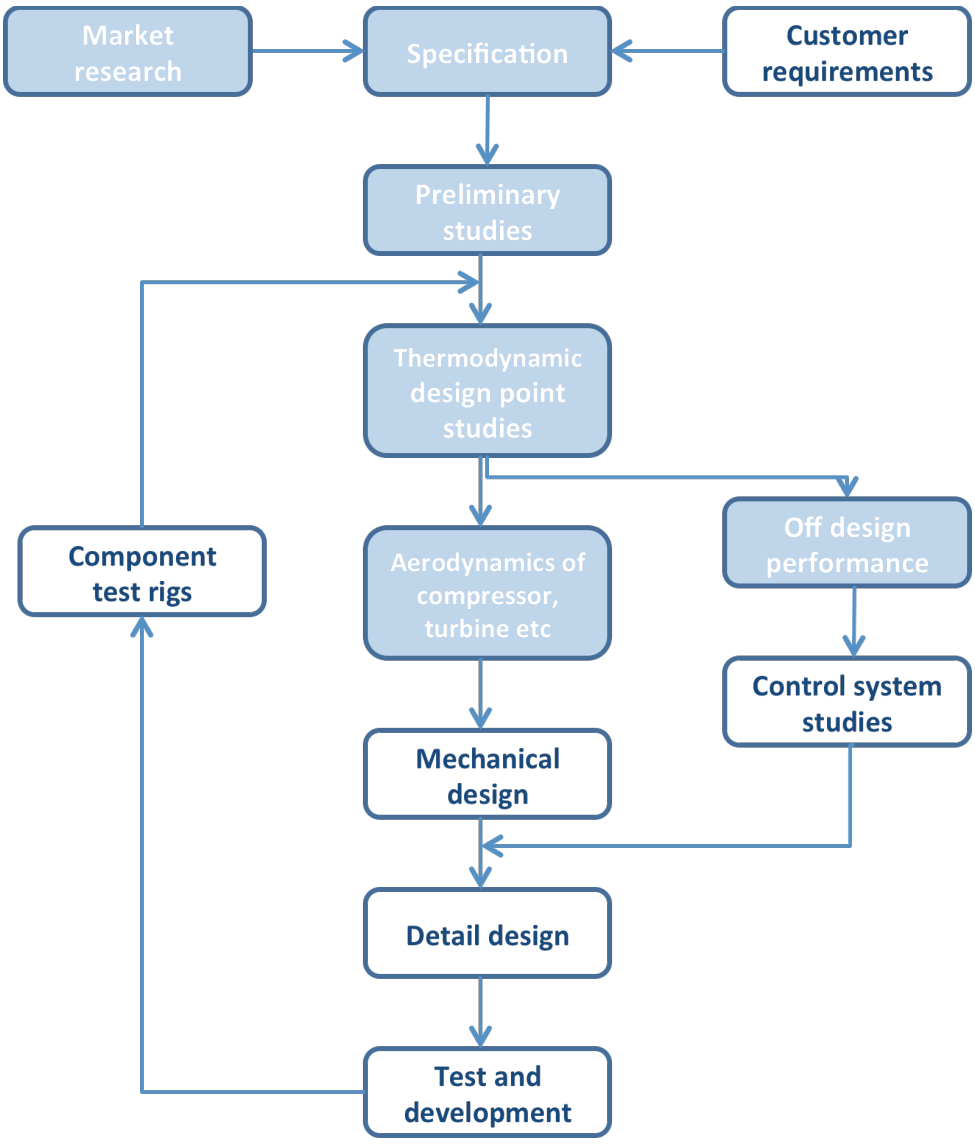

Figure 3.4: Engine design procedure, modified from [19]

The design steps which will be considered, to some extent or other, within this dissertation are depicted in Figure 3.4 with a blue background.

As described in Section 1.2 above, most civil aero-engine development studies are initiated once a new aircraft platform has been launched. It is mostly up to the organisation itself to decide whether or not to develop an engine to power the new or modified aircraft. One of the more important considerations when taking this decision is the expected market performance of the proposed aircraft, however unfortunately, this is not always well predicted. A typical case was when GE spent most its development time and effort designing the TF39 for the military C5 and left the market unchallenged for the then less popular B747. The Boeing aircraft eventually outsold C5 by a large margin [2].

Once a new engine is launched, most engine manufacturers may call in some potential customers, which in most cases are the airlines or the military staff, to get some feedback on what they would like from the engine. This then helps specify the design requirements and Figures of Merit (FOMs). The requirements assumed for this work are outlined in Chapter 4 whilst the FOMs are discussed in Section 5.1.

Requirements	Figures of Merit
Range	Initial investment
Payload	Direct operating cost
TOC thrust	Cost per seat mile
Growth capability	Off design performance

Table 3.1: Typical engine requirements and FOM; data obtained from [6]

Once the specification is outlined, the engine preliminary studies may be initiated. This entails, amongst other things, fixing the cycle parameters, such as turbine inlet temperature and overall pressure ratio. It must be appreciated however, that there are numerous constraints in fixing the cycle parameters. These can generally be classified into two main categories: the limitations of the available component technologies and the operational considerations which are dependent on the aircraft application. The cycle parameters assumed for this study are listed in Section 4.1 of the following chapter.

The design process then generally moves on to the thermodynamic design point analysis. The design point, as described in Section 3.2.2, is the operating point around which the engine's thermodynamic and aerodynamic performance is optimised. Included within this design stage are the projected efficiencies of the engine's components amongst which are that of the compressor and turbine units. In industry these calculations are carried out using specialised software either developed in-house or else sourced from one of the commercially available programs. One of the main outcomes from this research would be to establish anticipated design point efficiency and thrust output for the new engine.

If these meet the specified requirements, the geometry is fixed and the off-design performance is then considered. This is a critical process in any design study as the off-design operation dictates, to a large extent, the complexity of the control system which nowadays entails a considerable certification cost in itself.

In parallel with the off-design study, the aerodynamic design of the turbomachinery is usually undertaken. This specifies the exact contours and geometry of the components and also considers the manufacturing feasibility of the different components.

A successful candidate engine will then undergo detail and mechanical design studies which fine-tune the geometry to improve, amongst other things, the manufacturability and maintainability of the engine. This is then finally succeeded by an extensive testing phase to certify the engine as airworthy and thus safe to fly.

3.2.6.1 Compressor design

This dissertation outlines a compressor preliminary aerothermal design study coupled with some minor off-design analysis. The compressor is the heart of the modern aero-engine and because of the predominantly high temperature and pressure levels encountered, coupled with the small blade sizes, it requires a lot of attention and traditionally causes the most problems during in-service operation [20].

Because of the unpredictable nature of compressor behaviour, it is custom to cater for some shortfall in the predicted efficiency of the final design. Walsh *et al.* [7] suggest a 6%

efficiency margin for a high risk design down to a minimum of 2% for a high confidence, low risk, design.

One of the main objectives of the preliminary design of a compressor is to specify the number of compression stages required to meet the design pressure ratio. This is usually ascertained with the use of pitchline, or mean radius, design tools. These tend to use the blade and flow geometry as input to correlations which can predict the loss and deviation. Refinements may then be used to assess the blade loading at the hub and casing especially if the hub/tip radius ratio is low [25].

The duty, or stage loading, is the single most important decision in compressor design and determines to a large extent, the complexity of the problems that will be encountered and the level of efficiency to be achieved. Choosing an unrealistically high loading may cause extensive project delays and cost overruns. A typical case study is that of the IAE V2500 HPC [26]. This compressor, under the responsibility of RR, was initially earmarked to achieve a PR of 20 at an efficiency of 91%; however, after many modifications, costing the project millions of lost revenue, it only attained a PR of 16 and 88.7% efficiency.

Once a promising design layout is specified, the compressor is further analysed with the use of more exact means such as full three-dimensional, Navier-Stokes, computational fluid dynamics (CFD). The design can then iterate between the various stages of the design process and there is a considerable input from other engine design disciplines such as whole engine modelling and metallurgical science.

The compressor characteristic, which describes the behaviour of the compressor, is then generated and the working range within this characteristic is determined. Any need for variable geometry or bleed is finally established with the use of off-design prediction models.

3.3 The working fluid

Air, which is the working fluid of the engine, is considered, for all intensive purposes within this dissertation, to behave as a thermally perfect but calorifically imperfect gas.

A thermally perfect gas obeys the ideal gas equation [27], where the compressibility error z, has a value of unity.

$$P = z\rho RT \qquad \textit{(equation 3.7)}$$

This assumption is valid because for gas mixtures whose static pressure is low in comparison with their critical pressure, which for air is 3.77MPa [28], and the mass content of water vapour is less than 10% [7], the compressibility error z, can be considered negligible. Figure 3.5 shows the compressibility of air at the compressor inlet and outlet conditions.

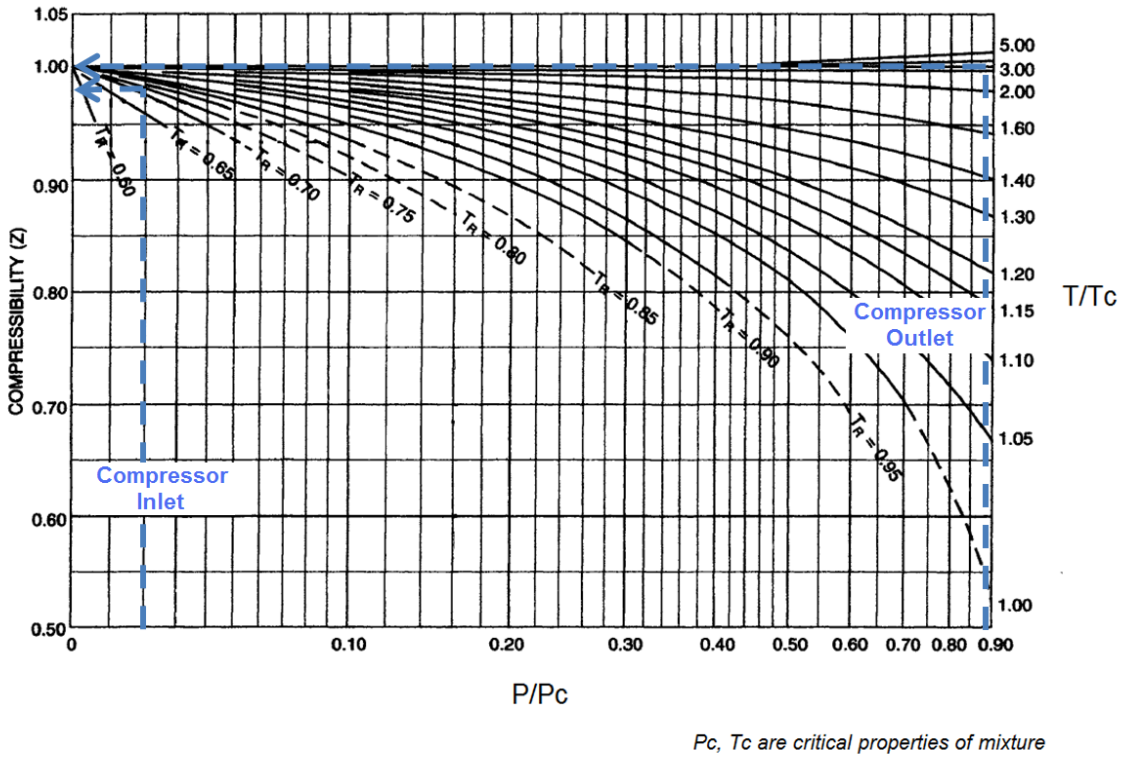

Figure 3.5: Compressibility of air at compressor inlet and outlet, modified from [28]

Even though the gas behaves as a thermally perfect gas, the specific heats at constant pressure and volume, C_p and C_v respectively, and hence their ratio, γ, vary considerably over the temperature range of 216K to 2200K [5]. However, the accompanying change in pressure, which occurs within aero-engines, has negligible effect on their magnitude and may thus be neglected. C_p and γ are calculated within this report using the empirical equations outlined in [7].

Finally, the gas constant R, remains essentially stable at 287.05J/KgK, for all values of temperatures, pressures and gas composition within the engine.

3.3.1 Total and static thermodynamic conditions

The working fluid undergoes thermodynamic changes when passing through the various components of the engine. These changes can be explained with the use of the First Law of Thermodynamics for a steady-flow process. This states that the change in energy is a measure of the heat ($\dot{Q}$) and work ($\dot{W}$) input to the fluid within the system.

$$\dot{Q} + \dot{W} = \dot{m}\left\{\left(h_2 + {}^1\!/_2\, V_2{}^2\right) - \left(h_1 + {}^1\!/_2\, V_1{}^2\right)\right\} \qquad \textit{(equation 3.8)}$$

The term $(h + {}^1\!/_2\, V^2)$ is frequently encountered within thermodynamics and is generally referred to as the stagnation enthalpy (H) [29]. Also, for an ideal gas, the enthalpy and temperature are related by the gas coefficient c_p as shown in Equation 3.9 [27].

$$dh = c_p dT \qquad \textit{(equation 3.9)}$$

Hence, with the use of the above two equations, the stagnation temperature (T_o) can be defined as,

$$T_o = T + {}^1\!/_2\, c_p V^2 \qquad \textit{(equation 3.10)}$$

Finally, the total pressure (P_o) is derived by assuming an isentropic, or loss free, deceleration from a flowing (P_o, T_o) to a static (P, T) condition.

$$P_o = P\left(\frac{T_0}{T}\right)^{\gamma/\gamma-1} \qquad \textit{(equation 3.11)}$$

3.4 The compression module

There are several reasons for compressing the air prior to combusting it. Without a compressor the engine will be unable to start from rest, behaving more like a ramjet. Also, even if this limitation is overcome, at low forward speeds, the engine would produce very little work as the efficiency would be appalling. This is primarily because, the working fluid should, as suggested by the Carnot cycle, be heated at the highest pressure within the engine to achieve the best possible efficiency [30].

Most large and medium sized aero engines today make use of an axial flow compressor; this is however, by no means the only possible manner how to compress air. Axial flow compressors are used because they permit a low engine weight coupled with a small frontal area for the required cycle flow and pressure ratio. The use of an axial flow compressor is assumed for this study and hence any mention to the compression section within this dissertation will be with regards to this statement.

Axial flow compressors employ a number of stages to yield the cycle pressure ratio. Each rotor stage adds energy to the flow and hence causes an increase in pressure and temperature of the fluid. The measure of work input by the rotor is related to the temperature rise of the air. The associated pressure rise, for an isentropic process, may then be obtained with the use of the following equation.

$$\frac{P_{o1}}{P_{o2}} = \left(\frac{T_{o1}}{T_{o2}}\right)^{\gamma/\gamma-1} \qquad \textit{(equation 3.12)}$$

It is worth mentioning that even if each consecutive compression stage adds the same energy input to the flow; the pressure ratio of the rear stages will be much lower than that of the upstream stages because of the reheat effect of the fluid. This is due to the fact that, for a given temperature rise, the stage temperature ratio, and the associated pressure ratio, diminish with higher inlet temperatures. This highlights the importance of achieving the best possible efficiency in the first stages as a small improvement in the latter will bear a large result on the overall performance of the compressor.

3.4.1 Flow description

The flow in a compressor is very delicate because it is forced to behave in an unnatural way by moving along an opposing pressure gradient. The bottleneck as to how much energy may be imparted to the flow within a stage depends mostly on the blade and annulus boundary layers. The boundary layer is the region of flow adjacent to a solid surface which is retarded with respect to the mainstream velocity due to the affect of friction.

The boundary layer is laminar on the leading edge (LE) of the blade however soon transitions to turbulent near the peak suction point. This is because, even though the flow is diffused in a blade row, it is momentarily accelerated in the forward region of the blade up to the throat, and then decelerated to achieve the required pressure rise. Even though a laminar boundary layer is desirable in respect of low blade profile loss, it is unable to support the opposing pressure gradient and hence tends to separate from the blade surface. This separated region causes a large mixing loss due to the increase in entropy of the disordered flow.

To delay flow separation, the blade profile is designed to transition, in a controlled manner, the laminar boundary layer to turbulent. Turbulent boundary layers cause greater profile losses however can support much higher opposing pressure gradients and hence are much more resilient to separation. The net result is normally an overall reduction of stage pressure loss.

In spite of the above argument, the turbulent flow often tends to separate towards the blade trailing edge and regions of low momentum such as fixed blade corners. The separated region can be limited by an appropriate choice of blade loading and by utilising three dimensional blade shapes such as sweep or lean [31]. Exceeding the allowable loading may result in large separation regions which dramatically reduce the performance of the compressor. However, higher loadings result in fewer compression stages and hence weight; thus, a proper balance is vital.

Even though, the flow in a compressor is usually described as behaving in a linear manner, it must be appreciated that the flow within turbomachines is highly complex and three dimensional. The boundary layers, described above tend to move towards the casing within

the rotors but towards the hub in stators. The former is a result of the outward centrifugal force outweighing the radial static pressure field which exists within all compressors to stabilise the flow. This is because the tangential velocity of the rotors and the associated boundary layers is greater than that of the mainstream flow. On the contrary, the stator boundary layer has no tangential velocity and therefore the radial static pressure field predominates [32].

The system is further convoluted because of the interaction between blade flow and the annulus boundary layer. The latter is also skewed as it migrates from the blade suction surfaces towards the pressure sides due to the tangentially varying pressure gradient which exists within each blade passage. This complex interaction manifests itself in a three dimensional flow behaviour, such as blade corner stall, which is not properly modelled by conventional methods.

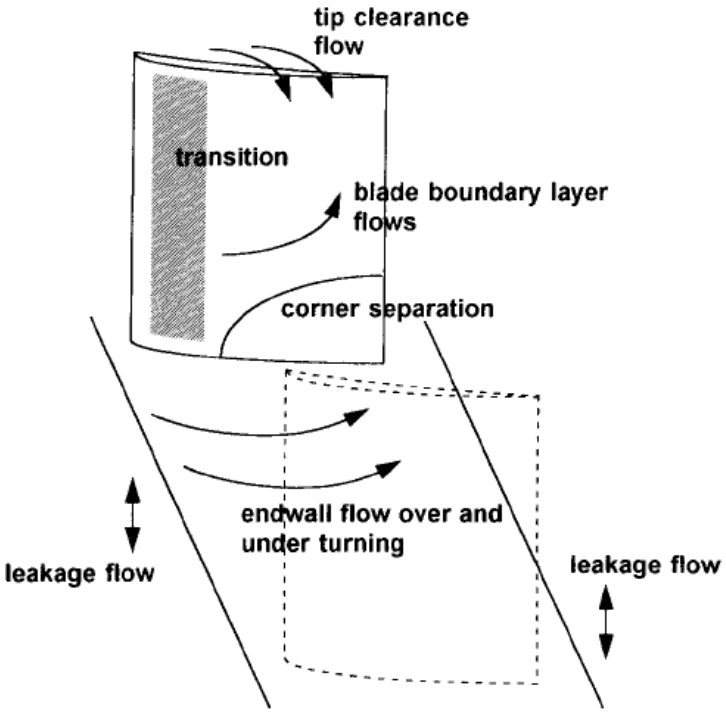

Figure 3.6: Three dimensional flow within rotors, obtained from [33]

Given the importance of predicting the transition from a laminar to a turbulent boundary layer, there have been numerous investigations and public reports on this matter. One such report is from Abu-Ghannam *et al.* [34], which states that for the turbulence level existing

within conventional compressors, an adverse pressure gradient will almost always induce transition at a critical value of Reynolds number (Re).

$$Re = \frac{\rho V L}{\mu} \qquad \textit{(equation 3.13)}$$

Moreover, it is known that the overall losses within a compressor tend to reduce with increasing Re as the boundary layers become thinner and more resilient to separation [33].

The flow architecture explained above is further disrupted by the tip leakage flow. At blade ends where there is a clearance, such as rotor ends (casing) and shroudless stator tips (hub), the flow on the pressure surface tends to escape over the blade tip and interacts with the suction surface flow. This leakage vortex dominates the flow behaviour near such regions and hence its influence can be mitigated by minimizing the clearance as much as mechanically feasible. Cumpsty [25], reports that the optimum clearance is around 1% blade chord, however, this level of precision is difficult to achieve in the rear stages due to the small blade sizes.

An optimum level of clearance exists because a small clearance (<1% chord) is thought to re-energise the blade boundary layer and hence mitigates the affects of corner separations and blade stall [35]. On the other hand, larger clearances are undesirable because they tend to increase disproportionally the blade loss and lower the maximum achievable pressure rise at stall due to the large scale disruption of the endwall flow [25].

The magnitude of tip clearance is small in proportion to the blade height in the initial blade rows, however as the blade rows become smaller towards the rear of the compressor this clearance occupies an ever greater percentage of the blade span. Hence, tip clearance flow has the greatest influence on compressor behaviour in the latter stages, and it is here where it determines, to a large extent, the occurrence of surge. Surge is explained in Section 3.4.5.

Given the complexity of the flow within compressors it is worth appreciating how preliminary design tools, based on simple pitchline empirical correlations, worked effectively in designing respectable compressors in the past before the advent of more complex media we make use of today.

3.4.2 Annulus blockage

The growth of the annuli boundary layers cause even greater concern than the localised disturbance of flow near the end wall region which is described above. Because these layers contain slow moving flow, they cause what is referred to as blockage.

Blockage, as described by Cumpsty [25], is a term used to quantify the percentage of the annulus area available to pass flow and which is, to a some extent, undisturbed by the end wall boundary layers. The prediction of blockage in preliminary design is an arbitrary process and is renowned to be the greatest single cause of inaccuracy for predicting multistage compressor performance. This is predominantly because, the blockage, which may reach anywhere from 10-20% in actual compressors [36], varies greatly between different designs, and depends profoundly on parameters such as tip clearance, stage loading [37], and three-dimensional flow profiles.

Furthermore, blockage, not only decreases the chocking mass flow [14], but also reduces the work done by the rotor blades on the mainstream flow. This is due to the fact that, it causes a degradation of the velocity profile, from that originally specified during blade design. It is known that the velocity tends to become more peaky and non-uniform along the length of the compressor but settles down to a constant form after the first few stages.

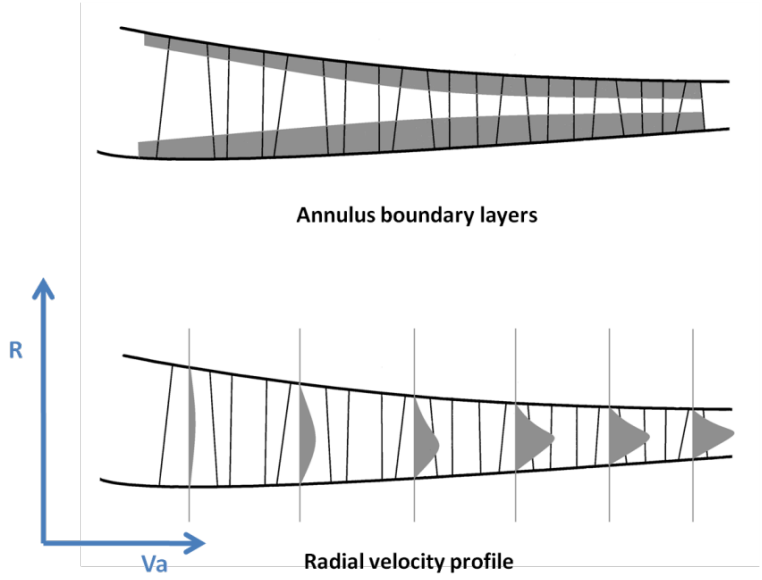

Figure 3.7: Annulus blockage

The increase in throughflow velocity outside the annuli boundary layers causes a reduction in stage efficiency and work input, because the flow angles will not match the blade shape. Different techniques are available to correct for this phenomenon. Cumpsty [25] and Aungier [36] favour the practice whereby the actual annulus geometrical area is increased somewhat, by a predicted blockage factor, to account for the reduced blade work and flow capacity throughout the span. However, the author of this dissertation prefers the use of the work done factor, λ. This is because it is well documented and easy to implement in a computerised preliminary design system. λ is an empirical adjustment of the stage work and is used to correct the differences observed between the calculated and actual stage performance. Howell [38], recommended a value of λ of 0.86 well inside multistage compressors; however, the present work assumes the following values of λ.

Stage	1	2	3	4 and greater
λ	0.98	0.93	0.88	0.83

Table 3.2: Work done factor values; data obtained from [19]

Finally, it is assumed that, since the velocity profile at the face of the HPC is already altered by the affects of the LPC, interconnecting duct and possibly bleed off-take, the value of λ, for any given stage of the HPC, is equivalent to that quoted above for the subsequent stage. This adjustment was deemed necessary because the values of λ listed in Table 3.2 are thought to be most representative of compressors having a uniform inlet flow at their front face. This correction effectively reduces the HPC stage work input; however, it is believed to model better the actual engine environment.

3.4.3 Stage work input

The work input in each compressor stage can be conveniently quantified with the use of a simplified derivation of the steady first thermodynamic law, Equation 3.8.

$$\dot{W} = \dot{m} c_p \Delta T_{0s} \qquad \textit{(equation 3.14)}$$

This equation clearly shows that, as was stated in Section 3.4, the stage work is directly proportional to the fluid's temperature rise. Also, it is evident that, for a constant axial velocity stage, the work input can be approximated to the Euler equation, Equation 3.15 [19].

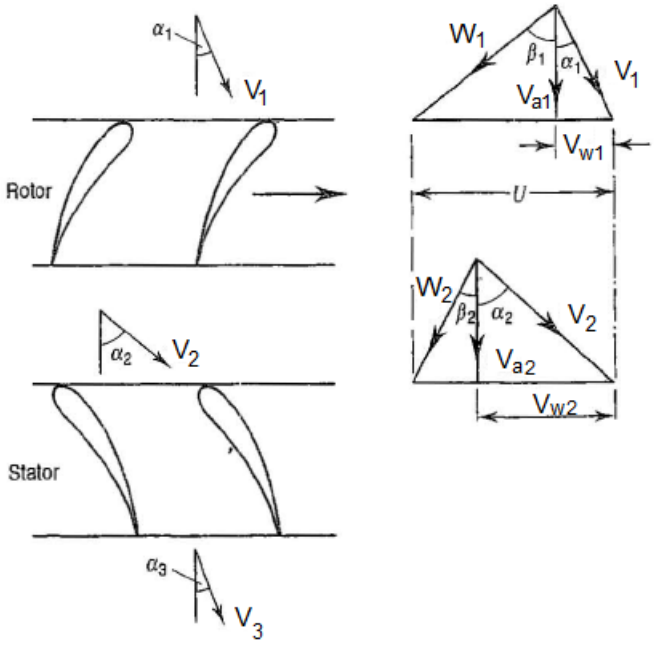

Figure 3.8: Stage velocity triangles, modified from [19]

$$\dot{W} = \dot{m}\lambda U V_a(tan\beta_1 - tan\beta_2) \qquad \textit{(equation 3.15)}$$

Hence, as illustrated in the above equation, there is a great incentive for increasing the blade speed (U) or the flow axial velocity (V_a). Increasing either one will increase the stage work input without influencing the flow diffusion and hence boundary layer health. The flow diffusion is represented in Equation 3.15 by the term $(tan\beta_1 - tan\beta_2)$.

The stage work may hence be increased either by further diffusing the flow or by increasing the blade relative Mach number (M). The former approach necessitates better control of the boundary flow through more detailed blade and annulus profiles and hence necessitates a general improvement in component technology.

The second option is restricted in application by stress considerations and also by compressibility losses which occur at high Mach numbers. To limit centrifugal stress on the

blade root fixings, the tip velocity is restricted to around 350-500m/s depending on the material type [7]. Increment in this figure requires better material and fabrication techniques.

Furthermore, this route towards increasing stage work input by increasing the blade relative Mach numbers necessitates a better understanding of transonic induced losses so as to design blades which can better handle such flow. High speed flow is thus the subject of a more thorough description within the following section.

3.4.4 High speed flow

As explained in the previous section, there is a great incentive for increasing the blade relative Mach number. Such an option is desirable in HPC design to reduce the component length and weight; however, it is of paramount importance in fan design. All current production civil engines employ a single stage fan; hence, the fan pressure ratio (FPR) as dictated by cycle analysis needs to be achieved within a single stage. This is essential to minimize the noise and weight of the engine and necessitates the use of highly supersonic blades to yield the 1.7:1 pressure ratio demanded by recent designs.

The demand for a single stage fan and minimum stage count thereafter usually results in the first few stages having some regions of transonic flow. Compressibility effects are of most concern in the first few stages. This is because, as the air is heated along the compressor, the speed of sound increases in proportion to $\sqrt{T}$ and thus the blade relative Mach numbers decline for a given flow velocity.

Transonic flow however, generally results in higher overall losses for a variety of reasons. A transonic blade is acknowledged to be a compressor blade in which the relative Mach number increases from below unity at the hub to a value slightly higher than M1 at the tip. The axial velocity V_a, is assumed to remain subsonic throughout. Kerrebrock [39], reports that the high transonic loss is not merely a consequence of the additional shock induced loss, but rather, a general amplification of subsonic losses experienced at speeds approaching M1. Hence any methodology for increasing the transonic efficiency needs to encompass a holistic approach to reducing all the different loss sources experienced within this flow regime.

Moreover, it is known that, some of the more desirable design attributes which operate best in high speed flow are small blade profile thicknesses and LE radii and also, small blade spacing and thus high solidity $\left({}^{blade\ chord}/_{spacing}, \sigma\right)$ [31].

The recommended maximum rotor tip Mach numbers assumed for this dissertation are M1.4 for the fan and M1.2 for all other compressor rotor stages.

3.4.5 Compressor stall and surge

The flow structure described above is applicable to operation at or near the design point. When the compressor is subjected to a lower mass flow, the compressor behaves very differently and may even react in an unsteady manner. This unsteady behaviour is referred to as compressor surge or stall. Predicting the onset of compressor instability is essential in the design process as operation close to this region induces elevated blade vibration and is thus a mechanical as much as an aerodynamic constraint [26].

Compressor stall is different from the blade stall described above. As was mentioned in Section 3.4.1, most blade rows operate satisfactory with some region of separated flow towards the trailing edge. Cumpsty [25], remarks that the compressor as a whole may work in a stable manner even if many of the blade rows are stalled.

A single-stage compressor will be unable to operate stably with extensive regions of separated flow within the blade passage; however, within multistage compressors, the same blade row may be allowed to operate in a stalled manner because of the stabilising effect of the other un-stalled stages. Therefore, because of this coupling effect, blade stall is not a good criterion for imminent compressor instability.

Compressor instability at low speed usually manifests itself as rotating stall. Rotating stall is a mechanism which allows a compressor to adapt to a flow which is too small for the given blade geometry. In such an operating regime, the flow is shared unequally within the annulus. Two types of rotating stall have been observed, full-span and part-span stall. Whether the instability will trigger full-span or part-span stall depends on the stall cell size and compressor characteristics [40].

Part span stall, which is the milder of the two, is common in the front stages of compressors at sub-idle speeds, however it usually disappears as the compressor accelerates towards the normal operating range [1]. The reason why rotating stall exists at such low speeds is because of stage mismatching at off-design. At low compressor speeds, the density ratio across the compressor decreases rapidly. At low values of density ratios, the flow annulus area at the rear of the compressor limits the flow through the compressor. This forces the front stages to operate at higher loadings and thus causes the latter to stall [32].

At a microscopic level, the higher loadings in the front stages may allow the tip leakage vortex to disrupt the blade suction boundary layer causing a large scale tip stall. This may extend through several adjacent blade passages forming a stall cell.

Corner stalls may also be inductive to rotating stall. Hah *et al*. [41] report how an incipient stall cell in their test compressor was triggered by an initial corner stall disturbance. This eventually migrated to the blade tips and formed a stationary stall cell.

Further loading of the front stages may cause the stationary stall cell to detach and rotate around the compressor annulus at around 30-70% of the rotor speed [33]. Even though this cell rotates in the same direction as the rotor, it seems to rotate in an opposite direction when viewed by stationary observer. The part-span stall frequency is typically around 100Hz and the stall cells tend to increase in number with higher loadings [42].

Furthermore, part-span stall, unlike full-span stall tends to occupy a small part of the compressor length and thus has a limited impact on the overall performance of the compressor.

Part-span stall may transition to the much more disturbing full-span stall; however, the latter is more prone in stages having a low aspect ratio (blade height/chord) such as those found towards the rear of the compressor. Full-span stall is considered to be a more serious phenomenon than surge, which is discussed next, as it is much more difficult to recover from and in some circumstances may necessitate a complete shutdown of the engine.

Full-span stall is characterised by a large stall cell extending throughout the compressor length, as evidenced in Figure 3.9. This type of stall results in severe vibration which may

lead to rapid high-cycle fatigue failure [7]. Also, the efficiency, pressure ratio and flow capacity of the compressor may diminish by up to 50% when compared to normal operation.

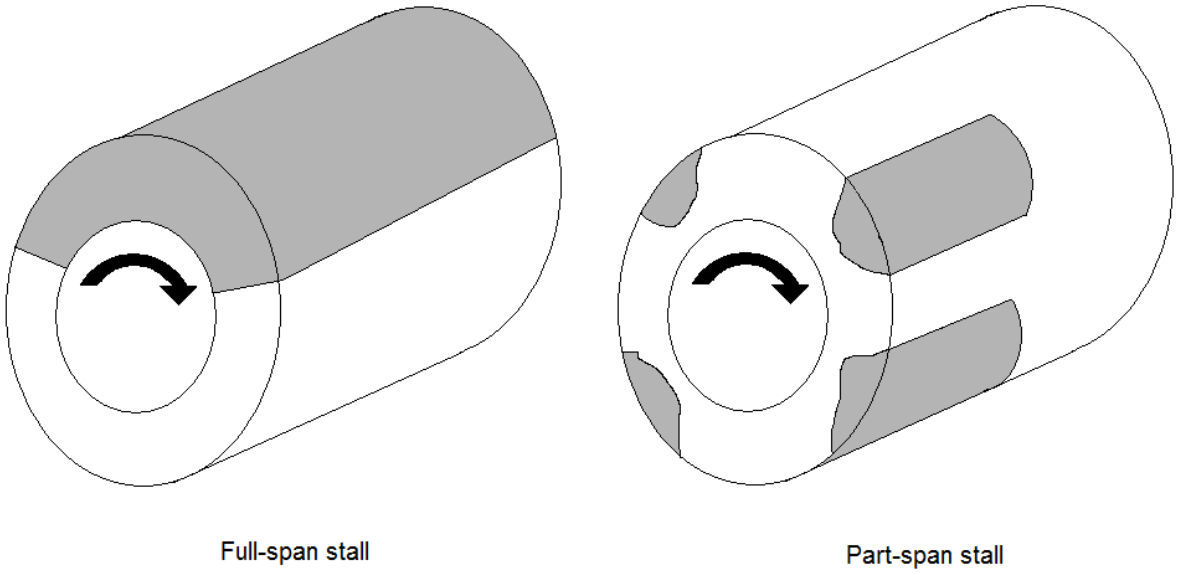

Figure 3.9: Rotating stall

Either type of stall may trigger surge. Surge is a mode of instability whereby the compressor adjusts to a low flow in a quasi-axisymmetric manner. During surge the inlet mass flow varies with time as the compressor oscillates between stalled and un-stalled operation. Also, unlike stall, the surge frequency is influenced, to a large extent, by the downstream components rather than the compressor itself, and is usually in the region of 5-10Hz [7].

Surge is normally characterised by a reversal of flow from the combustor or diffuser to the compressor inlet. It must be appreciated that this causes awkward bending stresses on the compressor blades and it is not uncommon for some blades to detach. This debris may then cause further extensive damage elsewhere. Furthermore, even though surge may be highly destructive to the compressor if prolonged, it is normally easier to recover from than full-span stall. However, it has transpired that on some occasions recovery from surge triggered full-span stall [7], therefore its importance should not be underestimated.

Finally, it should be appreciated that any kind of compressor instability is highly undesirable and is potentially dangerous to the aircraft and its occupants. Also, even though modern

compressors are protected against such events by the engine control system, surge can still be encountered within the normal flight envelope if the engine is damaged by an external source.

3.4.6 The compressor characteristic

The compressor characteristic depicts in a graphical manner the compressor performance and behaviour at any given flow and speed. The operating or working line is a locus of points throughout which the compressor operates during normal operation. This line is determined by the capacity of the downstream components, namely that of the turbine. If the turbine is choked, as is usually the case above idle operation, this line is unaffected by inlet flow Mach number and hence remains fixed within the normal flight envelope.

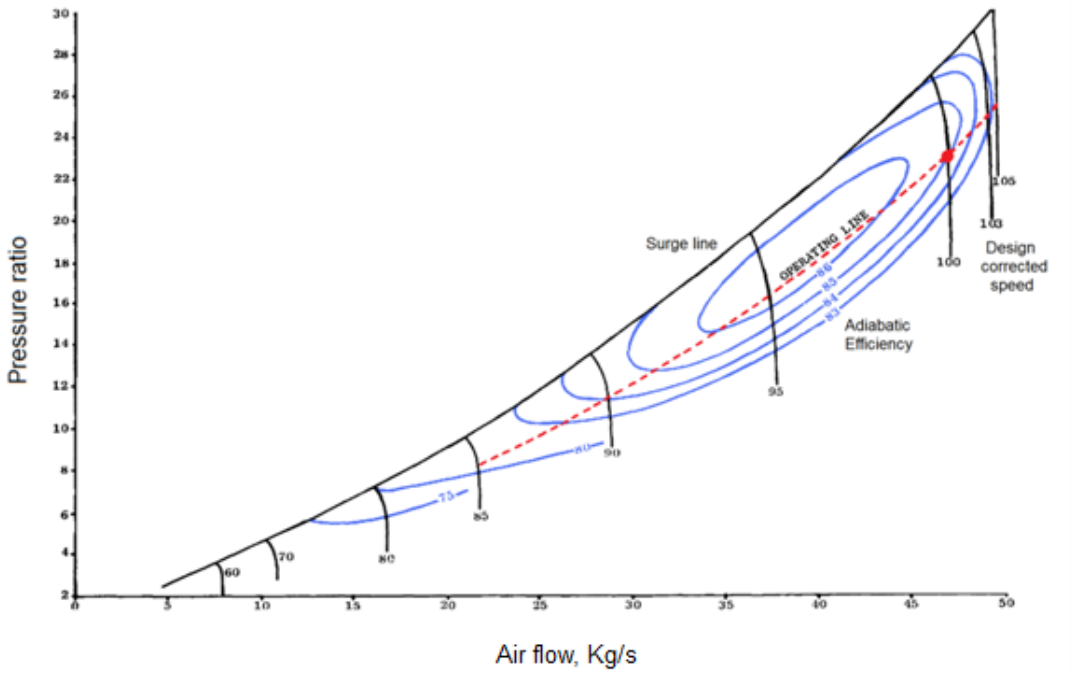

Figure 3.10: The compressor characteristic

The upper stability limit is depicted as a single curve and is usually referred to as the surge line. The surge line is a where the compressor first encounters either stall or surge.

Many design features affect the surge line shape, however, there is a general tendency for this line to be higher at intermediate flows for compressors which have low solidities (blade chord/blade spacing), low radius ratios (blade tip radius/root radius) and a rising hub line

[43]. Also, the complexity of the surge line depends on whether or not the flow limiting stage changes with operating speed. Closely matched stages may exhibit complex surge lines [12].

Although not implicitly depicted, the lower limit of the speed lines indicates the chocking mass flow. This flow is the maximum flow the compressor may handle and it is caused by the flow reaching sonic velocity in one or more blade throats.

The working line passes through the design point since this is where the compressor geometry is optimised. It is interesting to note that, as depicted in the above figure, the maximum efficiency is normally achieved at a speed slightly less than the design point. This is because, when operating at a slightly lower speed, the compressor geometry would still be relatively adequate for the given flow hence the off-design losses are minimal. Also, at a lower speed the profile and compressibility losses are reduced because of the lower inlet velocity within each blade row. This is quite useful in civil aircraft applications because it implies that when the thrust requirement is reduced slightly from the top of climb thrust, as is the case during an extended cruise period, the compressor performance remains adequate.

Also, it is desirable to have a working line as high as possible yet without infringing on the surge line. This permits the use of fewer stages and thus results in a lighter and shorter compressor. However, operating too close to the surge line may result in operability issues and also causes elevated vibration levels within the compressor. Such a situation was experienced on the TF30 which was installed on F111 and F14A [2]. This engine was renowned for its surging tendencies and in fact resulted in some crashes because of this issue.

To avoid a similar situation, a surge margin is usually specified. The surge margin is an measure of the separation between the surge line and the working line [17].

$$Surge\ margin = \left(\frac{PR_{surge} - PR_{working}}{PR_{working}}\right)_{fixed\ mass\ flow} \qquad \textit{(equation 3.16)}$$

The specified surge margin depends on the aircraft type and mission requirement but usually guarantees an allowance for the following,

1. build tolerance and in service deterioration,
2. inlet distortion due to crosswinds or abnormal attitudes,
3. working line shift during transients.

A military fighter may experience severe inlet distortions at high speed because of armament firing or high angle of attack requirements; however, this is not the case for a civil aircraft. Hence, the latter usually specify a smaller surge margin near the design point. A typical value is around 15% [17]. On the contrary, the part speed surge margin may be higher for a civil aircraft than for a military fighter. This is mainly because the former is designed for a longer service life. During the life of the compressor, the surge line tends to lower because of blade tip clearance increase due to casing/rotor rubs. Such rubs occur during transients owing to the differential thermal growth of the different components [19]. Also, to complicate things further, the working line also tends to rise during in-service deterioration.

To protect against compressor instability at part speed it is usual to specify 20-25% surge margin for HPCs and 15-20% for LPCs or booster stages [7]. The higher margin for HPCs is because these are influenced from instabilities arising from the upstream LPCs. The latter however are exposed to a much less turbulent air.

If, for any reason, the working line intersects the surge line at any operating point above idle, remedial action is necessary. Such action may dictate the use of variable stators, bleed valves or re-matching stages.

Variable stators were pioneered by GE in the early 1950s when designing the J79 [8]. They are used in the front end of multistage compressors to off-load the front stages. It was mentioned in a previous section that the front stages are forced to operate at higher loadings at part speed. This tends to stall these stages and thus variable geometry may be used to alleviate such a scenario. When closed, the variable stators, re-match the compressor stages to perform better at lower speed, however, by doing so, they drastically limit the choking mass flow. Hence, they are designed to open as the compressor accelerates to higher speeds. Variable stators are thought to be necessary when the pressure ratio from a single spool exceeds a value of around 7 [5].

Bleed valves are used to dump compressed air overboard. This is intuitively wasteful as the compressed air has had work done upon it. However, bleed valves are a lower cost and a more reliable option when compared to variable stators. Bleed air can, depending on the point of application, lower the working line or even modify the surge line [7].

As much as 5 to 25% of the core air may be bled off whilst starting [7]. Consequently, the sfc is worsened somewhat and the TIT rises significantly as less air is available for cooling. Bleed valves are seldom used as a sole means of controlling the off design performance of the compressor and are mostly used in conjunction with variable geometry to optimise the benefits of both.

Moreover, if a more thorough solution is needed to improve the off-design performance of the compressor, the required pressure ratio may be split into two or more spools. Another approach is to re-match the compressor stages to perform better at low speeds. The former approach necessitates a drastic redesign of the engine and is seldom used to rectify a performance problem once the compressor is built. It is more common to specify the number of spools during the preliminary design of a compressor. Different companies have different philosophies on this matter. Rolls Royce favours the use of three spools and minimal variable geometry, whereas General Electric and Pratt and Whitney tend to be more biased towards perfecting the use of variable stators and bleed control. It must be emphasised that no single approach is significantly better than the other; each has its own strengths and weaknesses.

Stage re-matching is often used as a last ditch approach towards improving the low speed performance of the compressor. This is a technique whereby the initial stages are permanently off-loaded by re-staggering the blades. This technique however, suffers from the significant drawback that, the front stages which normally contribute most towards the design pressure ratio are not utilised at their optimum potential.

Off design prediction has nowadays been perfected to such a degree that compressor instability is rare even during the engine development phase. This is because the compressor geometry can be approximated to other designs, from an extensive in-house database, to predict the performance at off-design operation before the compressor is ever constructed.

3.4.7 Compressor dimensional analysis

The compressor characteristic described in the previous section is valid for a unique combination of environmental and fluid conditions. Hence, by using the above approach a slightly different characteristic needs to be plotted for the entire engine operational envelope.

In practice, the technique of dimensional analysis is used to simplify matters somewhat. From experience and testing, it is known that the main variables effecting compressor performance are the following,

1. inlet temperature and pressure,
2. fluid density and gas composition,
3. fluid Reynolds number,
4. compressor size and efficiency,
5. mass flow,
6. pressure ratio.

Using the principle of dimensional analysis as described in [19], this list of variables is reduced to just five, more manageable quantities. It is worth noting that the fluid density is substituted by the gas constant R. The use of this quantity together with the temperature and pressure makes the density value superfluous. Also, for civil aero engines, the working fluid is air hence the gas composition property may be neglected. This technique generates the following relationship.

$$Compessor\ performance = f\left\{\frac{P_{02}}{P_{01}}, \frac{T_{02}}{T_{01}}, \frac{m\sqrt{(RT_{01})}}{D^2 P_{01}}, \frac{ND}{\sqrt{(RT_{01})}}, Re\right\} \qquad \textit{(equation 3.17)}$$

Furthermore, the efficiency term, η, is often used to relate the temperature ratio, to the pressure ratio, $\frac{P_{o1}}{P_{o2}} = \left(\frac{T_{o1}}{T_{o2}}\right)^{\gamma\eta/\gamma-1}$ as it is thought to be a more tangible quantity.

It may now be appreciated how a compressor characteristic similar to that shown in Figure 3.10, but utilising the above mentioned quantities, is much more meaningful and may be used throughout the entire flight envelope. The only variable missing in the aforementioned diagram is the Reynolds number. This is actually thought to be a third dimension to this chart.

The Reynolds number is known however, to have only a second order affect on compressor performance. It has a significant influence only when considering engine relighting at high altitude due to the low inlet pressure. To include this quantity, the above characteristic may be corrected for Re effects with the use of correction factors. However, the influence of Re on compressor performance is neglected throughout this dissertation.

3.5 Blade nomencluture

This section outlines the terminology which will be used throughout this report to describe the flow structure and its relation to the blade profile. Figure 3.11 lists all the relevant nomenclature. Note that this diagram depicts a stationary blade row. For rotor rows, the velocities and angles are adjusted to be relative to the rotor velocity.

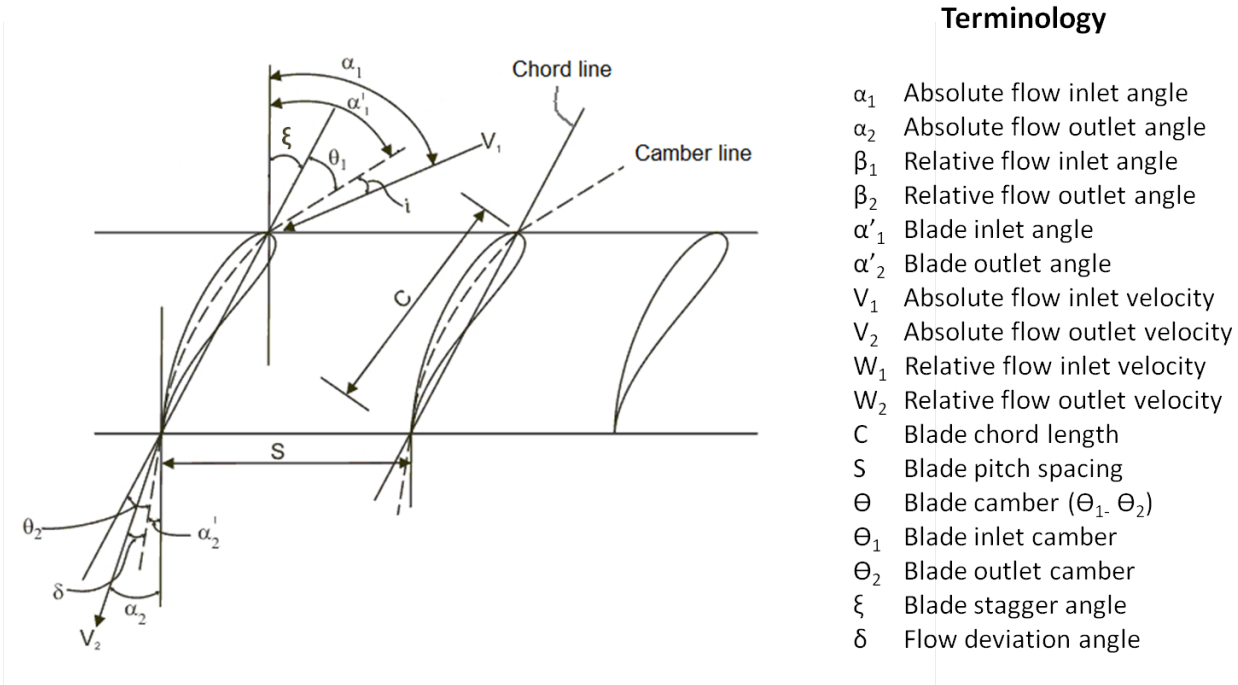

Terminology

α_1	Absolute flow inlet angle
α_2	Absolute flow outlet angle
β_1	Relative flow inlet angle
β_2	Relative flow outlet angle
α'_1	Blade inlet angle
α'_2	Blade outlet angle
V_1	Absolute flow inlet velocity
V_2	Absolute flow outlet velocity
W_1	Relative flow inlet velocity
W_2	Relative flow outlet velocity
C	Blade chord length
S	Blade pitch spacing
Θ	Blade camber (Θ_1- Θ_2)
Θ_1	Blade inlet camber
Θ_2	Blade outlet camber
ξ	Blade stagger angle
δ	Flow deviation angle

Figure 3.11: Blade nomenclature, modified from [19]

3.5.1 Incidence selection and theoretical optima

With reference to the above figure, the blade incidence is the angle between the blade camber line and the relative flow direction. This is similar to the angle of attack used in external aerodynamics however the latter is measured with reference to the chord line [36]. Due to this similitude and also because many of the early experiments were conducted using the angle of attack as reference, conversion factors are available for specified blade camber line shapes.

It might initially seem that the optimum incidence should be 0^o as this would imply that the blade LE is aligned with the flow. Even though this is not far from the theoretical optimum, different incidence design philosophies exist. Any one of these may be used to specify a design incidence during preliminary design.

Theoretically the optimum design incidence is that which yields the maximum loading for a given loss. This is the approach suggested by Carter [25]; however, even though this has a sound theoretical foundation, it is known that the incidences suggested by this method at low camber angles are erroneously large. Emery *et al* [44] suggest a method whereby the optimum incidence is chosen with the aim of achieving a smooth pressure distribution on the suction surface. This method is based on the valid assumption that the suction surface pressure distribution is the criterion which limits blade loading and loss. Nevertheless, the results from experiments or designs using this method are not well documented in public literature hence the author prefers the use of Lieblein's approach which is much better documented and reviewed.

Lieblein's describes a method whereby the design incidence is chosen to yield minimum loss. As discussed before, this is not the best ideology; however, it is known that Lieblein's method results in incidence magnitudes which are very close to Carter's theoretical optimum at moderate to large camber angles. Also, the results approximate very closely those of Emery *et al* throughout most camber angles in common use. Hence, this approach is expected to yield meaningful results for most blade designs and is thus the one used within this dissertation.

The minimum loss incidence is thought to be that which locates the flow stagnation point exactly on the blade LE. This is known to reduce velocity spikes in this region. Such velocity profiles contribute to the overall profile loss even though they appear to have minimal impact on the boundary layer health. Lieblein's incidence correlation is listed in Equation 3.18. Also, the accompanying formulae are suggested by Aungier [36] as empirical fits to the experimental results published in [32]. Note that some of the terms in the following equations will be explained in the following sections.

$$i^* = K_{sh} K_{t,i} (i_o{}^*)_{10} + n\theta \qquad \textit{(equation 3.18)}$$

$$K_{sh} = (1\ NACA65)\ or\ (1.1\ C4)\ or\ (0.7\ DCA) \qquad \textit{(equation 3.19)}$$

$$K_{t,i} = (10t_b/c)^{0.28/[0.1+(t_b/c)^{0.3}]} \qquad \textit{(equation 3.20)}$$

$$(i_o{}^*)_{10} = \frac{\beta_1{}^{0.914+\sigma^3/160}}{5+46\exp(-2.3\sigma)} - 0.1\sigma^3 exp\left[(\beta_1 - 70)/4\right] \qquad \textit{(equation 3.21)}$$

$$n = 0.025\sigma - 0.06 - \frac{(\beta_1/90)^{1+1.2\sigma}}{1.5+0.43\sigma} \qquad \textit{(equation 3.22)}$$

Lieblein formulated his theory from test results conducted in the early 1950s using NACA65 blades [44] at very low Mach numbers. Also, the blades used in these experiments had a circular arc camber line hence this approach is mostly valid when the blade's maximum camber is at or close to 50% chord. Furthermore, because the theory is based on tests conducted at negligibly small Mach numbers Lieblein's method should be used with caution when compressibility effects become relevant. Cumpsty [25], suggests that the use of this method should be restricted to a flow Mach number of 0.8 or less. Also, this approach does not consider incidence variation with Mach number even though it is known that blades having a sharp LE may exhibit some 4° variation in their minimum loss incidence between a speed range of M0.5 and M0.8 [25].

Finally, like all other design philosophies, the results from these experiments were obtained from cascade tests which are known to have a somewhat different flow structure to that of actual compressors. This difference is partly due to the way the experiments are conducted. As reported in the 1965 NASA report [32], the flow direction in cascade tests is altered by varying the blade stagger angle and keeping the absolute flow inlet direction constant. This is the opposite of what happens in actual compressors and results in a 1-2° difference in the minimum loss incidence for a given blade geometry. Also, the spanwise velocity profile in cascades is kept nearly constant whereas in compressors it degrades significantly in the rear stages of the compressor. This worsening of the velocity profile is due to the annulus boundary layers which are absent in cascade tests and cause the profile to peak significantly. In the aforementioned report it is suggested that the mid-passage incidence of the rear compressor stages should be increased slightly when using Lieblein's correlation.

Moreover, any cascade correlation only yields valid results for the mid-passage height in a compressor environment. Adjustments to Lieblein's incidence predictions are available to correct the design incidence for the blade ends. The corrections are reported in [32]; however, this level of precision is considered to be too detailed for preliminary design purposes hence is neglected within this report.

To overcome some of the deficiencies associated with this method, Aungier [36], developed further empirical correlations, based on the original Lieblein incidence equation. The formulae listed in this reference aim to adjust the original predictions for high speed flow and camber line shapes other than those listed in the original Emery *et al.* report [44]. In spite of this knowledge, this author chose not to correct for these effects but rather use the original incidence prediction correlations listed above. This is mainly because the latter correlations are not documented well enough to prove their validity or otherwise. Also, controlled diffusion blades typically have a blunt LE; hence, one might expect the minimum loss incidence not to vary much within the normal operating range. Such blades are assumed to have a K_{sh} of 1 within this thesis.

Finally, it must be noted that the incidence selection within actual compressors may not necessarily be as predicted by any one of the above theories [32]. This is because, as explained in the previous sections, any compressor will also have to operate at off-design; hence, consideration is also given to this matter. It is sometimes suggested that the incidences of the initial stages may be increased slightly and conversely those of the rear stages reduced from the predicted optima. This is to anticipate for the fact that the first stages are pushed towards stall and the rear towards choke when operating at part speed. This approach sacrifices design point efficiency for off-design control simplicity since fewer variable stages or bleed may then be needed to operate satisfactory at off-design.

3.5.2 Blade stagger and camber

The blade stagger angle, ξ, is fixed to obtain the required incidence. It is worth noting that specifying a relatively large ξ may lead to insufficient choke mass flow due to small throat openings [36]. The throat opening is the shortest staggered spacing between adjacent blades.

Also, a small throat opening implies that the flow will reach sonic conditions within the blade passage at a relatively low operating speed; hence, the passage shock will bear a greater influence on flow characteristics within the passage.

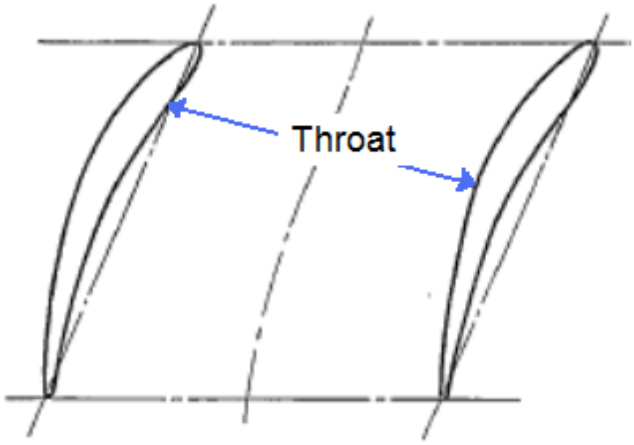

Figure 3.12: The throat opening, obtained from [45]

Conversely, highly staggered blades tend to have a relatively high pressure rise at stall [46]. This implies that the surge point will be at a relatively low mass flow compared to lower staggered blades. However, high stagger cascade test results tend to show that the maximum efficiency of such configurations occurs at a much higher flow than the stalling pressure rise [47]. This is a useful attribute for industrial machines since such designs can be optimised for maximum efficiency yet have a naturally large surge margin. On the other hand, designing towards maximum efficiency implies low stage work and hence a long and heavy compressor. This is undesirable for aero applications where weight considerations predominate.

The camber angle, Θ, is designed to achieve the required fluid deflection. The camber is chosen with consideration to the blade incidence and predicted deviation. The latter will be discussed in Section 3.5.4.

$$Fluid\ deflection = camber + incidence - deviation \quad \textit{(equation 3.23)}$$

The camber angle is a measure of the blade loading and is sometimes related to the lift coefficient which is conventionally used in aerofoil theory. The camber of subsonic blades may be quite substantial to achieve the desired stage work input. Supersonic blades have

negligible camber because of the higher relative flow velocities. Calvert et al. [31] remark that ideally, for such blades, the point of maximum camber, a, should be located just after the shock structure where the boundary layer is thinnest. However, if the shock were to cause the boundary layer to separate, a large camber angle within this region will impede the flow from re-attaching resulting in large areas of separated flow. Furthermore, moving 'a' rearwards shifts also the blade loading. This increases the flow deviation since the reduced blade force towards the trailing edge is unable to turn the flow effectively [25].

Carter [45], conceives that the two most important variables controlling the aerodynamic performance of subsonic blades are the position of maximum camber, a, and thickness. With regards to the former, the author notes that decreasing 'a' is expected to yield the following performance characteristics.

1. Suction peak velocity increased and hence the critical Mach number, when the flow first reaches sonic velocity within the blade passage, is lowered,
2. the blades tend to be more inclined to exhibit sudden stall,
3. the throat opening is enlarged,
4. the low incidence performance is improved.

These performance attributes tend to dictate the design of the stages within the compressor. The initial blade rows which are subject to the highest Mach numbers are designed with a rearward position of 'a' to optimise high speed performance whereas, the rear stages normally have a more forward position of maximum camber. Forward cambered blades have good negative incidence performance which is ideally suited to the rear stages.

Finally, to specify the location of the point of maximum camber along the blade chord, the designer usually chooses parabolic arc camberline. This was the primary reason why such camber line shapes were conceived; however, circular arc camber lines are generally known to have better surge margin and overall performance and hence their use is assumed in this dissertation. This assumption implies that 'a' is at 50% chord for all blade types mentioned throughout this thesis.

3.5.3 Blade thickness and profile shapes

Similar to blade camber, the blade thickness, t_b, and the location along the chord at which this maximum occurs has a great influence on the flow profile within the blade passage.

Data published in 1960 [45], shows that a small thickness is generally desirable for aerodynamic reasons; however, mechanical considerations dictate a minimum level below which the blade strength would be unacceptably weak and prone to vibration. Also, thicker, blunt leading edges are much more resistant to erosion and are sometimes employed in the LPCs, such as the case of the RB211-535C [20], to better resist foreign object damage. Furthermore, even though most compressor blades nowadays have a maximum thickness of around 5% chord (t_b/c), a significant portion of published literature quote test results conducted using blades of 10% t_b/c, hence correction factors are generally necessary [25]. This dissertation assumes the use of 0.05 t_b/c unless stated otherwise.

The position of the maximum thickness has a significant influence on the performance of the blade row. Carter [45], notes that forward locations of blade maximum thickness result in the same performance attributes as those listed for forward cambered blades above. Figure 3.13 shows how forward locations of blade maximum camber or thickness tend to amplify the suction surface velocity. Such blades can support lower loadings as the flow is more prone to separation due to the significant adverse pressure gradient after the velocity peak [48].

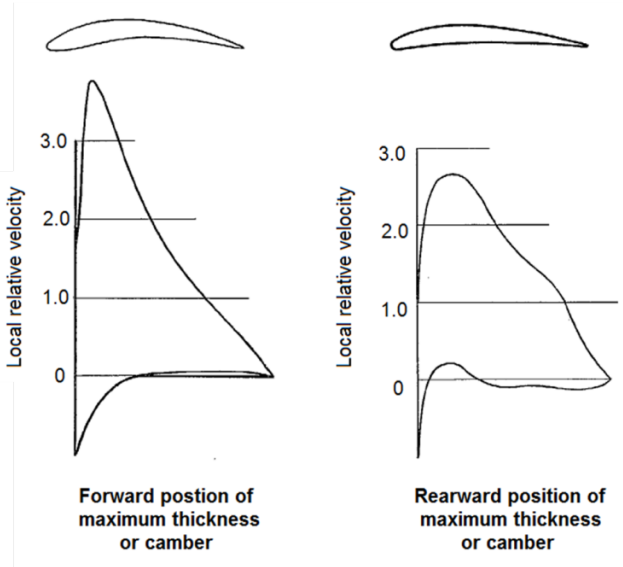

Figure 3.13: Blade thickness and camber, modified from [45]

Traditionally, standard blade profile types have been used to outline the thickness distribution along the blade length. The thickness at local chord lengths is determined once the maximum thickness, t_b, and camber line shape are specified.

Most American literature on compressor cascades assume the use of a NACA65 blade profile. This profile has t_b at 40% chord and was derived from aircraft wing aerofoils in the late 1940s [36]. The original aerofoil was modified slightly to make it more suitable for compressors. Amongst these modifications was the introduction a slightly thicker trailing edge to make the blades easier to manufacture. This profile is one of a few which also specifies a camber line shape; however, it is common practice to place this thickness distribution on a circular arc camber line. The latter approximates very closely to the original NACA65 camber line. This profile was used extensively by GE up to the late 1950s but was eventually superseded by the DCA which has superior high speed performance [11].

The C-series blade profiles, most notable of which the C4, were in widespread use by the British compressor industry. The C4 is similar to the NACA65 however the location of t_b is slightly more forward at 30% chord. Moreover, the LE of the C4 is more blunt thus has good erosion resistance but lacks respectable high speed performance [36].

Both blade types were eventually replaced by profiles such as the DCA which have superior high speed performance. In the 1950s, GE switched from using NACA65 to DCA at around M0.8; however, this changeover point was eventually brought down to even lower speeds as the Stamford engineers realised that the performance of this blade was equal to or better than the NACA within most operating regimes [6]. This profile has a t_b at 50% chord which partly explains the good high speed performance of this blade [25]. In the early 1970s Gostelow [49] reported that the use of this profile was, by then, considered a conservative design choice as most newer compressors opted towards the use of controlled diffusion blades.

Unlike the other blade profiles, controlled diffusion blades are not a specification of any particular blade thickness distribution, but rather, describe a design philosophy whereby the profile is specifically tailored for the required blade loading. Controlled diffusion blades usually have a significant region of laminar flow on the suction surface leading edge which promotes low blade profile loss. Nevertheless, the primary quality of such blades, is that they are designed to evade flow separation near the trailing edge thus can tolerate much higher

loadings [25]. Furthermore, because of these attributes, such blades normally exhibit a wider operating range than conventional designs. The profile loss can also be expected to be overestimated by around 20% when using the conventional loss correlations. Gallimore [33], states that if a nominal compressor were re-bladed from conventional to controlled diffusion blades, the efficiency would be expected to improve by around 1%. The use of controlled diffusion blades is assumed within this dissertation. However, because of the scarce data available on this subject within the public domain, the use of conventional correlations is often used and then modified accordingly. Figure 3.14 identifies some of the more typical design intents of controlled diffusion blades.

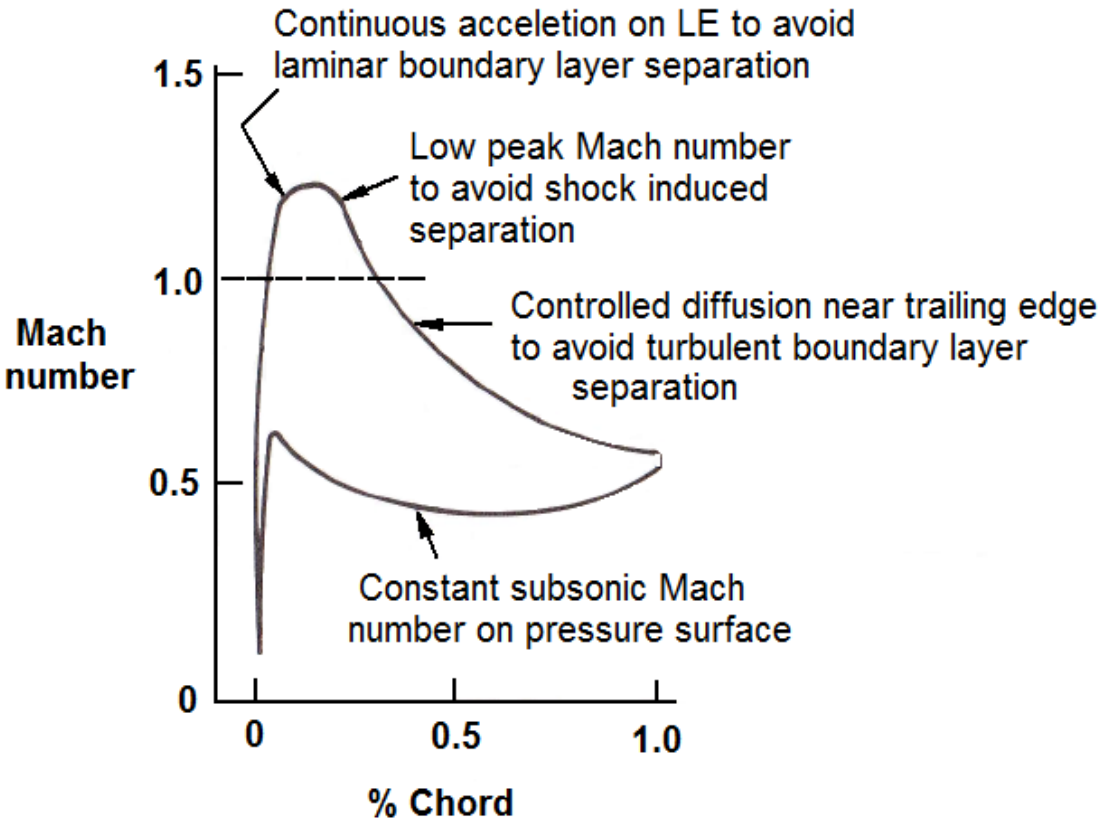

Figure 3.14: Schematic representation of Mach number distribution for controlled diffusion blades, modified from [25]

3.5.4 Flow deviation

As described in Section 3.5.1, there is a tendency for the turbulent boundary layer to separate as it approaches the blade trailing edge causing what is known as deviation, δ. The separated region varies for different loadings and blade profiles. It is known that, for a given loading controlled diffusion blades have a much lower deviation when compared to other conventional profiles such as the DCA. However, many of the empirical deviation correlations where intended for use with the standard profiles hence, an empirical adjustment is usually necessary to obtain a more representative deviation magnitude for today's blades.

Carter's deviation equation was obtained using C4 test results and was in widespread use up to the early 1960s. GE used this correlation up to around 1950 but also added an empirical adjustment, of around 2°, to better conform to their experimental data [6], [11].

$$\delta = \theta\sqrt{\sigma}\left[0.23\left(\frac{2a}{c}\right)^2 + 0.1\left(\frac{\beta_2}{50}\right)\right] \qquad \textit{(equation 3.24)}$$

It is worth mentioning that, as was stated in a previous section, increasing 'a' is expected to yield additional deviation which is detrimental to the flow turning ability of the blade. Boyce [12], modified this correlation to take into account the affects of blade profile, stagger and compressibility effects, allowing this model to be applicable to a wider range of designs; however, there is very limited data on the validity of this approach hence it is not used within this report.

Similar to Carter's correlation listed above, Lieblein formulated his own prediction model. Lieblein used the same NACA65 test results used for his incidence correlation but also included a profile adjustment coefficient similar to Boyce's approach. Equation 3.25 lists the original Lieblein's correlation accompanied by some empirical equations outlined by Aungier [36] to approximate the experimental data.

$$\delta = K_{sh}K_{t,\delta}(\delta_o{}^*)_{10} + m\theta \qquad \textit{(equation 3.25)}$$

$$K_{t,\delta} = 6.25\left(\frac{t_b}{c}\right) + 37.5\left(\frac{t_b}{c}\right)^2 \qquad \textit{(equation 3.26)}$$

$$(\delta_o{}^*)_{10} = 0.01\sigma\beta_1 + [0.74\sigma^{1.9} + 3\sigma]\left(\frac{\beta_1}{90}\right)^{(1.67+1.09\sigma)} \quad \textit{(equation 3.27)}$$

$$m = \left.0.249 + 0.074\left(\frac{\beta_1}{100}\right) - 0.132\left(\frac{\beta_1}{100}\right)^2 + 0.316\left(\frac{\beta_1}{100}\right)^3 \right/ \sigma^{\left[0.9625 - 0.17\left(\frac{\beta_1}{100}\right) - 0.85\left(\frac{\beta_1}{100}\right)^3\right]} \quad \textit{(equation 3.28)}$$

Note that Lieblein's equation is strictly only valid for circular arc camber lines since these are the type used in Emery's *et al.* report [44] from which Lieblein obtained his data. Also, even though Lieblein originally intended his deviation model to be used solely at his design incidence, it may be used throughout a large incidence range because it is known that deviation is only a weak function of incidence up to stall [25].

Finally, all of the above listed deviation correlations were obtained from cascade test results. Similar to the incidence case, the 1965 NASA report [32] outlines some correction factors which may be applied to make the predictions more applicable to compressor flow. Also, all the deviation equations listed above assume that the Re is sufficiently high, to avoid premature boundary layer separation, and that all the blades are only `moderately loaded. Increasing the blade loading will cause further deviation but this is not accounted for in any of the above models.

The work within this dissertation assumes the use of Lieblein's deviation model but also includes an adjustment of 2^o to account for the lower deviation expected from modern controlled diffusion blades.

3.6 Blade loading

A limit on axial compressor blade loading was sought from the earliest days of compressor design. As the blade loading is increased, the flow separation on the suction surface increases. This not only sets a limit on the maximum permissible flow deflection and hence pressure recovery, but also raises the mixing losses downstream of the blade trailing edge.

Initially loading coefficients were obtained from aircraft airfoil theory as most designers were already familiar with this field. Hence one of the earliest loading coefficients in mainstream use was the lift coefficient which is the lift force per unit blade area divided by inlet or vector-mean dynamic head. The use of this coefficient for estimating the blade loading was however for the most part unsuccessful, mostly because the complex, highly turbulent and dynamic flow within compressors is not representative of that experienced by an aircraft wing. Consequently, other loading coefficients were tested, such as, lift coefficient multiplied by solidity, ratio of change in tangential velocity to axial velocity, ratio of axial velocity to tip speed and so forth [11]. One notable effort was that by Howell. Howell developed a loading parameter consistent with a separation criterion used in boundary layer theory at the time [50]. This parameter involves the product of mean velocity lift coefficient as a function of the overall velocity ratio. Even though this parameter had a sound theoretical foundation, no extensive experimental investigations were carried out to further his theory, and as such his loading parameter remained for the most part unused.

A loading criterion which found more widespread use was the de Haller number. This originated from diffuser analogy and assumes that the pressure recovery, within a compressor blade row, cannot exceed more than 50% of the inlet dynamic head. This effectively sets a limit on the velocity ratio within the blade passage. This limit is illustrated in Equation 3.29.

$$\frac{W_2}{W_1} \geq 0.7 \qquad \textit{(equation 3.29)}$$

The primary asset of this parameter is its simplicity and thus suitability for preliminary design. However, because of its simplicity it disregards any blade characteristic and hence may not be representative of modern, highly loaded compressor environments. Nevertheless, it is known that, in spite of this deficiency, the de Haller number is a better predictor of end-wall stall than the more complex Diffusion Factor described below [25]. Because of this quality, Aungier [36], further developed this correlation to include the affects of blade geometry assuming a circular arc camber line. Aungier's empirical correlation is illustrated below. Also, this has been found to be a good predictor of surge at speeds close to the design point. However, at very low speeds it is thought to be too pessimistic and is thus considered unreliable.

$$\frac{W_2}{W_1} \geq \frac{\left(0.15+11^{t_b}/_c\right)/\left(0.25+10^{t_b}/_c\right)}{1+0.4\left[\theta\sigma/_{\{2\sin(\theta/2)\cos\xi\}}\right]^{0.65}} \qquad \textit{(equation 3.30)}$$

A more elaborate loading criterion called the Diffusion Factor (DF) was developed by Lieblein [51] in the early 1950s. The DF is a measure of the velocity gradient on the blade suction surface [19]. Large velocity gradients cause thick boundary layers which tend to separate causing undue deviation and loss. The DF started being used by the industry at about the same time as it was published. Smith [11], reports how GE first utilised this loading parameter in the late 1950s when developing the J85.

$$DF = \left[1 - \frac{W_2}{W_1}\right] + \frac{\Delta W_\theta}{2\sigma W_1} \qquad \textit{(equation 3.31)}$$

The above correlation demonstrates how the stage work may be increased, by increasing the blade speed U, without impacting the flow diffusion and hence the DF [25]. Also, for a given DF, higher solidities σ, can tolerate larger diffusions. This trend is evident in modern compressors which have much higher solidities compared to the earlier generation.

In spite of its qualities, the DF suffers from several limitations. Also, considering the importance of this correlation and the fact that it is used extensively in this report, Appendix A2 provides a more thorough understanding of the assumptions used in deriving it. Only some minor aspects listed in the appendix will be discussed here.

One of the main drawbacks of using the DF is that it does not account for different blade thickness and profile types. Some profiles such as the C4, suffer from much higher suction surface loadings, for a given DF, compared to other profiles such as DCA or NACA65. Also, as explained in Section 3.5.3, the thicker the blade profile, the more the suction peak is increased, and thus the greater the loading. Nevertheless, the DF neglects this fact and assumes that the blading has a t_b/c of 0.1. These limitations do not necessarily limit the use of this criterion; however, they illustrate how the allowable DF has steadily increased over the years from around 0.4 in the 1980s to something like 0.5 today [22]. This was mainly achievable because of thinner, better profiled blades which can tolerate much higher suction surface loadings.

Furthermore, even though the DF is considered to be a better criterion for blade stall than the de Haller number, it still does not account for three-dimensional flow features such as corner stalls and hence its use is much less predictable near blade ends where the flow is much more three dimensional [41].

The DF was eventually even correlated against cascade loss. The test results have been summarised as limiting values of DF which are outlined in Table A.2 of Appendix A2. Values in excess of those listed are an indicator of blade stall and hence are treated as maxima within this dissertation.

The de Haller number and the DF are both used within this dissertation. The latter is used to quantify the blade suction surface loading and hence boundary layer health, whereas the former is used as a predictor of the proximity of the operating point to the point of instability or surge.

3.6.1 Vortex flow

It is important to consider the blade loading not only at the pitchline radius but also near blade ends. This is because; these regions are highly loaded and hence prone to instability. Vortex theory is a method whereby the flow at other than the mid-passage may be predicted to allow an evaluation of the flow characteristics near blade ends.

Rotors impart swirl to the flow so that it may further diffuse in the stators. The presence of swirl in the flow creates an increasing static pressure field across the annulus. This balances the centrifugal effect of the swirling flow hence effectively stabilising the system. This swirling flow is known to be in radial equilibrium. Note that when the flow has no swirl, i.e. at entry or exit from the compressor the concept or radial equilibrium does not apply.

A thorough treatment of radial equilibrium is beyond the scope of this section; however, it is worth pointing out that different blade design types have been devised, which to some extent or other, respect the concept of radial equilibrium. These allow the blade shape to be optimised at different radial locations along the span so that it may better suit the local flow conditions and hence work more effectively.

Small industrial compressors may, on occasion, disregard vortex flow and opt for untwisted blades to lower costs. Even though vortex blades are thought to have a small efficiency advantage over untwisted blades, they are used exclusively in aero engine compressors because such designs produce a much better surge margin and axial velocity distribution compared to the simpler untwisted configurations [52]. The latter consideration implies that the rear compressor stages effectively have a better work-done factor and hence, pressure rise per stage compared to untwisted designs.

Furthermore, it must be emphasised that, even if the full radial equilibrium equation is satisfied by the blade design, the calculated air angles in the rear stages of the compressor will still not be as predicted. This is because, as explained in a previous section, annulus blockage causes a higher peak axial velocity at mid-heights, which is not accounted for by the radial equilibrium equation. This will result in a performance loss for these stages since, unless analysed by some more complex means, such as CFD, the blade and flow angles will not coincide.

This thesis assumes the use of constant reaction blades. The reaction, Λ, is a measure of how much of the stage static pressure rise is contributed to by the rotor row. Most designs opt for 50% reaction in preliminary design at the pitchline radius. This is a logical decision because it uniformly distributes the flow diffusion between the rotor and stator [36].

$$\Lambda = \frac{\text{static pessure rise across rotor}}{\text{static pressure rise in stage}} \qquad \textit{(equation 3.32)}$$

This design philosophy assumes that the axial velocity, work input and reaction are constant along the blade span [36]. However, these conditions cannot all be satisfied by the radial equilibrium equation hence the actual flow will not be exactly as predicted. This effectively implies that, even though this design strives to attain nearly constant reaction throughout the blade height, the latter varies considerably in actual compressors.

This is nevertheless not a major impediment for choosing this vortex type. Constant reaction blades have been used successfully in numerous compressor projects and are known to allow a higher work input per stage compared to some other designs [36]. This is a welcome quality for short-haul engines where the compressor weight and length may bear more relevance than efficiency compared to longer-haul engines where the importance of efficiency predominates.

3.7 Stage loading and design point efficiency

The stage loading, sometimes also referred to as the work or temperature coefficient is a measure of the rotor aerodynamic loading [36]. Philpot [17], describes the choice of compressor loading as one of the most crucial issues facing the designer. This is because it involves a complex compromise between efficiency, weight, surge margin and other mechanical considerations such as stress and vibration.

Choosing a high stage loading generally implies reduced compressor efficiency, however because of improved design analysis tools this trend has diminished somewhat over the last decade or so. Also, different applications dictate different loadings. Combat engines are designed with a considerably higher compressor loading compared to civil applications. This is because, even though cost and weight are important considerations for the latter, the importance of efficiency and fuel burn lead toward lower loadings. The stage loading parameter, ψ, is outlined by the following equation.

$$\psi = \frac{c_p \Delta T_{0s}}{U^2} = \frac{\Delta h}{U^2} \qquad \textit{(equation 3.33)}$$

Furthermore the stage loading and blade loading, which was discussed in Section 3.6, are also related. However, for a given DF or de Haller number, the stage loading may be increased by increasing the flow coefficient, φ. The φ is a measure of the volume flow rate within the compressor and determines the relative velocities relating to each blade row [25].

$$\varphi = \frac{V_a}{U} \qquad \textit{(equation 3.34)}$$

For a given stage loading, empirical results are available as graphical plots which may be used to predict the compressor efficiency during preliminary design [22]. One such plot is illustrated below.

Figure 3.15 was used rather extensively during this work. Its use has been both to quantify an initial efficiency guess for a given loading, and also to validate the calculation results once a more detailed efficiency value had been calculated.

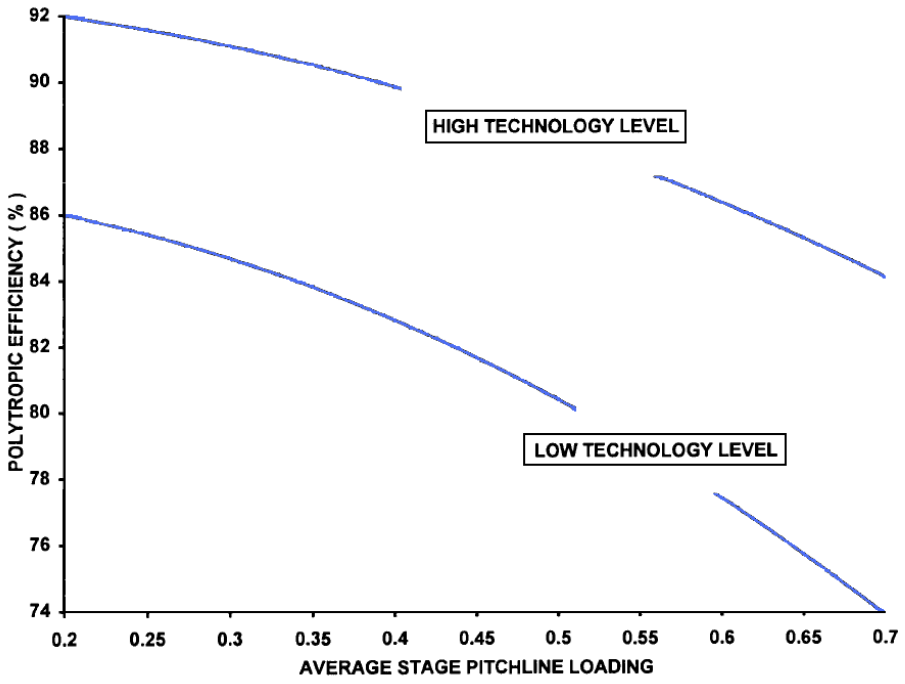

Figure 3.15: Compressor efficiency vs. stage loading, modified from [7]

Normal design practice for commercial aero engines is to use a stage loading of around 0.35 to 0.5 [7]; however, this may be allowed to vary throughout the compressor. Some designs specify a conservative loading for the front and rear stages and a rather higher value for the mid stages. This design philosophy stems from the fact that the middle stages operate closer to their design point throughout most of the operating range whilst the front stages are forced towards higher loadings at part speed. Also, the rear stages are sometimes offloaded to lower the exit Mach number thus improving the diffuser and combustor efficiency [36].

Previously it was stated that, for a given blade loading, it may be possible to increase the stage loading, ψ, by designing for a higher flow coefficient, φ. Howell [38], also suggested that a relatively high φ of around 0.9 is desirable for optimum efficiency. Thus, it may seem odd how modern compressors, such as the HPC of the IAE V2500 reported by Tubbs [26], tend to have a design value of φ nearer to 0.55. A higher mean value of φ also results in a smaller and lighter compressor which is very desirable for aero engines [33].

In spite of the above arguments, there are several incentives for keeping φ low. A smaller value of φ is beneficial because of the following [25].

1. Prevents high dynamic pressures at outlet which reduce the efficiency of the diffuser and combustor,
2. retards chocking to a higher mass flow,
3. improves stability and increase surge margin,
4. lowers the hysteresis when recovering from a stall or surge,
5. reduces the likeliness of the compressor exhibiting full span stall.

Note that, the stability term mentioned above is a measure of the ability of a compressor to smoothen out disturbances in the radial or circumferential plane.

Finally, since it is sometimes decided to allow a higher ψ in the middle stages, it may also be necessary to raise φ within the compressor from an inlet value of around 0.5 to a mid stage value nearer to 0.75 [7]. This is then slowly decreased again towards the rear of the compressor to achieve an exit value of between 0.5 and 0.6.

3.7.1 Efficiency terminology

Whenever the term efficiency has been referred to within this dissertation so far, it has been assumed that this is actually the polytropic efficiency, η_p, which is being quoted. The polytropic efficiency reflects the true aerodynamic quality of the design and is independent of PR [19].

In engineering practice however, it is more common to use the isentropic or adiabatic efficiency, η_{isen}. This is a measure of the overall efficiency of the machine and relates the outlet to the inlet parameters of the component. The main disadvantage of using this system in turbomachines is that the latter is dependent on the PR of the compressor.

$$\eta_{isen} = \frac{PR^{(\gamma-1)/\gamma}-1}{PR^{(\gamma-1)/\gamma\eta p}-1} \qquad \textit{(equation 3.35)}$$

For the same aerodynamic quality, or polytropic efficiency, a compressor with a lower overall PR will attain a greater isentropic efficiency hence this system is biased towards low PR compressors. For this reason alone, the latter efficiency is not used throughout this report unless explicitly mentioned so.

3.7.2 Loss generation and efficiency prediction

The aerodynamic loss within compressors is caused by several sources. In theory, loss generation can be described as an increase of entropy within the system. Entropy is the fundamental measure to quantify inefficiency because it evaluates the disorder of the system on a molecular level. Nevertheless, it is intrinsically difficult to calculate and to comprehend and is thus seldom used directly. It is more common to measure and classify the loss in accordance to the location of its source.

The aerodynamic loss model used within this dissertation is a modification of the Aungier's loss classification [43] and is described below.

1. **Blade profile loss**

   This accounts for loss incurred due to the blade's boundary layers. These layers cause friction on the solid surfaces but also tend to separate toward the trailing edge. As described above, the magnitude of the separation depends on the blade loading and fluid's characteristics [25], [36]. Also, this occurrence forms a wake at the trailing edge which then mixes out with the mainstream flow downstream of the trailing edge. Any mixing process is inherently inefficient because it tends to increase the overall entropy [35]. Furthermore, the wake is known to get bigger with an increase in blade trailing edge thickness; however, this tendency is not very pronounced for diffusing flows [22], [32].

2. **Annulus loss**

   Annulus loss is similar to blade profile loss however this includes any loss incurred directly from the presence of the annulus boundary layers.

3. **Leakage loss**

   This loss is primarily generated by the tip leakage vortex which causes mixing losses downstream of the blade row. However, even though this is the largest leakage flow, it must be appreciated that there are additional leakage paths, such as those present between the blade fixings and the disk, which are not considered within this work due to their minor contribution to overall aerodynamic loss.

4. **Secondary loss**

   This includes such losses due to mixing caused by corner stalls and other three-dimensional flow features which are not accounted for in the previous categories.

5. **Shock loss**

   This name is a bit misleading because this loss not only includes shock-induced losses but also the amplification of subsonic losses which is known to occur in transonic flow [53]. In this thesis it is assumed that the high speed losses only become significant once the peak suction surface Mach number exceeds the sonic value. This is thought to be a valid assumption considering that for controlled diffusion blades, the incidence, and hence losses [36], are not considered to change significantly with Mach number.

Once the blade geometry is specified, it is then necessary to calculate a more accurate efficiency prediction value than that used earlier in the design process for the initial specification of the blade profiles. The initial efficiency 'guess' may be obtained by a method similar to that discussed in Section 3.7. The technique used to calculate a more accurate efficiency potential within this report is based on the literature of Aungier [36] and is outlined below.

Aungier uses a modified empirical correlation, which presumably includes profile, annulus and secondary loss parameters into one term. This makes use of the Equivalent Diffusion Factor, D_{eq}, outlined in Section A.2, which is similar to the DF. D_{eq} however, may also be used at off-design incidences not just at the Lieblein's design incidence.

$$\overline{w}_{subsonic} = \frac{2\sigma}{cos\beta_2}\left(\frac{W_2}{W_1}\right)^2 \left\{K_1\left[K_2 + 3.1\left(D_{eq}-1\right)^2 + 0.4(D_{eq}-1)^8\right]\right\} \quad \textit{(equation 3.36)}$$

$\overline{w}_{subsonic}$ is an average subsonic loss coefficient outlined in Equation 3.37. Also, K_1 and K_2 are functions which should ideally be obtained from experimental results. However, for the purposes of this dissertation, they are defined below.

$$\overline{w} = \frac{\Delta P_o}{{}^1/_2 V_1{}^2} \quad \textit{(equation 3.37)}$$

$$K_1 = 0.0073 \quad \textit{(equation 3.38)}$$

$$K_2 = 1 + \left(\frac{s}{h}\right) cos\beta_2 \qquad \textit{(equation 3.39)}$$

Aungier, assumes that $\overline{w}_{subsonic}$ does not change significantly when the inlet Mach number is lower than the critical value, M_{crit}. M_{crit} is the inlet Mach value at which the flow on the suction surface first attains a sonic value, W_{sonic}. The magnitude of M_{crit} depends appreciably on the blade geometry; however, from data provided in [25] and [19], it is further supposed that this is 0.8 for controlled diffusion blades having a 0.05 t_b/c. When the inlet Mach number, M_1, exceeds M_{crit}, Aungier corrects $\overline{w}_{subsonic}$ as follows. It should be noted that, the use of the following equation should be restricted to cases where $M_1 \leq 1$ since the bow shock waves in front of the blade LE are not considered. Finally, for simplicity, this author assumes that $\frac{W_{sonic}}{W_1} \propto \frac{M_{sonic}}{M_1}$.

$$\overline{w}_{transonic} = \overline{w}_{subsonic}\left[1 + \left\{\left(\frac{M_1}{0.8} - 1\right)\left(\frac{1}{M_1}\right)\right\}^2\right] \qquad \textit{(equation 3.40)}$$

The leakage loss is treated separately within this dissertation. The model utilised is a modification of that originally developed by Lakshminarayana in 1970 [54]. With respect to the following equation, $\Delta\eta_{leakage}$ is the reduction in row efficiency due to tip clearance. Also, for the purposes of this work, each and every blade row is assumed to have a tip clearance δ_c of 1% blade height. This magnitude is thought to be quite representative of modern compressor designs.

$$\Delta\eta_{leakage} = \frac{1.4\,\Psi\delta_c}{hcos(\beta_1+\beta_2)}\left[8 + 10\sqrt{\frac{2\Phi\delta_c}{c\Psi cos\,(\beta_1+\beta_2)}}\right] \qquad \textit{(equation 3.41)}$$

Finally, Saravanamuttoo et al. [19] outline a procedure whereby the stage isentropic efficiency may be deduced once the loss coefficients have been finalised. Also, because of the relatively low stage pressure ratio, it may be assumed that the stage isentropic and polytropic efficiencies are equal in magnitude.

$$\eta_p = \Lambda\eta_{Brotor} + (1-\Lambda)\eta_{Bstator} \qquad \textit{(equation 3.42)}$$

$$\eta_B = 1 - \frac{\bar{w}}{\Delta P_{th}/_{1/2\rho V_1{}^2}} \qquad \textit{(equation 3.43)}$$

$$\frac{\Delta P_{th}}{1/2\rho V_1{}^2} = 1 - \frac{cos^2\beta_1}{cos^2\beta_2} \qquad \textit{(equation 3.44)}$$

3.8 A general turbine design overview

This section aims to give the reader a brief background on the turbine design requirements. The compressor component is the primary focus of this dissertation; however, because of the close coupling between this and the turbine, it is thought that a brief knowledge of turbine aerodynamics would be an asset in understanding some of the design choices made later on within this dissertation.

The turbine flow is quite similar to that existing within compressors. The main difference between the two is that the former has an accelerating rather than diffusing flow. This allows for higher loadings than is usually customary in compressors and is the key reason why the turbine section of a gas turbine has far fewer stages compared to the compressor.

Furthermore, similar to the compressor, a turbine stage consists of a stationary and a rotary blade row. However, in spite of this similarity, the stator, also called a nozzle guide vane (NGV), precedes the rotor and is used to accelerate and direct the flow onto the rotors which then extract energy to drive the compressor.

A main concern in turbine technology and which is, to a large extent, absent in compressor design, is the temperature capability of the components. As will be discussed in an earlier section, modern turbines must tolerate very high temperatures, sometimes even exceeding 2000^{o}K. Also, the reliability, maintainability and time between overhaul are also very demanding hence material technology plays a very fundamental role in this field.

Modern turbine blades are elaborate pieces of engineering often constructed from single crystal or directionally solidified nickel or cobalt based alloys. HPT blades almost always have complex internal cooling geometries which allow the blades to operate at temperatures far in excess of their blade metallurgical limits. The cooling air is tapped from a suitable location within the HPC and delivered to the blades via holes within the disks or casing. The effectiveness of the cooling system is such that the blade metal temperatures may be reduced by up to 300^{o} for each 2% core cooling air per blade row [19].

However, because much of this flow is not utilised to generate work within the turbine its magnitude is strictly controlled to limit the efficiency penalty associated with its use. Also, any cooling air ejected from the blade surfaces tends to disrupt the mainstream flow and thicken the blade boundary layers inducing separation [17].

Furthermore, in addition to the cooling air requirement mentioned above, the compressor is usually required to supply excess pressurised air for cabin environmental control, anti-icing and bleed supply for engine starting and hydraulic pressurisation. The airflow model used within this dissertation is outlined below.

Magnitude (% core flow)	Air system model
5% overboard	Extracted at 50% through HPC
12% turbine cooling flow	Extracted from HPC delivery 75% does work within the LPT turbine 25% yields no work output
0.5% disk cooling	Extracted at 50% through HPC 100% does work within LPT
1 % disk cooling	Extracted from HPC delivery 50% does work within the LPT turbine 50% yields no work output

Table 3.3: Secondary air system model; data obtained from [7] for the assumed TIT value specified in Chapter 4

3.8.1 Turbine loading and efficiency potential

Similar to the compression scenario, the turbine work requirement has to be split between a number of stages to limit the stage loading. The chosen loading value, which is analogous to that outlined in Section 3.7, directly specifies the turbine efficiency potential for a given technology level.

The proper determination of the turbine efficiency in preliminary design is of most importance because a 1% shortfall in this value may well affect the engine's overall sfc by a similar amount [7]. A well known efficiency prediction tool is the Smith chart. This is the turbine counterpart to the compressor correlation depicted in Figure 3.15 and shows contours of isentropic efficiency versus stage loading and flow coefficient. The Smith chart can be used to estimate an initial efficiency guess once the latter two are specified [55].

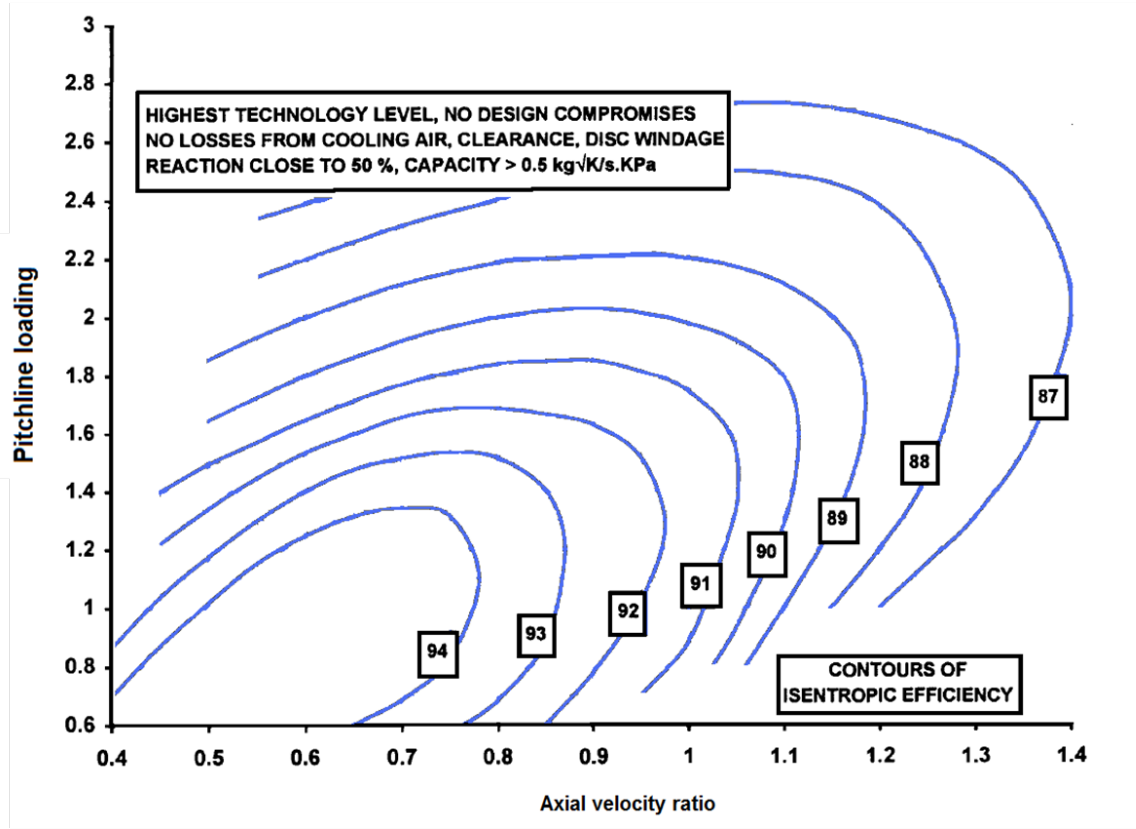

Figure 3.16: Smith chart, modified from [7]

Simplicity is considered the main asset of this design tool; however, it is also, in some respects its prime weakness. This is because, this chart embodies several assumptions which must be factored to obtain a realistic efficiency magnitude for a given turbine design. The following are some of the more important assumptions used in deriving this chart [56].

1. Reaction assumed to be close to 50%,
2. tip clearance is not considered,
3. variation of efficiency with aspect ratio not considered,
4. axial velocity is constant across the stage,
5. blades are uncooled,
6. Mach number changes do not affect performance.

Aungier [56], derived a correlation to correct the predicted efficiency for some of these limitations; however, it is thought, that this level of precision is beyond the scope of this work. To simplify matters, the actual turbine efficiency is assumed to be 95% [7] of the chart

value. This accounts for the differences between the actual turbine geometry and the generic design assumed in developing this chart.

Figure 3.16 identifies an optimum efficiency for any given level of flow coefficient, φ. The reasoning behind this trend is that for a low φ, the flow deviation within each blade row will be significant and hence the separation losses will also be high. On the contrary, a high φ results in significant profile losses due to the excessive Mach numbers relative to the blades. Hence, the φ in actual turbines is usually restricted to around 0.5-0.65 in HPTs and 0.9-1.0 in LPTs [5]. The lower than optimum φ in HPTs is chosen to allow for larger blade heights and hence reduced secondary and leakage losses. Also, the relatively high φ in LPTs is mainly due to the fact that these often rotate at a slow speed because they are coupled directly to the fan shaft. This choice then allows a higher ψ and thus fewer stages for a given work output.

In addition to fewer stages and thus lower weight, a higher design value of φ yields lower blade stress and rim load for a given RPM. Also, the cooling flow requirement is reduced because the turbine blades will have less camber and thus a smaller wetted area [57]. The end result is usually the fact that the designer will specify a slightly higher φ than the indicated optimum [6]. This sacrifices design point efficiency for lower weight and cooling flow complexity.

Furthermore, even though a higher ψ yields fewer stages and lower weight, the design value is usually restricted to 1.5-2.0 for HPTs and 2.0-2.5 for LPTs [7]. The higher LPT loading is because these stages have a higher aspect ratio, less cooling flow and a lower percentage tip clearance compared to HPT blades and are thus aerodynamically more efficient. Also, should any turbine blade be overloaded, the turbulent region near the trailing edge would cause excessive heat transfer and hence blade metal temperatures. This consideration usually merits more importance in HPT design because of the predominantly high local temperatures.

3.9 Method of analysis and general assumptions

This section outlines some general solution techniques used in turbomachinery preliminary design. It was deemed necessary to present this literature towards the end of this chapter because some of the theory involved presupposes a general level of knowledge of the material discussed within the previous sections.

The component's preliminary design layout is usually set using pitchline analysis which solves the governing equations for inviscid flow at one radial position along each blade row. This may then be augmented by selective use of boundary layer and hub-to-shroud analysis. Pitchline analysis is a one-dimensional, aerodynamic flow technique which allows rapid assessment of the part's performance through the use of empirical flow equations. Most of the established blade row performance systems such as deviation and loading assessments were specifically catered for use in pitchline analysis. This approach has found widespread use since it is known that the overall performance of a component may be well approximated by a mean-line analysis, especially near the intended design point [56].

Boundary layer analysis strives to correct the inviscid flow solution for the affects of friction by assuming that viscous effects are only significant near solid surfaces. Even though this is a gross simplification of the flow in the turbomachine, boundary layer analysis has been used successfully in numerous design projects because it offers considerable computational advantages over the full, three-dimensional, Navier-Strokes solutions and is thus highly suitable when comparing different designs during preliminary design. Boundary layer analysis finds more use in diffusing flows, as it is in such cases that boundary layer separation, on either the blade or endwall surfaces, can cause stall or even surge [36]. The benefit gained from boundary layer analysis is far more modest in the accelerating flow of turbines as this flow is much more tolerant to separation. In actual fact, various turbine components have been designed successfully without the use of boundary layer analysis [56].

Hub-to-shroud analysis also finds widespread use in preliminary design. A variant of hub-to-shroud analysis which is mostly used in preliminary design is called through-flow analysis. This method solves the flow equations in the hub to shroud plane at one or more intermediate stations between the blade rows. The through-flow technique is mostly used in preliminary design when the blade loading is suspect at radial locations along the blade height other than that previously examined in pitchline analysis. Also, when using this technique it is normal to assume that the stream surface curvature and the gradient of entropy along the blade height are both negligible. The resulting solution is then usually referred to as simple radial equilibrium [56]. The combined use of pitchline, boundary layer and through-flow analysis yields a quasi three-dimensional solution to the flow field.

Moreover, it is customary to assume that the flow behaves in an axisymmetric manner. This allows the flow governing equations to be solved at one tangential location along the component's length thus greatly simplifying the flow solution. This technique is universally used as the inaccuracies involved do not noticeably affect the relevance of the results.

Finally; in compressor preliminary design the flow is also considered to be adiabatic. This is a reasonable assumption considering the fact that the magnitude of work done on the flow by the compressor is a lot larger than the amount of heat transferred by the flow to or from its surroundings. However, this limitation is violated in turbines as the latter are usually cooled by compressor delivery air and hence there is considerably mixing.

The work within this dissertation uses an axisymmetric pitchline analysis as most of the empirical correlations presented so far are specifically catered for such use. Hub-to-shroud analysis is also used to augment the latter for a more in depth analysis and performance prediction. The prediction technique for compressor stall was outlined in Section 3.6 and was deemed especially useful for analysing the onset of compressor instability. As was discussed in a previous section, the end-wall region is often the cause of compressor stall or surge; therefore, a general treatment of the flow within this layer was indispensable when comparing the performance of different designs. Finally, because of the premise presented above, this work assumes an adiabatic flow within compressors and a mixed, cooled flow in turbines.

Chapter

4

Engine parameters

4.1

- Engine E2/101

4.1 Engine E2/101

This dissertation concerns a compressor study for an engine within the 20Klbf thrust category to power a short-haul aircraft similar to the ERJ-190. Henceforward this engine will be referred to by its designation E2/101. The author chose this label because, as far as he is aware of, no other engine in design or production bears this designation, hence the outcome of this study will not reflect upon any particular existing or proposed engine. Furthermore the prefix 'E' in this designation shall be replaced by 'C' or 'T' when the author is specifically referring to the compressor or turbine section of this engine respectively.

With reference the arguments discussed in Section 3.2, the main parameters of this engine are listed in Table 4.1 below. Furthermore, E2/101 is assumed to be unmixed, i.e. the cold and hot streams are discharged separately and not mixed to form coherent flow in a common propelling nozzle. The fan is also coupled directly to the turbine through the fan shaft, without any intermediate gearbox.

T_{ssl}	85000N/19.1Klbf
T_{cruise}	21000N/4.7Klbf
TIT	1650^{o}K
TIT_{cruise}	1530^{o}K
OPR	32.5
BPR	5
FPR_{bypass}	1.68
FPR_{core}	1.32
Compressor PR	24.6
Air mass flow through core	20kgs/s

Table 4.1: E2/101 main parameters

Notes

i. *As mentioned in Section 3.2.2, the engine design point is taken to be the initial cruise condition.*

ii. *All values listed in Table 4.1, except for T_{ssl} and TIT, are assumed to be at the cruise design point. This is because they vary as the engine is throttled away from the cruise setting [7].*

iii. *The FPR varies between the bypass and core streams because of the vastly different mean blade speed in each section.*

In addition to the data provided in Table 4.1, the following table lists the assumed parameters. These concern the engine components that are beyond the scope of this study but are nevertheless required to compute the resulting engine efficiency.

Fan polytropic efficiency η_{fan}	88%
Combustion efficiency η_{comb}	99.9%
Mechanical efficiency η_{mech}	99.5%
Intake pressure loss	0.5%
Bypass duct pressure loss	2.5%
Inter-compressor pressure loss	1.8%
Compressor exit diffuser pressure loss	2.0%
Combustor pressure loss	4.8%
Inter-turbine pressure loss	1.5%
Core propelling nozzle pressure loss	0.75%
Propelling nozzle Cd	0.97
Propelling nozzle Cx	0.99

Table 4.2: E2/101 assumed parameters

Notes

i. *All values listed in Table 4.2 are assumed to be at the cruise design point.*
ii. *Combustion efficiency is the ratio of fuel burnt to total fuel input.*
iii. *The fuel is assumed to be kerosene with an LCV of 43100KJ/kg [23].*
iv. *The mechanical efficiency is assumed to include bearing and windage losses.*
v. *The pressure losses quoted in Table 4.2 above are the percentage reduction in pressure in relation to the inlet total pressure of the component.*
vi. *The intake loss incorporates installation and engine duct losses.*
vii. *The combustor pressure loss is thought to include both the cold (friction) and hot (momentum change due temperature rise) losses.*
viii. *The propelling nozzle coefficient of discharge, Cd, compensates for nozzle blockage due to flow separation and boundary layer growth on the annulus walls. This is the ratio of nozzle effective area to actual geometric area.*
ix. *The propelling nozzle thrust coefficient, Cx, corrects for the lower momentum of the stalled and boundary layer flows within the nozzle. It is the ratio of actual thrust to predicted thrust.*

The requirements from E2/101 for the present study are the following.

Compressor polytropic efficiency η_{comp}	88%
Turbine polytropic efficiency η_{turb}	89%
sfc_{cruise}	$1.85x10^{-5}$ [kg/s]/N
sfc_{ssl}	$0.96\ x10^{-5}$ [kg/s]/N

Table 4.3: E2/101 required parameters

Furthermore, it is known that the aircraft's initial cruise altitude and speed are 11000m and M0.8 respectively. Additionally, the atmosphere is considered to conform to the International Standard Atmosphere (ISA) [58], which has the following characteristics.

Pressure Altitude (m)	Temperature (^oK)	Pressure (KPa)	Relative Humidity (%)
0	288.2	101.325	0
11000	216.7	22.628	0

Table 4.4: ISA conditions

Finally, the engine design is limited by the constraints listed in the following table due to the aircraft type and materials technology.

Fan diameter	1.9m
Engine length	2.3m
Fan tip Mach no.	1.4
LP & HP compressors rim speed	350m/s
LP compressor tip speed	500m/s
HP compressor rear tip speed	400m/s

Table 4.5: E2/101 constraints

Notes

ii. *The dimensional constraints are similar to the published dimensions of the CFM34-10E5[3] which powers the ERJ-190.*

iii. *The limiting compressor speeds are a result of material strength capability and were obtained from the guidelines published in [7]. The different compressor tip speeds are because the LPC can be made from titanium whereas the HPC needs to be made of nickel-based alloys due to the higher temperature.*

Chapter 5

Design analysis

5.1
- Design project overview

5.2
- Preliminary analysis
  - Turbomachinery design code, Turbodev
  - The fan stage
  - Preliminary analysis results and conclusions

5.3
- Detailed analysis
  - High reliability and long life
  - Compressor weight and length
  - Off design considerations
  - Operating range and performance retention
  - Low cost of ownership

5.4
- Finalised design
  - Stage by stage aerodynamic design
  - Design point exchange rates

5.1 Design project overview

The theoretical foundation necessary for understanding the compression optimisation task required for this work has been thoroughly discussed in previous chapters of this thesis. The compressor is intended for the E2/101 engine which is defined in the Chapter 4. Through a general design study, a preliminary compressor aerodynamic design and layout is suggested which, is believed, will be capable of delivering the required pressure ratio, or work input, for the requisite efficiency and performance level as stipulated in the previous chapter.

To evaluate and optimise the different compressor layouts a list of design FOMs was established in accordance with the principles discussed throughout the previous part of this thesis. This list is defined in Figure 5.1.

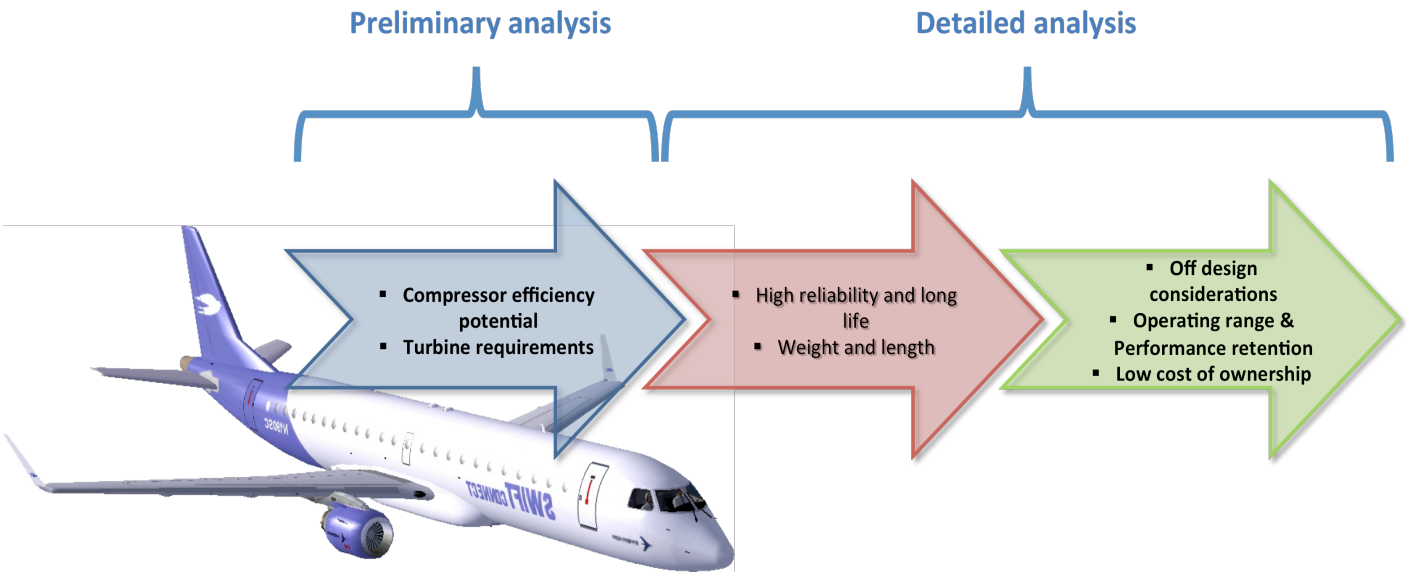

Figure 5.1: Compressor design figures of merit

The author thought it best to approach this design task by initially choosing the three most promising layouts, amongst all the alternative designs, in a preliminary assessment and then perform a more detailed performance analysis on these selected designs to finalise the preferred geometry. This approach was deemed to be more efficient and less time consuming than having to perform a detailed performance analysis on each and every candidate design

layout. Also, more time and effort could then be dedicated to the more promising designs and hence a better and more realistic solution might potentially have been achieved.

The preliminary analysis considered only the first two FOMs. The logic behind this approach is that if a candidate design failed to achieve the required efficiency at a satisfactory turbine loading it will, most definitely, be inadequate for the given application. Furthermore, it must be emphasised that engine reliability is almost always one of the more important requirements; however, for the intent of this work, it was thought more appropriate to incorporate it within the detailed analysis as more specific design parameters were needed to properly evaluate this criteria. The three most promising designs were then analysed in a more detailed and thorough assessment during the second part of the study.

The following section outlines all the alternative design layouts which were analysed in the preliminary evaluation. The results and conclusions from this assessment are then discussed in some detail in Section 5.2.3. The detailed analysis is described towards the second part of this chapter.

5.2 Preliminary analysis

A total of sixteen different compressor design layouts were thought to be, to some extent or other, adequate for the E2/101. The configurations assessed in this study are outlined in Table 5.1. Also, the accompanying efficiency, which is also listed, is a preliminary estimate obtained from an educated guess of compressor loading and a realistic mid-quality achievable performance, sourced from Figure 3.15.

Configuration name	Number of booster/HPC stages	Predicted efficiency of booster/HPC
C2/101_1	0/12	-/0.85
C2/101_2	1/12	0.88/0.88
C2/101_3	2/12	0.87/0.88
C2/101_4	3/12	0.89/0.9
C2/101_5	4/12	0.89/0.9

C2/101_6	5/11	0.89/0.9
C2/101_7	6/11	0.88/0.88
C2/101_8	7/11	0.89/0.86
C2/101_9	6/10	0.88/0.87
C2/101_10	5/10	0.87/0.87
C2/101_11	6/9	0.86/0.88
C2/101_12	5/9	0.89/0.88
C2/101_13	4/9	0.89/0.84
C2/101_14	4/10	0.89/0.88
C2/101_15	3/10	0.88/0.88
C2/101_16	3/9	0.88/0.87

Table 5.1: Compressor layouts

5.2.1 Turbomachinery design code, Turbodev

To aid this investigation, the author opted to develop a turbomachinery design code which allowed a quick analysis of a variety of key aerodynamic parameters of a given design. This code was programmed using Microsoft Excel and is named Turbodev.

This section aims to give the reader a general overview of how Turbodev tackles the turbomachinery design task and thus highlight some of the key strengths and limitations of this approach.

Turbodev is designed with several interlinked modules which, if properly utilised, may calculate detailed compressor geometrical and aerodynamic design properties coupled with some preliminary turbine analysis. It should be noted that the compression module is much more detailed and complex than the corresponding turbine counterpart. The latter's use within this work was restricted as a generic aid for the quick validation or otherwise of a given turbine design for the required compression geometry. This concept is further expanded in Section 5.2.3.2.

5.2.1.1 Turbodev compression module

Figure 5.2 below, depicts a generic overview of the compression module and the associated input requirements. This section outlines, in some detail, the computational techniques and user interaction required for the compressor design process.

1. **General data input**

   The aircraft operating altitude and cruise Mach number are specified by the user within the input module. This data is used to formulate the free air conditions used to define the fluid characteristics at the engine intake. Furthermore, the user may opt to specify compressor bleed flow requirements. The standard used for this thesis was to simulate bleed off-take within the HPC part only. This is considered normal engineering practice and implies that no air is extracted mid-way through the booster or LPC. Also, no bleed is extracted in the inter-compressor duct when operating at the design point. The HPC's bleed air requirements are listed in Table 3.3.

2. **Compressor characteristics**

   The input module also allows the user to specify the compressor annulus type and inlet casing diameter. The annulus shape can be defined as constant casing, hub or mean pitchline diameter. The preliminary assessment results, listed below, assume a constant hub diameter booster compressor and a constant-casing diameter HPC. Different aero gas turbines tend to have slightly varying design philosophies in this regard; however, this choice is quite common as it allows a smoother inter-compressor duct and somewhat lower HPC loadings.

   Furthermore, the primary compressor variables, which the user must also specify, include such things as the required compressor pressure ratio, number of stages and air mass flow. The user may also specify an upstream compressor pressure ratio, efficiency and inter-compressor pressure loss, if any. This data is used to calculate the air properties at the compressor front face. Also, this system is thought to cater for all known designs as different types of booster and fan stages can be simulated together with any form of inter-compressor duct. The present study assumes a generic inter-compressor duct loss magnitude of 1.8% [7].

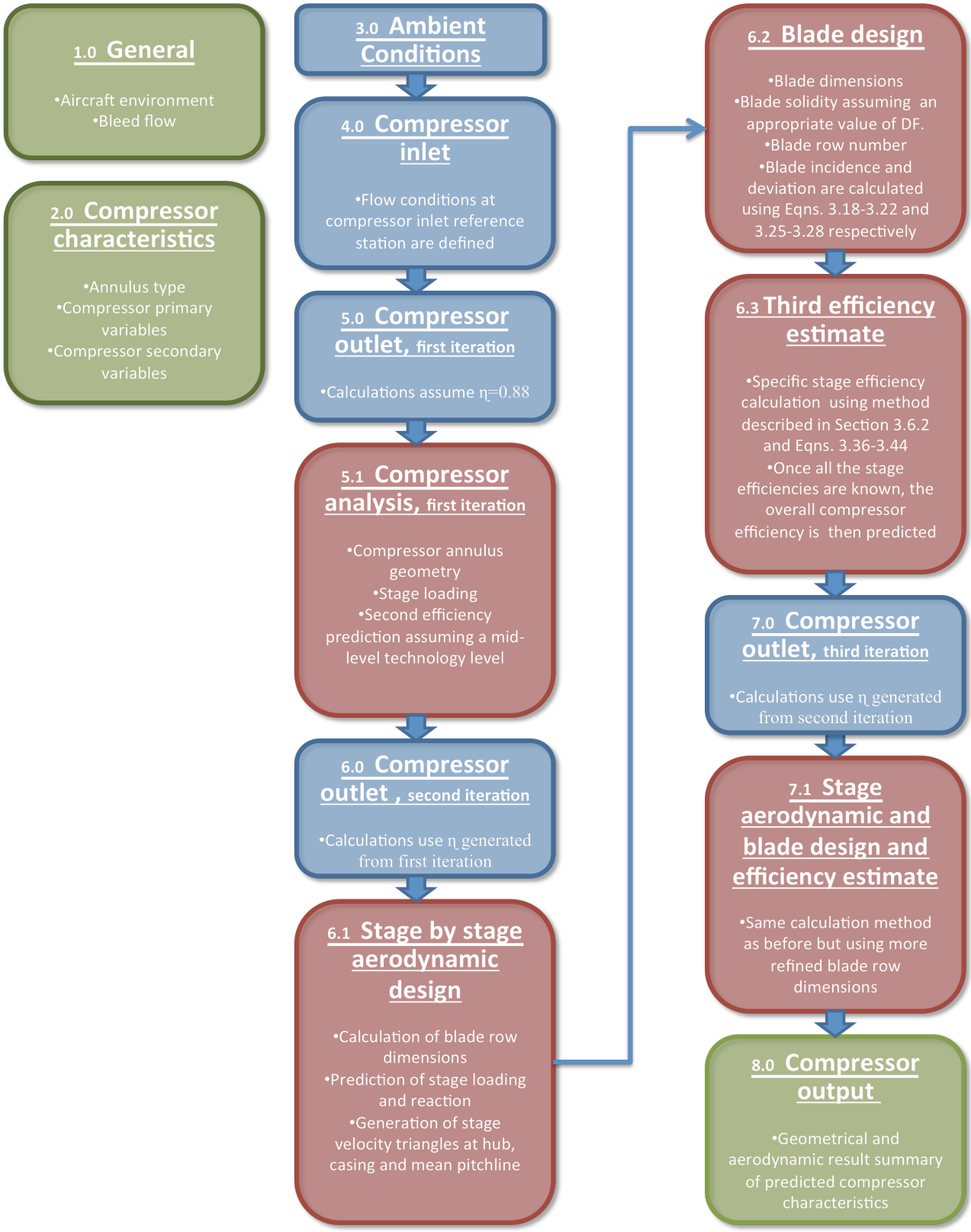

Figure 5.2: Turbodev compression module

Finally, the compressor secondary variables include a list of supplementary data which may be used to refine the compressor design. This section allows the user, amongst other things, to vary the stage loading along the compressor. This is a useful feature since some mid-stage loadings may be increased somewhat compared to the initial and final stages as discussed in Section 3.7.

3. Ambient conditions

This is the initial part of the compression module and is used to calculate the free air properties in accordance to the aircraft cruising level and Mach number. The system assumes an ISA atmosphere as defined in Table 4.4.

4. Compressor inlet

The flow conditions at the compressor inlet reference station are defined. The booster and HPC inlet reference stations are defined as 2.3 and 2.6 respectively in accordance with the ARP755A reference standard defined in Appendix A.1. The fan blade row is simulated as a separate compressor, having a PR of 1.32, with zero inter-compressor duct pressure loss between this blade row and the initial booster stage.

5. Compressor outlet, first iteration

The flow properties at compressor outlet are initially guessed using an estimated efficiency of 0.88. Bleed flow, if any, is taken into consideration when calculating the outlet annulus area. Constant casing diameter annuli result in the smallest blade height at exit for any given requisite area. This may affect the overall attained efficiency since such designs tend to suffer from a greater magnitude of tip leakage loss compared to the other design types.

5.1 Compressor analysis, first iteration

The compressor mean blade loading, ψ_{mean}, is calculated using the results from the previous computations. A second, more refined efficiency guess is predicted using a relationship of ψ_{mean} versus η similar to that depicted in Figure 3.15.

6. Compressor outlet, second iteration

A second, more refined outlet geometry is calculated based latter efficiency magnitude. The computation method is similar to that described in Step 5 above.

6.1 Stage by stage aerodynamic design, second iteration

This iteration makes an initial attempt to define the stage by stage aerodynamic and geometrical stage design. The predicted blade heights assume that both the rotor and stator chords are equal in all the stages and that the spacing between each blade row is equal to 20% of the upstream blade chord. This is thought to be a realistic estimate based on data provided within [7].

The blade vortex is assumed to conform to a constant reaction design as outlined in Section 3.6.1. Furthermore, the hub reaction is constrained to a minimum of 0.3 [36] to avoid excessive flow diffusion in the stator row. The pitchline reaction is set to 0.5 unless otherwise constrained by the hub reaction. The latter restriction may sometimes constrain the design because the local reaction tends to vary significantly along the blade height as described in the aforementioned section of this thesis.

Finally, the stage velocity triangles at the hub, mean pitchline and casing are predicted using the geometric results from the previous calculations.

6.2 Blade design, second iteration

Turbodev then performs an initial attempt to suggest blade designs which will provide the required flow orientation. The blade incidence which corresponds to the flow inlet is calculated using the modified Lieblein's approach outlined in Section 3.5.1. For this purpose the blades are assumed to have a t_b/c of 0.05 and a K_{sh} of 1. Furthermore the incidence of the initial stages is increased by 1^o whilst that of the rear stages correspondingly decreased by 1^o. This is to cater for the off-design performance of the compressor as suggested in the literature review chapter.

Moreover, the blade deviation which relates the blade trailing edge to the flow at exit is calculated using Equations 3.25-3.28. The same blade geometrical assumptions stated above are again assumed for these computations with a further decrement of

2^o of the predicted deviation to simulate the improved performance of modern CDA blade designs.

Finally, to compute the blade number required for each row the mean pitchline DF is set at 0.48. This is considered a realistic magnitude considering today's three dimensionally designed blades which optimise the flow diffusion along the blade span and chord.

6.3 Third efficiency estimate

Once the blade and flow aerodynamic geometry are known, the stage loss is predicted according to the principles outlined in Section 3.7.2. For this purpose, the blade critical Mach number and tip clearance are assumed to be 0.8 and 1% blade height respectively.

The stage and overall compressor efficiency are then calculated using Equations 3.36-3.44.

7. Compressor outlet, third iteration

This step is similar to Step 6 above; however, the last computed efficiency estimate is used to predict a more refined annulus geometry.

7.1 Stage aerodynamic and blade design and final efficiency estimate

The solution method is similar to that described in Steps 6.1 to 6.3 above. Also, a more appropriate DF is used in accordance with the limits outlined in Appendix A.2. Minor improvements in blade geometry, such as more accurate blade chord lengths, are suggested based on the previous iteration. A fourth and final efficiency estimate is then calculated.

8. Compressor Output

The compressor output module presents to the user a summary of the more important results from the previous iteration. Blade row data is displayed in a simple interface which allows the user to grasp a detailed picture to the geometrical and aero-dynamical characteristics pertaining to the analysed compressor.

Finally, rotor and stator de Haller numbers are displayed in a graphical manner. This format allows the user to predict the compressor's overall aptitude towards stall or surge in an intuitive manner.

5.2.1.2 Compression module limitations

The more important limitations associated with this module tend to arise because of the assumptions listed above. However, it is believed, that the inaccuracies incurred through the use of these computations are minor and justified when considering the intended use as an educational aid for preliminary design.

A more practical limitation concerns the type of compressors this program is designed to handle. In its present form of development, only three to twelve stage compressors can be analysed. This deficiency was not considered to cause a major impediment for its use in this work because smaller compressors were simply analysed using manual calculations. Also, since the work required for such purposes was limited in this thesis, the author chose not to implement this capability within the actual programming structure, since this would have taken unnecessary effort and time.

Finally, the results generated by this program appear to be realistic and plausible. The efficiency estimates tend to converge which gives further credit to the computational technique. However, it was noted, that a few results tend to be slightly pessimistic for some highly-loaded designs and hence a good general knowledge of this subject is considered desirable when using this program. Turbodev is nevertheless thought to be a great asset and a good overall tool worthy of further development.

5.2.1.3 Turbodev Turbine module

1. **Turbine required data input**

   At this stage, the user is required to define some fundamental turbine design criteria, which will influence the overall turbine geometry and performance. Amongst the more important variables which must be identified are the turbine type and annulus design.

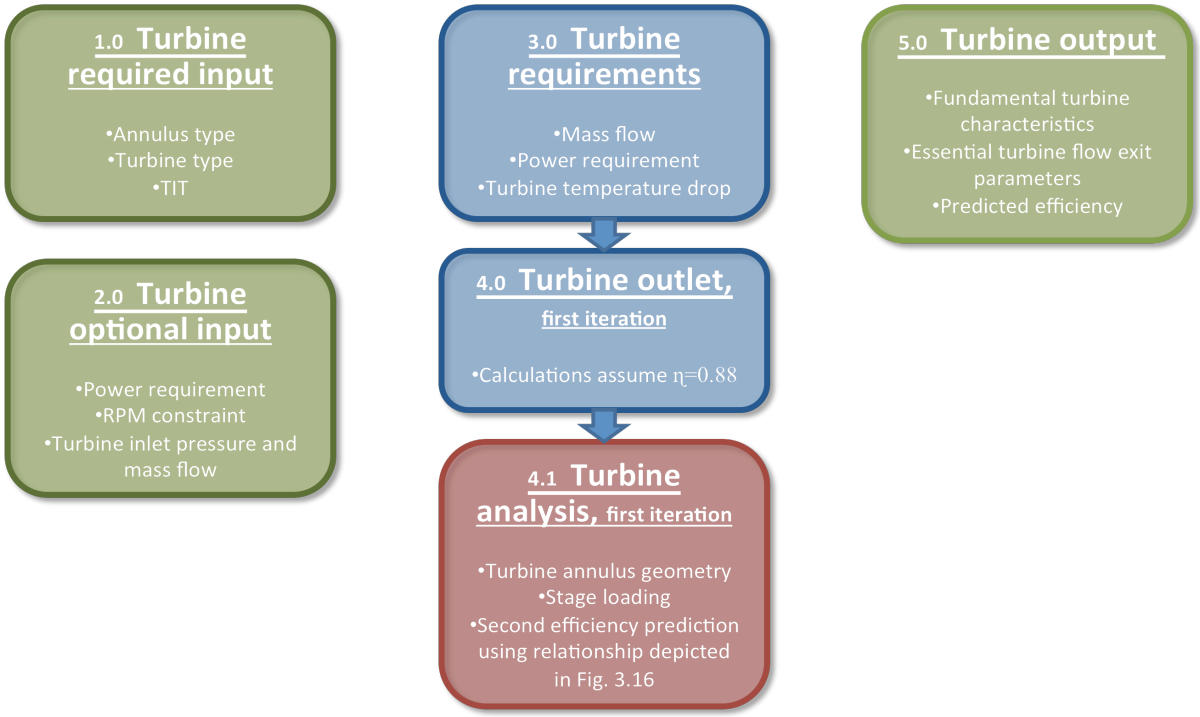

Figure 5.3: Turbodev turbine module

The scope of the annulus design data input is analogous to that implemented within the compression module. Also, akin to the compressor case, the preliminary results discussed below, assume a constant hub-line HPT and a correspondingly constant pitch-line LPT. This design choice is considered logical and common practice in industry. A constant hub-line design was chosen for the HPT to minimize, as much as possible, the influence of leakage flow on turbine efficiency. It is known that, this design results in rather taller blades which are less susceptible to leakage flow. On the other hand, a constant pitch-line LPT is thought beneficial for reducing the high turbine loading imposed by the slow co-rotating fan.

The turbine type identifies the turbine as a HPT or LPT. The relevance of this input field is made clear at a later stage. Another important user defined data is the turbine entry temperature. This is the stator outlet temperature as experienced by the first turbine rotor stage. The turbine entry temperature may not necessary be equal to the engine overall TIT since if the turbine being examined is not a HPT, this temperature will be a lower value.

2. **Turbine optional data input**

This section allows the user to define variables additional to those mentioned above. A beneficial feature of Turbodev is that, if this part is left empty, the program assumes that this turbine is designed to power the compressor defined within the compression module. That is, the turbine power requirement, mass flow, rpm and inlet pressure are compatible with the compressor defined in the latter module.

However, if the turbine has to be examined as a standalone module, each of these variables needs to be defined by the user to get meaningful results. User defined quantities have precedence over computer generated data.

3. **Turbine requirements**

This is the first section of the turbine computational module. The program initially defines fundamental turbine design variables generated from the input data set specified by the user. The turbine power requirement is either equal to that entered by the user or else set to a value appropriate to drive the analysed compressor. The latter value assumes 99.5% mechanical efficiency [7]. Hence, the actual turbine output power will slightly exceed the compressor requirement; however, this assumption is thought to make the results more meaningful and realistic.

Furthermore, the HPT power requirement also accounts for accessory drive and customer power extractions which are inevitably extracted from the HP spool. Walsh *et al.* [7] suggest a tentative magnitude of 0.1% compressor shaft power for the former. This value, which is also used in Turbodev, is thought to account for engine pump and generator requirements. Moreover, aircraft external power requirement is set at 80KW. This power, which is usually extracted through an integrated drive generator (IDG), is used to supply all the aircraft electrical requirements. The IDG used on the slightly larger CFM56-5B is rated at 90KW [59], hence the chosen value is thought to be realistic for an engine of this category.

The turbine mass flow is again a value generated automatically by Turbodev or defined by the user in the Optional Input section. The auto defined value assumes that the flow exiting the compressor plus a small percentage of fuel flow enters the turbine. The fuel flow value is computed from the combustor temperature rise. For

this purpose, the NGV temperature drop is assumed to be 70°C. Note also, that the auto-generated input is only available when the turbine is a HPT. For a LPT/IPT the user must define a mass flow value since the auto-generated value would be erroneous.

Furthermore, the turbine inlet pressure, unless otherwise defined by the user, corresponds to the compressor exit pressure less 6.8%. This value simulates the combined diffuser and combustor induced pressure losses. The magnitude of this loss is suggested by Lefebvre [23] as a realistic value for modern, annular combustors preceded by a dump diffuser.

4. Turbine outlet, first iteration

A preliminary guess of turbine outlet conditions is guessed by the program assuming a turbine efficiency equal to 88%.

4.1 Turbine analysis, first iteration

The data generated from the previous calculations is used to predict a more refined turbine annulus geometry and design parameters. Amongst the more important computations are an estimation of the flow coefficient and turbine loading.

A series of correlations outlined by Aungier [56] are used as empirical fits to Figure 3.16 which defines an optimum efficiency for a given loading. This magnitude of this efficiency is then decreased by 5% for the reasons outlined in Section 3.8.1 above. The latter efficiency term is used as the final educated guess of the turbine efficiency potential which is considered to be realistically achievable.

5. Turbine output

A general summary of the predicted turbine efficiency and primary parameters is displayed in an uncluttered manner. The detail and accuracy of this data is thought to be appropriate for the purposes of this work; however, it is acknowledged that, this module will require further development to be adequate as a more generic aid for turbine design. Nevertheless, the generated results are realistic and plausible which give credit to the theoretical foundation and assumptions.

5.2.1.4 Turbodev validation

Turbodev is a new turbomachinery preliminary design tool, developed as an aid to quickly analyse the aerodynamic qualities of any chosen compressor or turbine design. The decision to develop an entirely new design aid was based on the lack of available non-proprietary software which is suitable for use within preliminary design.

A similar design system to Turbodev is T-AXI [60] developed by Turner *et al.*. However, even though the latter's capabilities are very similar to Turbodev's, T-AXI is primarily intended for teaching practice, hence the results are rather theoretical in nature and not suited for preliminary design. Also, since T-AXI develops its own component geometry, it does not allow the user to specify any specific turbomachinery layout, which was a very important requirement for this present work.

Furthermore, given that Turbodev is a new turbomachinery analysis tool, it was deemed necessary to validate the results of this system against published data. A ten-stage HPC and a five-stage LPT were chosen as candidate designs for the validation exercise. The respective designs are depicted in the following diagram.

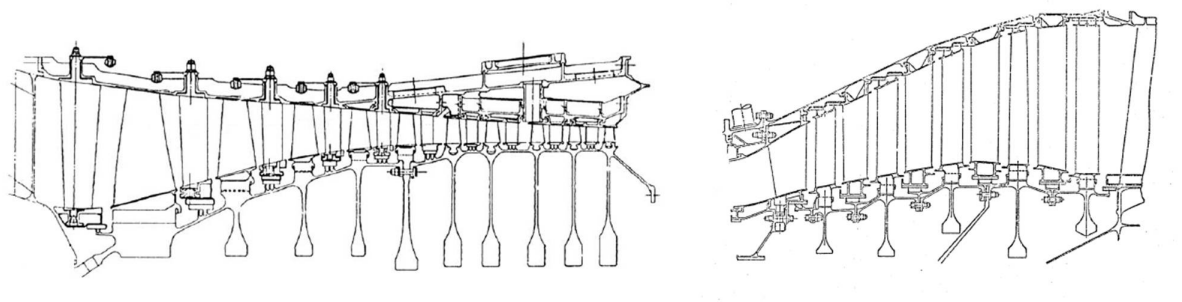

Figure 5.4: Energy Efficient Engine HPC and LPT; obtained from [61] and [62] respectively

1. **Compressor module validation**

The compressor chosen to validate Turbodev was from the Energy Efficient Engine (EEE) project managed by GE under sponsorship of NASA and conducted in the early 1980s. This compressor was chosen primarily because its performance and mechanical characteristics are very well documented in [61] and [63].

The EEE was a research project aimed at improving the overall engine performance for use on subsonic, long haul jets. Some of the more significant EEE goals were to improve sfc by 12% compared to the CF6-50C and reduce the latter's deterioration between overhaul to just 50% of the magnitude experienced on the CF6. The final EEE compressor characteristics are detailed below.

Compressor PR	23.0
No. of Stages	10
Polytropic efficiency	89.5%
Airflow	53.5kg/s
Annulus type	Constant pitchline Stages 1-6 Constant hub-line Stages 7-10
Bleed requirements	1.3% mid-stage (Stage 5) 2.3% Stage 7 (modelled as compressor delivery bleed within Turbodev)
Design point	Maximum climb, 10.67km, M0.8, ISA-8^{o}
RPM	12303
Blade geometry	Sourced from detailed report [64]
Stagewise distribution of temperature rise and DF	Sourced from detailed report [64]

Table 5.2: EEF, 10 stage second build, compressor characteristics, data obtained from [64]

For the intent of validating Turbodev, it was thought best to mirror the EEE compressor geometry exactly as documented in the aforementioned literature. Thus, a more realistic efficiency prediction can be generated which is directly related to the published data. Also, since the compressor design intents of the EEE and the current engine are different, the turbomachinery geometry which would be generated by Turbodev will most certainly not conform to the actual compressor. Furthermore, considering the fact that the EEE compressor is derived from a detailed parametric design and includes an unusual annulus shape, which cannot be modelled by Turbodev, the current approach to validating Turbodev was thought to be the most opportune for the current circumstances. Moreover, in addition to the above argument, even though a parametric study of each and every compressor design characteristic and its affect on compressor weight, direct operating cost and performance is the more traditional approach used in industry, this method is not feasible for the current study due to the limited non-proprietary knowledge available on this subject.

For the purpose of this validation, the Turbodev computations were altered slightly to accept the required compressor stage geometry as input. The EEE blade profiles and stage temperature rise were also programmed in directly. This data was obtained from the EEE detailed report [64]. In spite of these modifications, Turbodev's efficiency prediction correlations remained unchanged. Therefore, the affect of these alterations should not bear any impact on the performance of Turbodev and the results of this validation are thought to be accurate and a true representation of this system's capability.

Turbodev predicted an overall efficiency potential of 90.0% for the EEE configuration. The EEE Performance report [61], outlines a measured adiabatic efficiency, at the design point, of 82%. However, Cline *et al.* suggest that this magnitude should be corrected upwards by 2.6% to account for instrumentation induced losses and deterioration from previous high speed stalls. The resulting 84.6% adiabatic efficiency corresponds to a polytropic efficiency of 89.5%. This shows very satisfactory agreement with the predicted value. The error is only 0.6%.

2. Turbine module validation

Similar to the compressor validation exercise, the turbine chosen to validate Turbodev is from the NASA/GE EEE programme. This LPT, is a five stage, highly loaded turbine and attained an overall recorded efficiency of 91.5% [65]. The high aerodynamic loading was the result of a high engine BPR coupled with a close transition duct between the HPT and LPT which severely limited the rotor's tangential velocity of the initial stages. The following table outlines the primary turbine characteristics.

Turbine PR	4.18
No. of Stages	5
Polytropic efficiency	91.1%
Average Stage loading $(\Delta h/2u^2)$	1.39
Average flow coefficient (V_x/u)	1.11
Annulus type	Constant hub line
Design point	Maximum climb, 10.67km, M0.8, ISA-8^o

Table 5.3: EEF, 5 stage Block II, LPT characteristics, data obtained from [62]

The predicted Turbodev efficiency is 87%. This represents an error of 4.7%. This magnitude, although significant, is unsurprising considering the relatively simple way the efficiency prediction is generated within this module. The turbine computations are based on Aungier's [56] suggested approach, and are thought to be sufficiently accurate for the purposes of this study. It is anticipated that, with further refinement, the turbine module can generate the same level of precision that is built in the corresponding compression module.

In conclusion, even though this testing is by no means an extensive evaluation of Turbodev's capabilities, it reinforces the fact that the aerodynamic computations implemented within this system are sound and the results should be satisfactory for the intents of preliminary design.

5.2.2 The fan stage

The design of the fan stage was considered beyond the scope of this work. Fan design is a highly specialised field in gas turbine manufacture and is conducted by expert personnel using dedicated software. For the present study, the author simulated the fan blade row as a separate single stage compressor, upstream of the booster, connected to the latter by a loss-free inter-compressor duct. The assumed fan characteristics are listed below.

Mass flow	120kg/s	**RPM**	4500
PR bypass air	1.68	**PR core air**	1.32
Polytropic efficiency	0.88	**Power input**	5MW
Tip radius	0.95m	**Hub radius**	0.55m
Tip blade speed	440m/s	**Tip Mach number**	1.4
Hub blade speed	250m/s	**Hub/tip ratio**	0.57
T_o2	245°K	**P_o2**	32.7KPa
$T_o1.3$	290°K	**$P_o1.3$**	55KPa
$T_o2.3$	267°K	**$P_o2.3$**	43KPa

Table 5.4: Fan characteristics

Note

i. *The station numbers conform to the ARP755A standard outlined in Appendix A.1.*

5.2.3 Preliminary analysis results and discussion

A preliminary analysis was conducted to elect three designs, amongst all the alternatives, that appear to be most suited with regards to the two initial FOMs mentioned above.

5.2.3.1 Efficiency potential

The compressor designs outlined in Table 5.1 were analysed using Turbodev to obtain a more realistic efficiency potential of each one. Turbodev allowed a rather quick analysis of the different designs and the work associated with this program's development can be further justified if future work is conducted to enhance its overall capability and accuracy. A summary of the generated results is presented in Table 5.5. The results embody the assumptions stated in the previous sections of this thesis.

Configuration name	Mean stage loading of booster/HPC *(computed using Turbodev)*	Efficiency potential of booster/HPC *(predicted by Turbodev)*
C2/101_1	-/0.31	-/0.88
C2/101_2	0.29/0.3	0.89/0.89
C2/101_3	0.27/0.29	0.89/0.89
C2/101_4	0.36/0.26	0.88/0.89
C2/101_5	0.26/0.26	0.89/0.89
C2/101_6	0.31/0.26	0.88/0.89
C2/101_7	0.34/0.21	0.88/0.91
C2/101_8	0.31/0.2	0.88/0.9
C2/101_9	0.26/0.27	0.9/0.91
C2/101_10	0.28/0.29	0.89/0.9
C2/101_11	0.26/0.3	0.89/0.88
C2/101_12	0.31/0.3	0.88/0.88
C2/101_13	0.33/0.32	0.88/0.89
C2/101_14	0.33/0.29	0.88/0.89
C2/101_15	0.32/0.32	0.88/0.88
C2/101_16	0.33/0.35	0.88/0.88

Table 5.5: Preliminary analysis results

Based on the interpretation of these results, the author opted to further analyse compressor configuration numbers 10, 13 and 16. Each of these layouts showed real potential of achieving or exceeding the efficiency requirement stated in Table 4.3 of the previous chapter.

Finally, it must be noted that even though the three chosen designs appear to be suitable from an efficiency standpoint, there is very little margin of error allowed for the entire design process. Also albeit these designs may be considered as being rather conservative in nature, the required surplus efficiency potential suggested in Section 3.2.6.1 has not been achieved. This makes the whole engine design process potentially riskier and more prone to cost and time overruns. With this in mind, configuration 10 is the preferred alternative amongst the three finalists.

5.2.3.2 Turbine consideration

The three chosen compressor layouts were then validated according to the turbine suitability criterion listed in Section 5.1. This analysis consisted of a simple testing of whether or not the compressor layouts impacted negatively on turbine design.

A compressor layout may necessitate an excessive number of turbine stages to satisfy the required turbine efficiency as stipulated by the programme requirements. This may result in an unacceptably heavier engine overall even though the compressor design appears satisfactory as a standalone module. Hence, this testing served as an assurance that the required turbine performance can be met, within a reasonable degree of certainty, by the requisite amount of stages and geometrical constraints.

For the purpose of this study, it was supposed that the mean HPT pitchline radius was 133% that of the corresponding HPC radius. This effectively implies an inclined combustor and is used to allow higher HPT work coefficients. The higher rotor mean blade speed, at any given rpm, generates higher work output thus requiring fewer turbine stages. This is a common design option on modern civil aero gas turbine engines and is used in some of the more prolific aircraft engines currently in production.

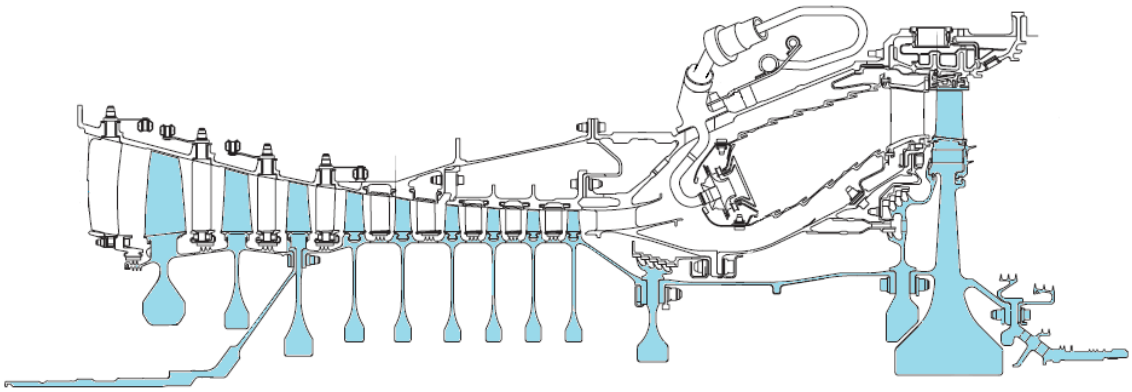

Figure 5.5: CFM56-5A's HP spool, modified from [13]

It is also worthy of mention, that such a configuration, will, as shown in Figure 5.5, allow a larger combustor length and volume for a given overall engine size. This is also expected to improve this component's performance and efficiency.

Table 5.6 presents a summary of the results obtained using the methodology described in Section 5.2.1.3.

Configuration name		No. of stages	Mean stage loading	Temperature drop (^oK)	Predicted efficiency
T2/101_10	*HPT*	1	1.33	259	0.89
	LPT	4	1.14	302	0.90
T2/101_13	*HPT*	1	1.43	278	0.88
	LPT	4	1.24	328	0.89
T2/101_16	*HPT*	1	1.57	315	0.88
	LPT	3	1.38	274	0.89

Table 5.6: Turbine analysis summary

It is evident that adequate turbine geometries may be designed to power the three different compression layouts. A single stage, moderately loaded, HPT, satisfying the minimum required efficiency of 89%, can only de designed for configuration E2/101_10. However, in spite of these results, all three configurations were deemed satisfactory in this regard because a more detailed turbine design study may yield slightly better efficiency potential.

Moreover, the results listed in Table 5.6 suggest that the LPT design is also not adversely affected. The results listed in the above table assume a 1.5% inter-turbine duct pressure loss [7] and a pitchline radius equal to that of the fan hub. It is worth noting that the E2/101_16 configuration has a significant weight advantage compared to the other designs since it is able to satisfy the LPT efficiency requirement with one less turbine stage. On the other hand, the E2/101_10 once again possesses the highest LPT efficiency of 90%. The author notes that, with some refinement, the 89% efficiency requirement can also be achieved in this design with one less turbine stage; however, it is thought, that this configuration represents an overall more conservative approach potentially yielding the highest engine efficiency for the least amount of development time and cost.

Finally, it worth considering how the three chosen designs compare to the current production engines mentioned in Section 1.3.1. From the data presented in the following table, it can be appreciated how the E2/101_16 configuration represents a highly-loaded turbomachinery layout which may be prone to several complex off-design behavioural issues and thus a long and costly development programme. The E2/101_13 appears to be a good compromise between the latter design and the more conservative E2/101_10.

Engine	LPC/Booster	HPC	HPT	LPT
CFM56-7B18	3	9	1	4
BR715-55	2	10	2	3
CF34-10E5	3	9	1	4
E2/101_10	5	10	1	4
E2/101_13	4	9	1	4
E2/101_16	3	9	1	3

Table 5.7: Stage row numbers of proposed and existing designs; relevant data obtained from [3]

5.3 Detailed analysis

The detailed analysis concerned FOMs, other than those examined in the previous study, which were thought to be of importance in identifying the optimum compressor design. These FOMs, in accordance of importance, are discussed below.

5.3.1 High reliability and long life

High reliability is considered a fundamental criterion of any aero engine. Historically, good reliability generally implied also a long life between overhaul, hence the two criteria have been grouped together within this report.

More so, good reliability is required by engines of short haul aircraft, such as the case of this project, because these aircraft tend to operate to regional airports which may not have a suitable maintenance organisation. Thus, if the engines had to suffer from frequent technicalities, the whole operation may be compromised and will eventually make the aircraft-engine combination unfavourable with the airlines.

Reliability however, concerns mostly the mechanical domain. High reliability is achieved by proper mechanical design and a good maintenance schedule. Nevertheless, the aerodynamicist can design the turbomachinery to be inherently more reliable and less prone to failure. Normal industry practice is to assign reliability indices to each and every component that may compromise the ability of the engine to operate. However, these indices are complex in nature and depend greatly on the manufacturer and component characteristics.

Unfortunately, reliability is not an easy property to quantify since it is a function of several parameters that affect, either directly or indirectly the engine's ability to function normally. Any failure, be it isolated or coupled can affect the engine's despatch capability. Also, some failures are more serious than others. Hence, the engine's overall reliability is a complex subject, often measured in terms of down time, time between overhaul or any other parameter used to reflect the overall system health.

With regards to turbomachinery, the primary cause of failure, from an aerodynamic point of view, is due to vibration. Vibration within compressors is normally caused by flutter. Flutter is blade excitation at the natural frequency which may eventually lead to failure if left uncontrolled.

Flutter may be caused when operating close to choke or surge [25]. Also, in some cases flutter can be initiated due to excessive amounts of bleed off-take [12]. The amount of bleed off-take that can usually be tolerated is between 12 and 17%. The bleed requirement for this engine, as outlined in Table 3.3, is lower than this amount hence this mode of flutter initiation is not considered critical for this study.

Flutter, as described above, can be caused when operating close to choke or stall. This, as shown in Figure 5.6, depends not only on the compressor map but also on the engine working line. The working line depends, to a large extent, on the turbine capacity which, unfortunately, is difficult to predict accurately at this stage. This is because minor variations of nozzle throat area have a significant influence on the final capacity.

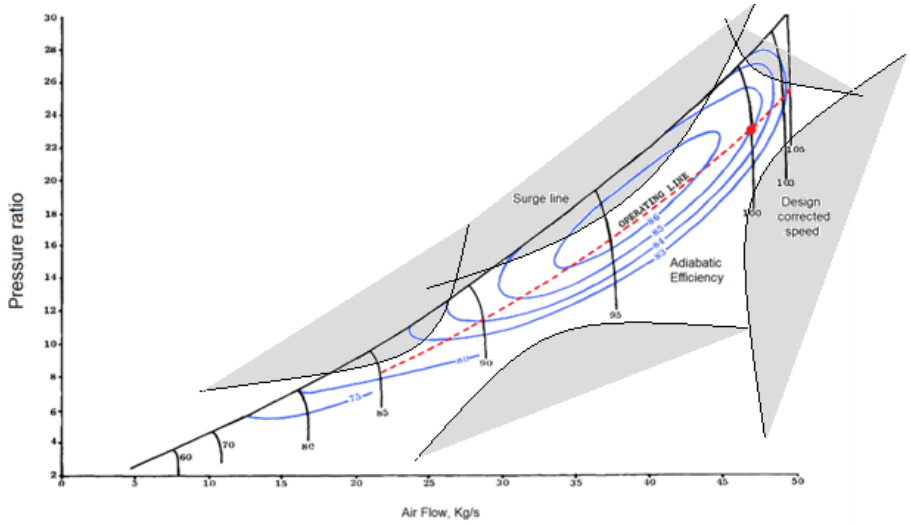

Figure 5.6: Common flutter initiation regions

Nevertheless, an estimate working line can be generated and the flutter margin calculated accordingly. This margin is a measure of how much the working line is removed from the flutter boundaries. This procedure, is not normally conducted during preliminary design, and

requires engine-specific data to predict the actual flutter boundaries. This data is normally obtained from similar engines the manufacturer has tested in the past.

Whatever the mode of flutter, it is normally initiated because of excitation induced by the blade wake. When the blades are heavily loaded they tend to stall. Blade stall causes Karman vortices in the aerofoil wake [66]. Whenever the frequency of these vortices coincides with the natural frequency of the aerofoil, flutter will occur.

In spite of the above limitations, some information regarding the compressor's aptitude towards vibration can be obtained at this stage. A measure of the magnitude of stall induced wake is the DF or de Haller number. The former is thought to be a better predictor of blade stall, whilst the latter is known to satisfactory account for end-wall stall [25].

The tendency for blade stall is limited within all the examined compressors because the DF within each blade row is limited to a maximum as suggested in Appendix A.2. This magnitude is thought to limit blade mixing loss due to excessive blade wake. Therefore, this limit is also thought to be beneficial in limiting blade excitation and thus flutter.

Furthermore, the de Haller number of each blade row is depicted in Figure 5.7 below. These depictions were obtained using Turbodev which has the capability to provide a graphical summary of this parameter. Note also that the stage loading has been optimised to balance the diffusion throughout the length of the compressor.

It can be noted that all the compressors exceed the minimum suggested de Haller number of 0.7 at one stage or another. The minimum recorded value of 0.585 was noted in configuration number 16. This was not unexpected, considering that this design is relatively highly loaded. Also, even though this is considered quite excessive, the 0.7 threshold is more of a guideline than a constraint. This is because, this limit, as discussed in Chapter 3, is derived from diffuser theory neglecting any form of specific compressor geometry or characteristics.

Nevertheless, the data suggests that C2/101_10 performs best in this regard, with the least amount of stalled flow. Also, it must be emphasised, that this criterion is by no means an exact reliability gauge. On the contrary, its use has been limited to serve as an indication of stalled flow which, in itself, may induce vibration.

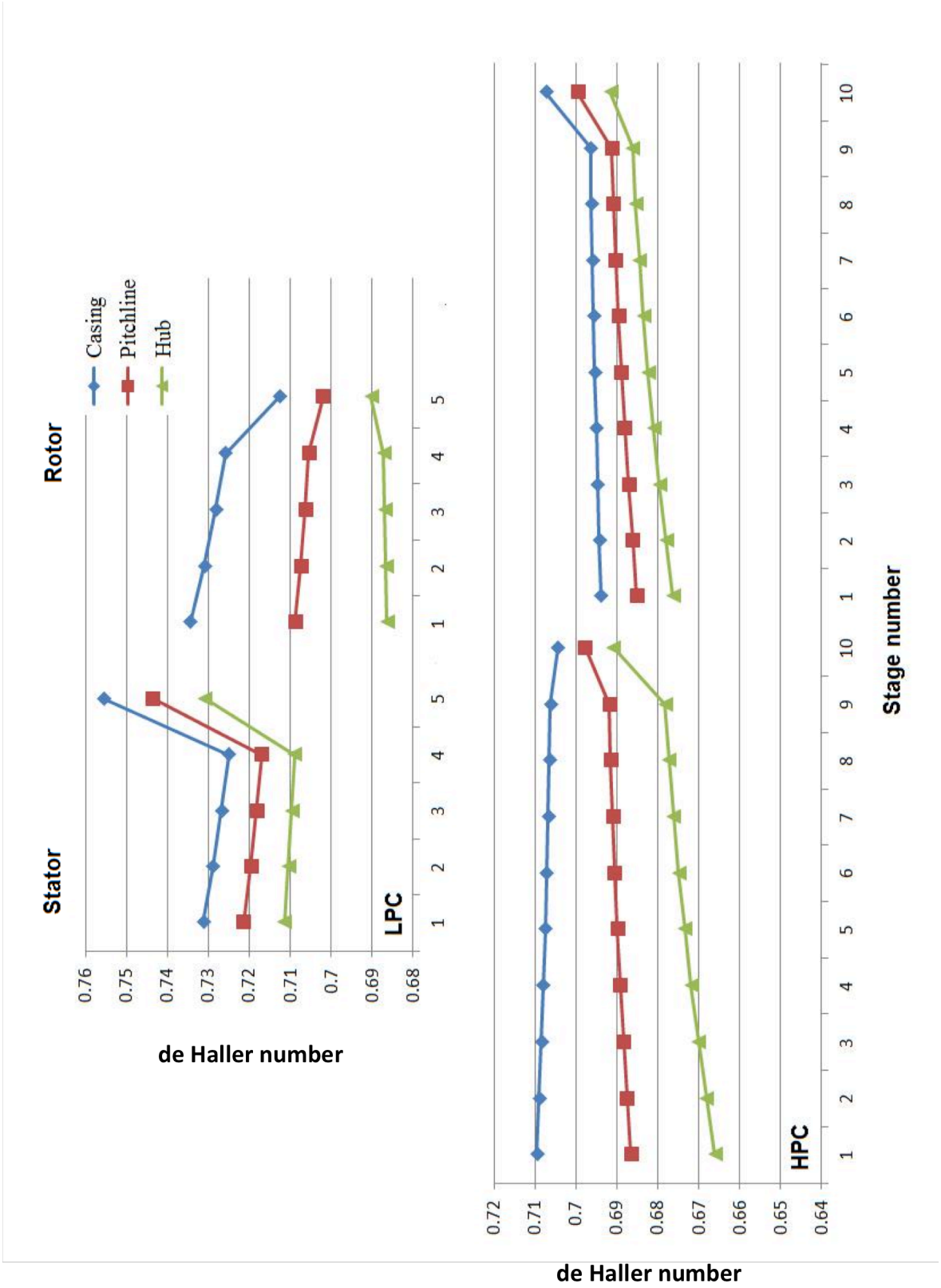

Figure 5.7a: Configuration C2/101_10 de Haller number synopsis

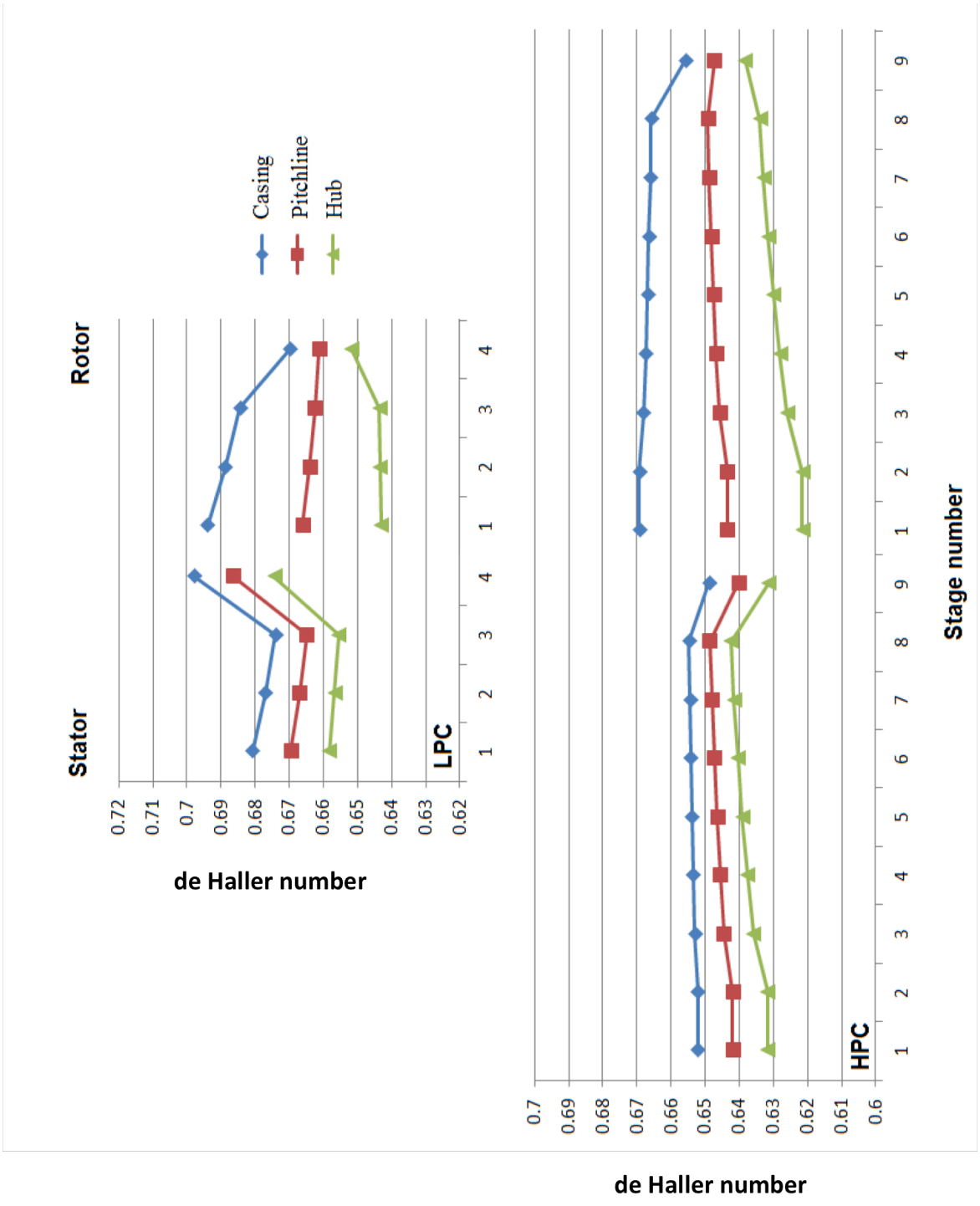

Figure 5.7b: Configuration C2/101_13 de Haller number synopsis

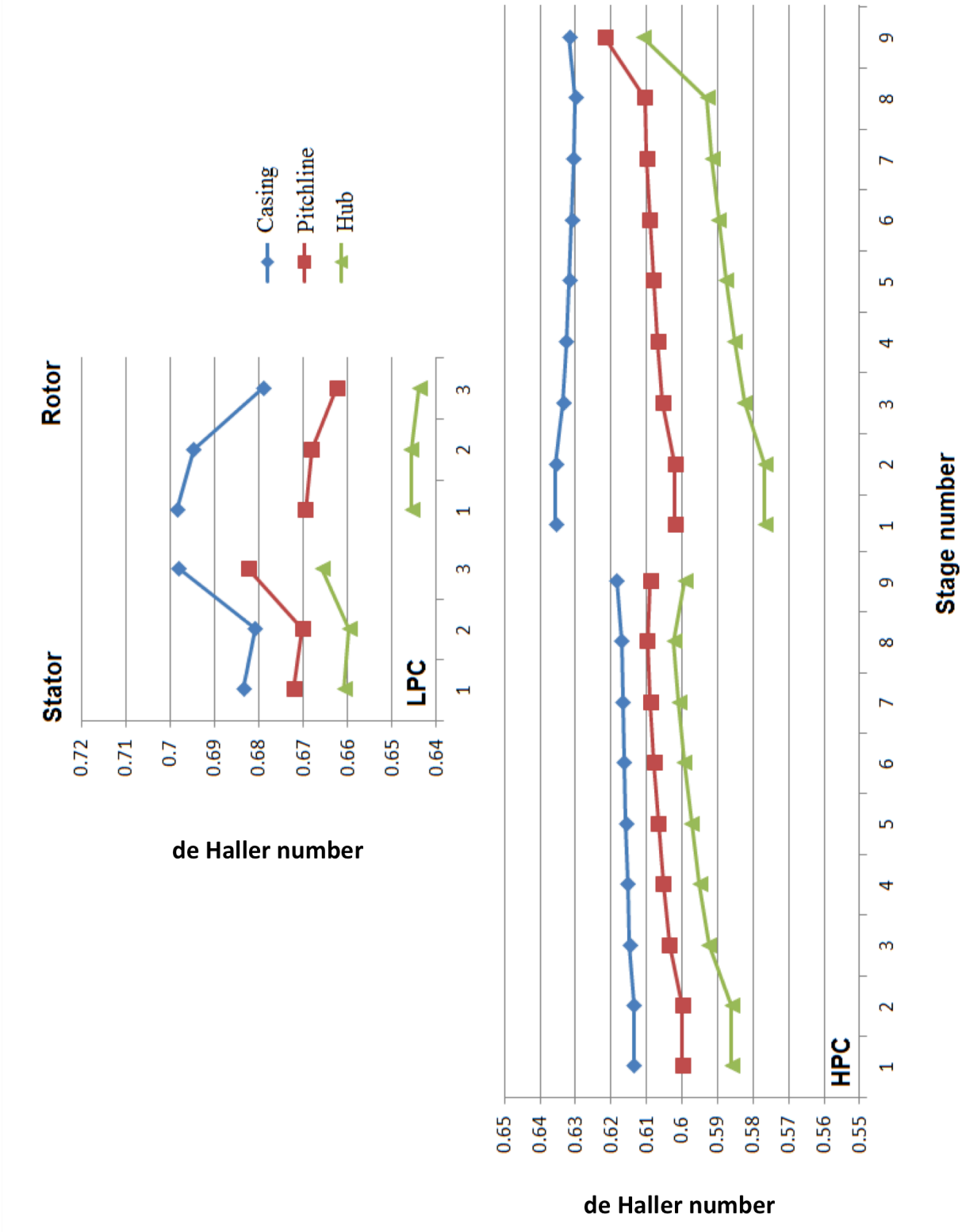

Figure 5.7c: Configuration C2/101_16 de Haller number synopsis

To conclude, reliability performance is known to be a very hard quantity to assess in preliminary design, especially considering the author's limited pool of industrial data. With this in mind, some form of aerodynamic instability can be assessed, which in itself may trigger failure due to vibration. The results suggest that, configuration 10, has the best performance in this regard.

5.3.2 Compressor weight and length

Overall engine weight is a prime consideration in any design endeavour. To this end, each component should be optimised towards minimum weight unless limited by the requisite performance or reliability.

Compressor weight prediction techniques are however, not well documented in the public domain and for this reason the author opted to use a modified empirical technique described by Sagerser *et al.* [67]. This practice is thought to be suitable for preliminary design even though it is based on research conducted in early 1970s. Furthermore, the weight estimate obtained by this method, is factored by 0.7, as suggested by Gerend *et al.* [68] to compensate for the improvements in design technology and material fabrication techniques over the last four decades.

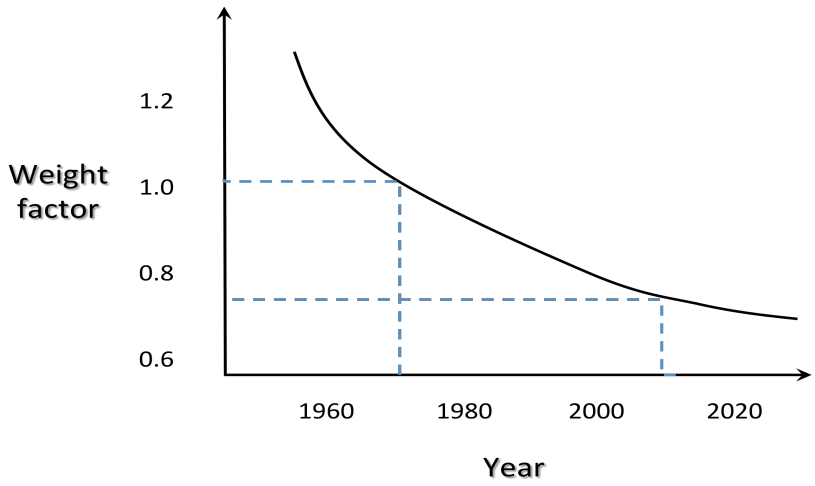

Figure 5.8: Weight decrement due to technology improvements over time, modified from [68]

Moreover, in addition to component weight consideration, the length is also of great importance. A shorter compressor implies a shorter and stiffer engine together with a more simplified bearing and support structure.

Engines of this size are normally supported by a bearing assembly at the front and rear of the HP shaft. This, as depicted in Figure 5.9, allows for a compact two frame system which supports the entire rotor assembly [6]. Moreover, the front frame, which locates the HPC rotor bearing, is normally utilised to transmit power from this shaft to the accessory gearbox via the accessory drive shaft. The power requirement for the accessory gearbox is outlined in Section 5.2.1.3.

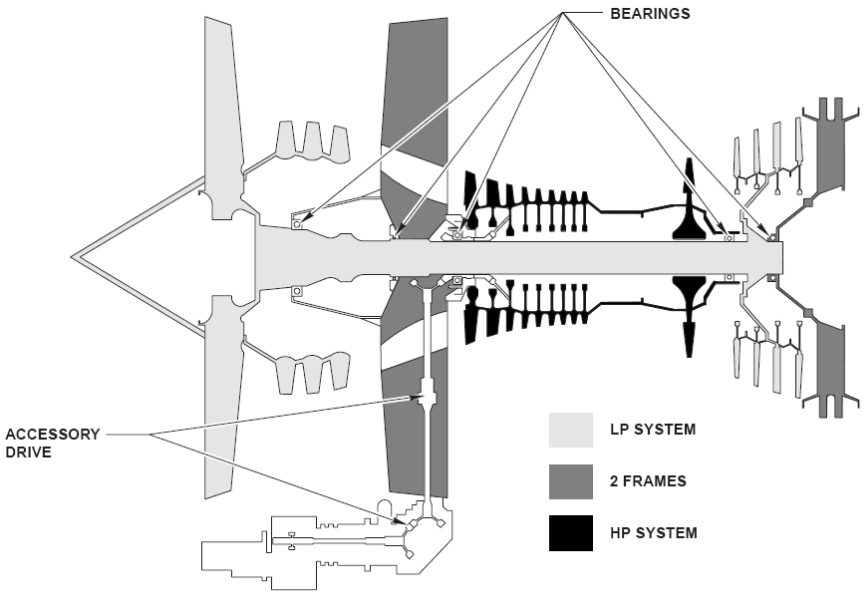

Figure 5.9: Engine rotor and frame assembly, obtained from [13]

One of Turbodev's capabilities is to generate a first order estimate of the compressor length (L_c). This length is calculated by sizing the axial blade chords, of each row, accordingly to limit the DF at the mean blade height. This value, as discussed in Appendix A.2, is realistic and even considered somewhat conservative, for modern designs.

In addition, the blade spacing is set equal to $0.2 * upstream\ blade\ chord$ as suggested by Walsh *et al.* [7]. Turbodev finally accumulates all the respective lengths to provide the user with an estimated overall compressor length.

Figure 5.10 summarises the results from these calculations. Also, the overall compressor length, which is also tabulated, assumes a 0.3m inter-compressor duct. This duct is usually designed to yield undistorted flow at the HPC face and may also be used to extract bleed flow for aircraft or engine requirements. Furthermore, located within this duct is usually a HPC inlet guide vane. This vane, which is depicted in Figure 5.5, is not unlike a variable stator vane, and is used to orient the flow in a manner best suited to the HPC's first rotor row. Finally, from a structural standpoint, the front frame assembly is usually located between the two compressors hence; the axial length of this duct is as much an aerodynamic as well a mechanical constraint.

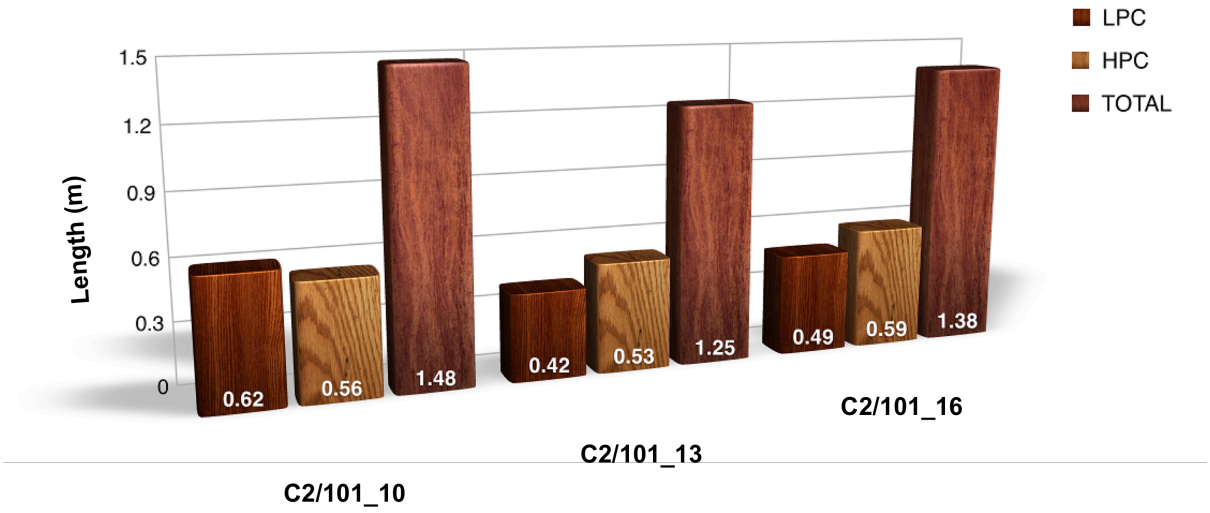

Figure 5.10: Compressor length (L_c) results

With reference to the above chart, it is evident that C2/101_13 is the shortest option from the three alternatives being considered. Also, it is noteworthy to mention that even though the LPC of this design has an additional stage compared to the C2/101_16, the latter is actually predicted to be slightly longer.

The weight prediction technique discussed above and used within this dissertation is based on the work of Sagerser *et al.* [67]. This work, which was intended primarily for vertical takeoff or landing (VTOL) engines, also incorporates adjustments to allow the engineer to use this information for conventional designs. More so, the compressor characteristics analysed within this present work are similar to those used for deriving the correlations in Sagerser's

report. This occurrence, together with the weight adjustment factor discussed above, is thought to yield meaningful and realistic results suitable for the current work.

The modified Sagerser's weight empirical correlation used within this report is as follows.

$$W_c = 17(\overline{D_m})^{2.2}(N)^{1.2}\left[1 + \frac{{}^{L_c}/_{\overline{D_{m,1}}}}{0.2+0.081N}\right] \qquad \textit{(equation 5.1)}$$

Figure 5.11 summarises the results from this correlation.

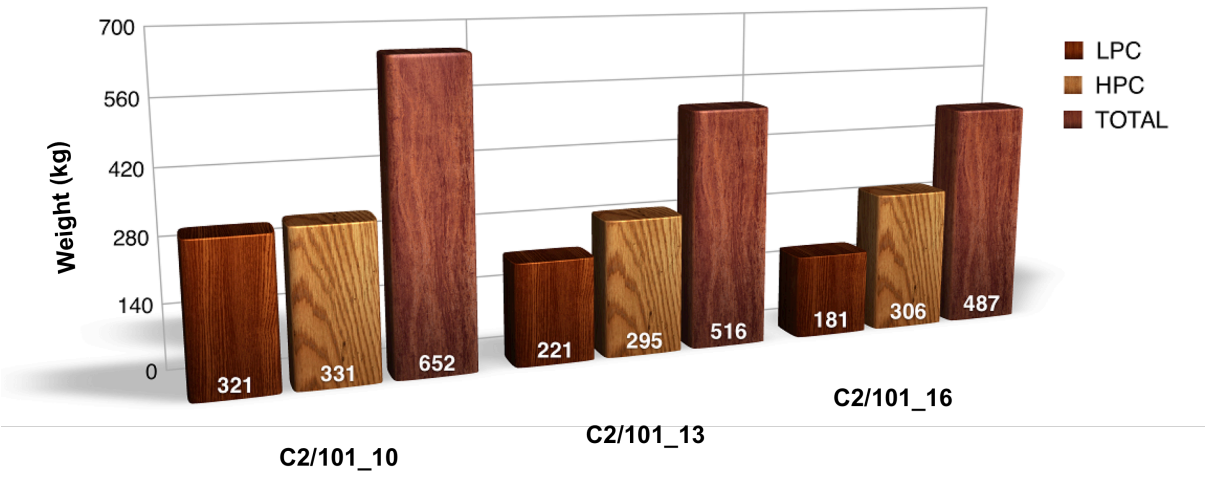

Figure 5.11: Compressor weight (W_c) results

Note that W_c shown above is assumed to include the rotor and stator blades, disks, seals and casing. Also, it is worth considering that the weight of longer compressors, namely configurations 10 and 16, might potentially be underestimated because this empirical method makes no allowance for shaft weight or corresponding weight additions due to complexities in bearing or strut assemblies that may be required.

Therefore, configuration number 13 appears to be the most appropriate design amongst the three alternatives with regards to compressor length and weight.

5.3.3 Off design considerations

Off design performance is very important for any gas turbine, be it industrial or aero. However, this issue is even more critical for aero engines because these engines undergo a lot more starts and transient operation compared to industrial machines. The aircraft flight profile dictates the extent of off design operation expected per operational hour. The flight profile modelled for this aircraft is outlined in Table 1.1. It is evident that only 33% of the total flying time is at the cruise condition. Hence, the majority of the block running time is expected to be carried out at off-design conditions.

Furthermore, as explained in Section 3.4.6, off design performance dictates, to a large extent, the complexity of the engine control system, which nowadays involves a significant certification cost in itself. Modern control systems are almost exclusively digital in nature and are referred to as Full Authority Digital Engine Control (FADEC) due to the extensive control and manipulation they offer on all the engine variables. Finally, even though off design performance and modelling is not considered part of preliminary design, a general aptitude of the compressor off design complexity task can be assessed at this stage.

Off design operation is considered complex because the blade rows will become mismatched in the sense that the aerofoil profile will no longer conform to the actual flow direction. It is known that when operating at slower than design speed, the front compressor stages tend to be pushed towards stall whilst the rear stages become chocked.

To counter this unbalance, the primary control systems may use bleed or variable geometry. Bleed air, depending on the point of application, lowers the compressor working line and may also alter the surge region [5]. In this regard, the bleed system affecting the LPC and HPC of this engine is intended to have a different outcome within the two compressors.

The LPC is expected to have a bleed outlet only at the compressor delivery within the inter-compressor duct; whereas the HPC, as outlined in Chapter 3, is also expected to have an inter-compressor bleed. The effect of bleed within the LPC is to lower to working line, whereas the HPC is also expected to undergo a modification to the surge line, in addition to the lowering of the working line due to the affect of interstage bleed. Finally, it should be

noted that, even though the use of bleed is intuitively wasteful, it is almost always used within aero engines, especially during the start sequence.

The other means the FADEC usually has at its disposal to suppress stage mismatching at low speed is the use of variable geometry. This technique involves the re-staggering of the stator blades to re-match the blade to the correct flow direction. The use of variable stators vanes (VSVs) is thought necessary when the PR in a single compressor exceeds 7 [27]. Also, Walsh *et al.* [7] outline how, for preliminary design, it is sufficiently accurate to assume that one variable stage is required per additional stage beyond five on a single spool. Aungier [36], however suggests that the required number of variable stages on a given compressor should be approximately half the total number of stages. This theory however is known to be inconsistent since few LPCs, if any, have any variable geometry, thus the former theory is used for the purposes of this work. Additionally, Aungier suggests a method whereby, the VSV re-stagger angle can be calculated for any required stage. It is known that, the magnitude of re-staggering required decreases down the length of the compressor, hence the reason why the number of variable stages is always less than the total number of stages on any given spool. In spite of the relative simplicity of Aungier's method, it is thought that this task is beyond the scope of preliminary design, thus is not included within this report.

Furthermore, it is customary to include a variable inlet guide vane (VIGV) within the HPC. The VIGV is not unlike a VSV in operation but is situated in front of the first rotor row. A VIGV is used, amongst other things, to control the rotor hub reaction and thus limit the stator hub Mach number [69]. Figure 5.12 shows such a design. This arrangement is similar to that assumed for the purposes of this study.

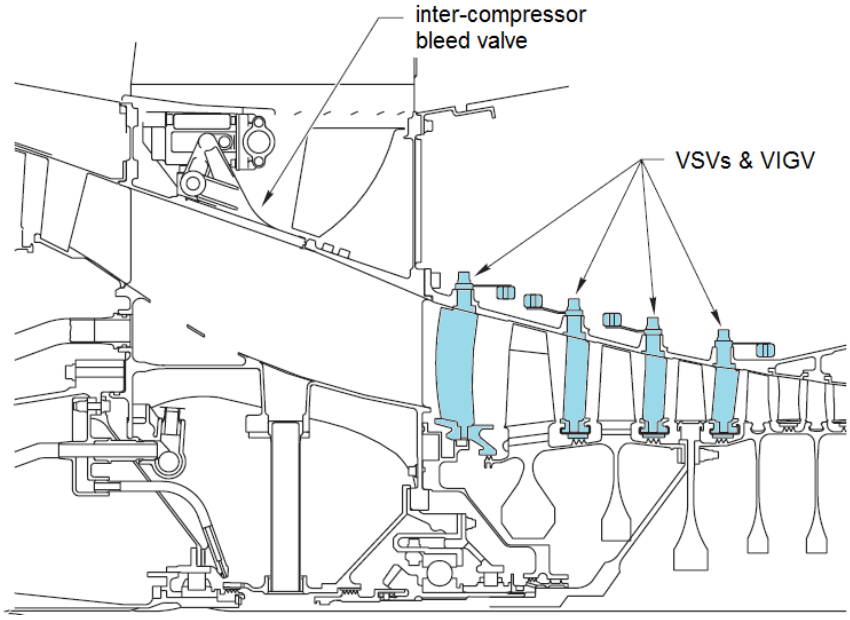

Figure 5.12: CFM56-5A inter-compressor mechanical layout, modified from [13]

VSV and VIGV positions are controlled by the FADEC and scheduled versus compressor non-dimensional speed. Other variables such as current altitude, fan speed and rate of acceleration or deceleration may also be included within the FADEC computations [13].

Furthermore, it is interesting to compare how other manufacturers tackle the off design operability problem in their short or medium range aero engines. RR always favoured the use of a three shaft layout over the more extensive use of variable geometry. This is reflected in their RB211-535C and E4 medium range engines which do not employ any variable geometry but are both three spool engines having an overall PR of 24 and 28 respectively [20]. Similarly Lycoming chose not to use variable geometry in their ALF502 and LF507 short haul engines [21]. However, in spite of the two shaft layout, they managed to get away with variable geometry on these engines by opting for a much lower PR and hence sacrificing fuel efficiency for weight and simplicity. Finally, CFM Corporation, of which GE is part, employs a more traditional approach for its CFM56 series short and medium range engines. This engine, which is widely renowned with airlines for its reliability, has a two shaft layout with some five to seven stages of variable geometry, depending on the exact model. Also, the author noted that the Walsh *et al.* [7] suggestion, estimating the required number of variable geometry, quite accurately predicts the number of VSVs and VIGVs for the CFM engines.

Thus it is understood that, the use of this method should also be valid for this work since the proposed engine is quite similar in geometry and performance to the CFM engine.

Configuration	Compressor	PR	Total number of stages	Variable stages required
C2/101_10	LPC	4.00	5	0
	HPC	6.15	10	5
C2/101_13	LPC	3.80	4	0
	HPC	6.47	9	4
C2/101_16	LPC	2.92	3	0
	HPC	8.40	9	4

Table 5.8: Variable geometry required according to Walsh *et al.* [7]

Table 5.8 summarises the results obtained when using the suggestion of Walsh *et al.* [7]. The outcome of these results highlights the shortcomings of such a simple correlation. Configuration number 10 HPC's PR of 6.15 is predicted to require 5 variable stages whereas configuration 16 having a much higher HPC PR of 8.40 is thought to need one less variable stage. Considering that it is the loss of PR across a compressor at low speed which causes the stage mismatching, this result may be a little unexpected.

Thus, if the results of Table 5.8 were employed, it implies that, configuration numbers 13 and 16 will require more use of bleed at low speed to re-match the stages across the HPCs.

With this in mind, it appears that configuration numbers 10 and 13 appear to be quite balanced in this category and expected to perform slightly better than the alternative C2/101_16 due to the latter's highly loaded HPC. Thus, the author expects that the off design performance of the former two is quite acceptable and should not pose any significant control difficulties later on during detailed design. It is expected that the number of variable stages suggested in Table 5.8 will be acceptable for both but configuration number 13 may require some more use of bleed air while operating at less than design speed.

5.3.4 Operating range and performance retention

It is all well and good to have an engine which is designed for a high level of performance when rolled out of the factory line but any customer will also be concerned with the system's ability to retain a specified performance when operating on-line. As will be discussed below, the importance of having a good operating range contributes significantly to this end. Thus, this FOM complements the reliability property, discussed in Section 5.3.1, in achieving long engine life and therefore maximising the customer's return on investment.

Operating range, as depicted in Figure 5.13, is the allowable range of operation between surge and choke at any given speed [12]. In other words, this region acts as a locus of possible working points; the compressor may operate at without any alterations of the surge or choke regimes. The normal operating range for aero gas turbines is around 6% at design speed.

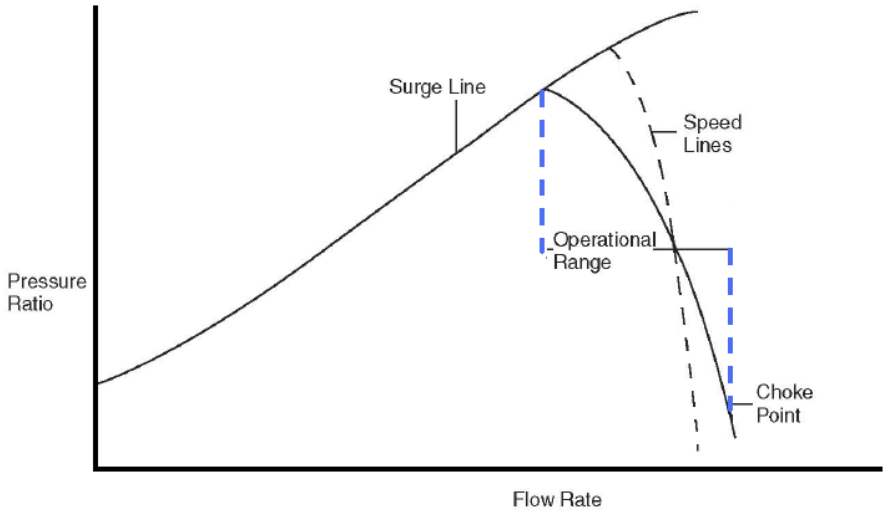

Figure 5.13: Operating range, obtained from [12]

The surge line tends to degrade over time due to dirt or blade damage incurred from foreign or possibly even internal objects. The most common cause of blade damage in aero engines is due to bird strikes. Furthermore, some magnitude in blade damage is usually tolerated to improve the engine's dispatch capability. This issue is very important for short haul engines, which tend to accumulate more takeoffs and landings, compared to longer-haul engines. This

is because, the occurrence of bird strikes below 2km altitude, increases dramatically; hence, if no allowance is given, any bird strike, no matter how damaging, would ground the aircraft until the proper spares are installed.

If designed accordingly, a larger operating range may allow more surge line deterioration and thus a better dispatch capability. This is due to the fact that the compressor operating point may be matched at a slightly higher mass flow with minimal associated reduction in efficiency and PR. In such a case, less bleed or VSV action will be required which will also improve the engine's initial and on-line performance.

Furthermore, due to the shape of the efficiency contours depicted in Figure 3.10, a flatter speed line characteristic, such as the case with a large operating range, causes a smaller efficiency penalty during working line transients. This implies that, if the working line migrates from the design condition, such as for example due to engine degradation [19] or operating altitude variations [17], the compressor efficiency will be relatively unchanged.

Boyce [12], outlines how high PR compressors tend to have a small operating range as depicted by the dashed line in Figure 5.13. Therefore, because of this fact, operating range issues concern mostly HPCs and not so much LPCs. Table 5.9 summarises the results relating to this work. Also, as outlined in the following table, it must be noted that, operational range is assessed as a relative rather than an exact measure. This is because, the exact compressor characteristic, would be hard to predict at this stage in the design process. The assessment listed in the Table 5.9 is based on a personal interpretation of the results in accordance with the theory discussed above. Nevertheless, some manufacturers may adopt a technique whereby the compressor characteristic of a similar existing compressor is adjusted, through empirical techniques to try and predict the behaviour of the new machine. Needless to say that, this level of detail and precision is hardly required for the purposes of this study.

Compressor	HPC PR	Relative operational range
C2/101_10	6.15	Large
C2/101_13	6.47	Large
C2/101_16	8.40	Medium

Table 5.9: Relative operational range

From the results depicted in the above table, it can be noted that operational range issues are not critical within any of the examined compressors because the PR is relatively low in each and every one. The 6% nominal operating range listed above should be achieved in each and every one. However, configuration numbers 10 and 13 appear to sustain a better operational range and hence are the preferred designs in this regard.

Furthermore, the ability of an engine to retain a minimum guaranteed performance when in service depends also on two other important factors. These, as explained by Pickerell [20], are the preservation of small tip clearance between the aerofoils and the static casings and secondly the retention of the aerofoil's profile, especially when operating in supersonic flow.

Incidentally, a shorter compressor, as discussed in Section 5.3.2, implies also a more rigid construction having the minimum axial distance between the aerofoils and the bearing supports. This fact also helps to maintain the required level of tip clearance as transient out of balance loads are reduced to a minimum. Such loads, if left uncontrolled, may induce tip shrubs which are the prime contributor to the increase in tip clearance over time.

Furthermore, the importance of a short LPC is considered more critical than that corresponding to a HPC because the former is usually cantilevered from the front bearing support and is thus more prone to radial displacements and hence aerofoil rubs. The corresponding LPC lengths are depicted in Figure 5.10.

Modern designs tend to incorporate rotor active clearance control. This is a system whereby, the HPC rotor casing is thermally controlled, with the use of bleed air, to adjust the expansion and contraction during transients. Thus, the rotor clearances can be maintained to a minimum during the entire engine operating range. This system, which can be incorporated onto any examined compressor design, improves compressor reliability and performance retention.

In addition to the above arguments, all compressor blades, especially those pertaining to the LPC, should be designed with a substantial thickness to chord ratio (t_b/c) and possess the required minimum blade leading edge radius to resist erosion. However, these criteria are not design specific because such attributes can be incorporated within any final design.

Considering all of the above arguments, it is thought that configuration 13 appears to have the best overall attributes and is thus the preferred design for compressor performance retention.

5.3.5 Low cost of ownership

The prime endeavour of any airline operation is to profit financially from its service. Unfortunately this type of business suffers from a very low profit to revenue ratio, especially compared to other customer service operations. It is therefore understandable that, any major purchase decision, such as an airframe powerplant, will be biased towards maximising the return on investment. This reality impacts the engine manufacturer in the design decisions that need to be taken to provide an engine, possessing the required level of reliability, at lowest possible cost of ownership.

The cost of ownership depends on initial purchase price and any additional recurring expenses such as fuel usage and maintenance costs. With regards to the latter, fuel burn is a factor of the engine's overall efficiency, as defined by Equation 3.4, and the propulsion system weight. Also, the information provided within Tables 1.3 and 4.3 suggest how the performance of the proposed new engine matches or exceeds that offered by current production engines in this category. Furthermore, if it assumed that the compressor weight is 50% of the gas generator weight, data provided by Gerend *et al.* [68] suggests that the total engine weight, for any of the three alternative designs being studied within this report, will be in the region of 1900kgs. If configuration 10 were to be chosen, the final engine weight will slightly exceed this figure, however, it is expected that the excess weight will be counterbalanced by a slightly better thermal efficiency. This magnitude, as evidenced by Table 1.3, also compares favourably with the other engines currently available on the market. Thus, it can be expected that the fuel burn of the new engine will be lower than that offered by any other engine currently in production for this type of aircraft.

Furthermore, maintenance related costs is a complex issue to quantify since it depends a great deal on the spares supply chain, the contract that is signed between the customer and the manufacturer and the level of experience the airline maintenance engineers have on this subject, and specifically on this type of engine. However, in spite of the lack of information that is available, any powerplant which offers good reliability and performance retention and a long overhaul life, coupled with a sound maintenance schedule will surely benefit the customer with a reduced expenditure. Each one of these subjects has been discussed in the

former sections of this chapter; hence the chosen design should present no significant hurdles in developing a fine engine, worthy of today's expectations.

Finally, the initial purchase price is the last part of the chain affecting the customer's engine related costs. This price is intractably related to the manufacturer's production process and capabilities. However, if one were to neglect the manufacturer's cost base, which varies drastically from country to country, the ability to produce a given engine at a reasonably price depends, to a large extent, on the number of engines that will eventually be produced as the design and development costs can then be shared between a larger amount of units. Moreover, the unit costs tend to reduce with time as the personnel and production line become more adapted and efficient in building the new engine. Furthermore, it is in the manufacturers' intent to try and adapt a given design to match the needs of a different aircraft with the least amount of modifications possible. This philosophy is very common in industry and has led to some very successful engines being developed with the minimum amount of time and effort. One notable case is the CFM56 which has a core adapted from the F101 military engine powering the B-1 bomber [2]. This approach also strives to increase the number of units produced hence collectively lowering the price of the different engines.

Fortunately, it transpires that, configuration number 13 offers real potential of adapting the HPC of this design to suit an engine of higher PR, possibly for a longer range aircraft, requiring better thermal efficiency. It is noted that if a zero stage is added in front of this compressor, the new design would be capable of delivering a 7.8 PR at a very satisfactory 90% efficiency. This compressor will then be suited for an engine requiring a PR of around 40 which is thought beneficial for a medium to long range aircraft such as the B767 or A330.

On the other hand, the HPC of configuration 10 will probably require an additional, highly loaded stage to match this performance, which will make it inefficient and thus unsuited for a longer range aircraft. Also, it appears that configuration 16 is too highly loaded to make it attractive for a more efficient, long haul engine. It is anticipated that, to make this design suitable for such an engine, the entire HPC will have to be redesigned to a lower PR by lowering the average stage loading, hence increasing the efficiency. Both of these alternatives offer a more expensive solution compared to the elegant redesign possible with configuration 13.

To conclude, it appears that the latter configuration possesses all the qualities required to make the final design financially attractive to the customer. Fuel burn, maintenance related costs and initial purchase price have all been considered hence the final design should offer a cost effective solution.

5.4 Finalised design

Based on the arguments raised in latter two sections of this chapter, it was concluded that C2/101_13 possesses the best overall attributes, amongst all the alternative designs, in meeting or exceeding the requirements outlined in Chapter 4.

Configuration 16 is considered too highly loaded to provide an adequate overall performance as offered by the other two designs. However, it must be noted that this design has the advantage of requiring one less turbine stage compared to the C2/101_13; hence the LPT of the former may potentially be significantly lighter, albeit at a slightly worse efficiency. Furthermore, configuration 10 also offers satisfactory performance and it even surpasses the chosen design in the efficiency estimates of the compressor and turbine modules. However, it was concluded that C2/101_13 outperforms this design in length and weight predictions and may also offer the customer a lower cost of ownership. These factors combined, led to configuration 13 being chosen as the preferred design, considered worthy of being investigated further in a more detailed design study.

Outlined below is a summary of the results generated during preliminary design pertaining to C2/101_13.

Compressor	No. of stages	Mean stage loading	Efficiency potential	No. of variable stages	Weight (kg)	Length (m)
LPC	4	0.33	0.88	0	221	0.42
HPC	9	0.32	0.89	4	295	0.53

Table 5.10: C2/101_13 result summary

Furthermore, even though turbine design is not considered part of this dissertation, the preliminary turbine design criteria relating to this configuration are outlined in Table 5.6.

5.4.1 Stage by stage aerodynamic design

This section will examine a stage by stage aerodynamic design of the chosen configuration. The majority of the data has been obtained through the use of Turbodev using the methodology outlined throughout the previous sections of this thesis. Also, the stage loading along the compressor has been refined to obtain a better, and more realistic, value of stage efficiency and overall compressor performance. Moreover, this data represents the final result from preliminary design within this thesis and should provide the engineers with sufficient and reliable information, allowing them to further examine this compressor within the subsequent stages of engine development as outlined in Figure 3.4.

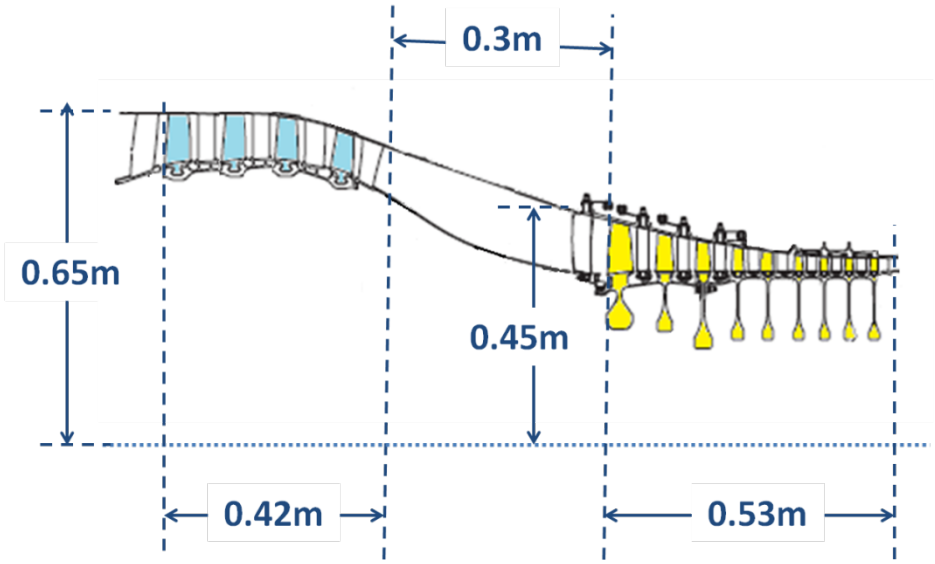

Figure 5.14: C2/101_13 configuration layout and dimensions

Note that the data presented herein is only a summary of that available in Appendix A.3. The reader is referred to this appendix for a more thorough list of all the information generated during this exercise.

LPC/booster

Mass flow	20kg/s	**PR**	3.8
Efficiency	90%	**Mean stage loading**	0.33
Length	0.43m	**Weight**	223kg
Annulus type	Constant hub line	**Number of stages**	4

Table 5.11: LPC/Booster performance summary

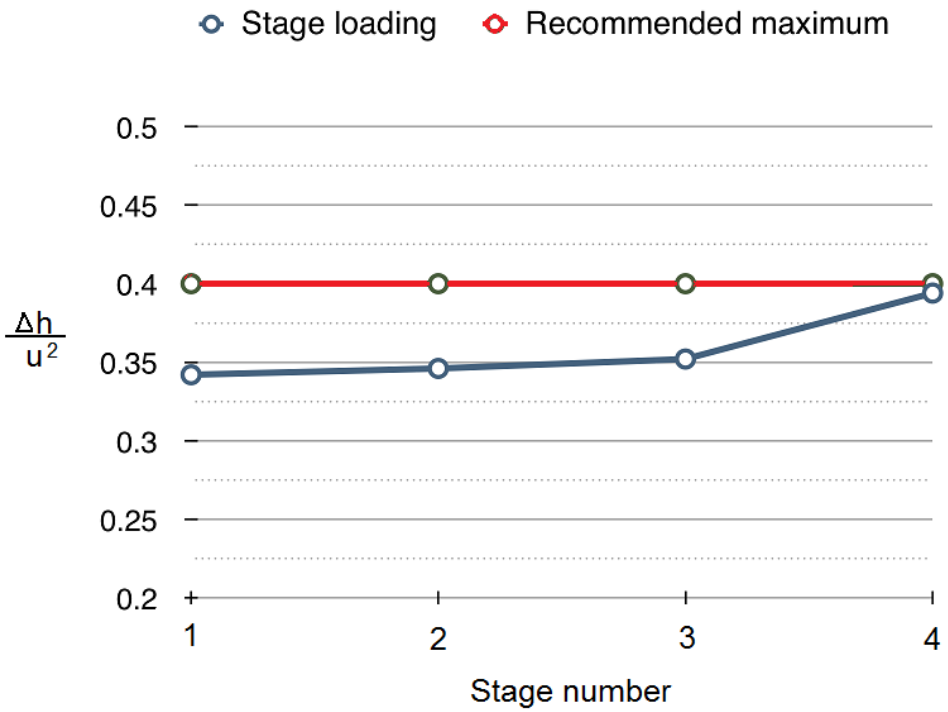

Figure 5.15: C2/101_13 LPC stage loading distribution

Note

i. *The recommended maximum stage loading* $\left(\Delta h/_{u^2}\right)$ *of 0.4 is derived from Figure 3.15. This value is the maximum for which an efficiency of 0.89 is realistically achievable.*

Note that the LPC efficiency outlined in Table 5.11 varies slightly from the value quoted in the earlier sections of this chapter due to the fact that, during the more thorough design analysis conducted at this stage, the compressor stage work was modified slightly, along the length of the compressor, to better match the stage loadings thus yielding an overall efficiency improvement of two percentage points. As a consequence of this change, the LPC length and weight have increased slightly by 0.1m and 2kg respectively. These minor drawbacks were deemed justifiable, owing to the improvement in efficiency and overall performance.

Furthermore, with reference to Appendix A.3, it is noteworthy that, because of the chosen vortex type, the stators can be approximated to constant camber blades. This may imply lower manufacturing costs; however, for an aero engine, normal variable camber blades will be used to maximise efficiency and performance. Nevertheless, this attribute may prove useful if an industrial version of this compressor, or the HPC, is developed in the future. The small penalty in efficiency and performance is normally justified for industrial use.

Finally, it is of interest to observe that the fourth stage of this compressor is quite highly loaded to achieve a near axial outlet flow. Due to this fact, the flow has a significant deviation at outlet from the stator, possibly indicating a stalled region. The flow direction at exit was predicted to be 1^{o} from the axial direction, hence the total deviation at stator outlet is in the region of 10^{o}. Moreover, the relatively high exit flow coefficient, which was required to keep the blade diffusion at an acceptable level, may cause higher than predicted inter-compressor duct pressure loss. It is anticipated that, the geometry of this stage may be refined slightly during detailed design, with the aid of more precise means such as CFD, to achieve a better overall performance and a more stable operation.

HPC

Mass flow	20kg/s	**PR**	6.47
Efficiency	89%	**Mean stage loading**	0.32
Length	0.53m	**Weight**	293kg
Annulus type	Constant casing line	**Number of stages**	9

Table 5.12: HPC performance summary

It is noteworthy that, even though a minor improvement, the HPC weight was decreased by 2kg from the previous estimates, thus compensating for the LPC weight increment. Furthermore, the data within Appendix A.3 indicates that stage 6 of this compressor is expected to achieve 90% efficiency. Nevertheless this magnitude is thought to be slightly optimistic due to the moderately large DFs within this stage. Even if this stage attains a more realistic value of 89% efficiency, the overall compressor performance should remain largely unchanged.

Furthermore, the LPC and stages 1-4 of the HPC can be manufactured from titanium composites thus reducing weight and cost. However, the use of nickel alloys will be required from stage 5 onwards due to the predominantly high temperatures.

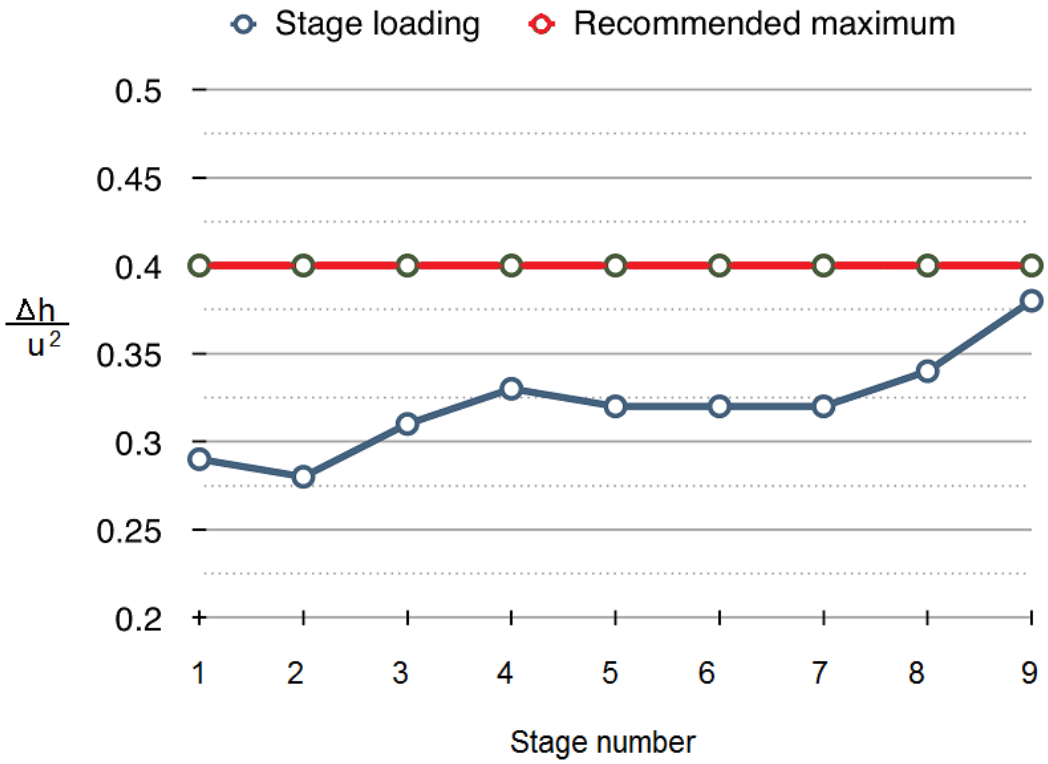

Figure 5.16: C2/101_13 HPC stage loading distribution

Note

i. *The recommended maximum stage loading* $\left(\Delta h/u^2\right)$ *of 0.4 is derived from Figure 3.15. This value is the maximum for which an efficiency of 0.89 is realistically achievable.*

To conclude, the rotor within Stage 9, is noted to be quite highly staggered, thus making it susceptible to all the performance related issues discussed within Section 3.5.2. A notable attribute of highly staggered blades is that they suffer from a low chocking mass flow. Furthermore, it is anticipated that the flow temperature rise of stage 4 may have to be decreased somewhat to offload this stage. This would be beneficial due to the fact that this is the first stage employing fixed stators; hence, the blade geometry will least conform to the actual flow characteristics at off design. In addition to the above arguments, it is apparent that the final stages are again quite highly loaded thus may affect negatively the performance of the diffuser and combustor. Nevertheless, this compressor layout is expected to sustain good overall performance, and all the aforementioned deficiencies can be tackled during detailed design to limit their performance penalty.

The data within Appendix A.3 encompasses the final results from preliminary design. Sufficient data has been acquired to enable any design bureau to conduct a proper and thorough detailed aerodynamic and mechanical design of this proposed compressor configuration.

5.4.2 Design point exchange rates

The section will examine the performance related issues associated with an underachieving, or possibly, overachieving final design. A design point analysis study has been conducted through which, the penalty or surplus in engine efficiency and thrust, induced by a variation of the final component efficiency from that predicted in the previous section, is quantified.

This study is important because it highlights the importance of having the final compressor design achieve the above listed performance levels. If the final design, were to underachieve, the whole engine will underperform, necessitating a higher fuel flow for the required level of thrust, reducing engine life and performance.

A significant variation in efficiency margins of the compressor between preliminary and detailed design is not uncommon unfortunately. A recent case study was discussed in Section 3.2.6.1, wherein the efficiency of the IAE V2500 HPC underperformed by 2.3% from the

initial estimates [26]. This led to a major alteration of the compressor layout, necessitating a longer and more expensive engine development programme.

For the purposes of this study only the design point exchange rates associated with the compressor have been examined, assuming that all the other components perform as outlined in Chapter 4. The only exception was the turbine performance, for which the assumed efficiency was derived from Table 5.6.

	Datum value (%)	Change in value (% points)	sfc_{cruise} (%)	Specific thrust (%)
LPC	90	+1	-0.12	+0.54
		-1	+0.14	-0.57
HPC	89	+1	-0.21	+0.81
		-1	+0.24	-0.85

Table 5.13: E2/101 design point exchange rates at 11,000m ISA 0.8M.

Notes

ii. Specific thrust is equivalent to $^{engine\ net\ thrust}/_{air\ mass\ flow}$.

iii. Design point sfc_{cruise} *and specific thrust are equal to* $1.82x10^{-5}$*(kg/s)/N and 174.4Ns/kg respectively.*

It is noteworthy to mention that if the expected efficiency levels are realised, the sfc_{cruise} will be $1.82x10^{-5}$(kg/s)/N. This magnitude represents an improvement of 1.6% compared to the requirement outlined in Table 4.3. This is a very welcome conclusion, considering that each percentage point in sfc results in millions of dollars of fuel savings for the airlines each year.

Finally, the results outlined in Table 5.13, conform to the observations made in Section 1.4, whereby the performance of the HPC is normally the most critical. This results from the fact that the HPC normally imparts a large work input to the flow and hence, even a small degradation in the performance of this component has a noticeable impact on the engine's overall operation. Moreover, the broad performance of compressor C2/101_13 is thought to represent a general improvement over the current production engines available on the ERJ190 and should be a good candidate for future study and possible commercial development.

INTENTIONALLY LEFT BLANK

Chapter 6

Concluding remarks

6.1

- Work overview
- Turbomachinery preliminary design tool
- Work objectives review
- Compressor comparative design and conclusions
- Future work
- Work contribution

6.1 Work overview

This dissertation concerned a compressor design optimisation task intended for a short-haul aircraft, namely the ERJ-190. A market research confirmed the opportunity for a commercially viable engine within the 20Klbf thrust category. Current production engines are relatively dated; hence it is likely that the market will welcome a new powerplant possessing a general overall improvement in performance and reliability. Also, in addition to several new aircraft in production or in the final phases of development that will require powerplants within this category, Embraer is also considering re-powering their E-Jet family using more modern and efficient engines [70]. All these arguments combined, empower the belief that a newly developed engine can be designed and be profitable within this thrust category.

The assumed engine specifications have been outlined in Chapter 4 of this dissertation. The hypothetical engine, named E2/101, was conceived to outline the compressor working environment. Also, this engine is thought to represent a natural but conservative evolution compared to current in-service engines. It is expected that the market will be more receptive to a conservative but reliable design, based on proven technology, rather than a radical, highly developed engine. This is due to the fact that reliability concerns for short-haul engines are deemed very important due to the nature of the airline operation. Therefore, the engine specifications utilised within this report, are thought to be representative of a realistic new powerplant for this type of aircraft.

Furthermore, a literature review chapter thoroughly describes all the technical aspects necessary for understanding the substance of this thesis. Incorporated within this section are all the assumptions and justifications used for the examination of the flow within turbomachines. The chosen method of analysis is biased towards empirical correlations, derived from experiments having similar component geometry and flow conditions to that studied within this report. Even though the majority of the correlations were obtained from experiments conducted in the early 1970s and 80s, the results are thought to be representative of modern compressors. When this assumption was violated, correction factors were applied to the correlations, to adjust the outcome to better represent modern designs.

Moreover, the general approach used to solving the preliminary design task is similar to that actually conducted within any aero engine design organisation; however, it has been slightly modified to better suit the author's capabilities and pool of knowledge. Nevertheless, this dissertation should have exposed the reader to a realistic engine development experience.

6.1.1 Turbomachinery preliminary design tool

A compressor design and layout has been suggested which, is believed, will be capable of delivering the required work input for the requisite efficiency and performance level. For this aim, a turbomachinery design code, named Turbodev, was developed using Microsoft Excel. This is capable of analysing a chosen compressor or turbine design and provides the user with a detailed performance and geometrical analysis.

Turbodev is specifically catered for turbomachinery preliminary design and is composed of several inter-linked modules. It must be emphasized that, unlike other software, Turbodev, does not incorporate whole engine modelling, but was designed to specifically handle either the compressor or turbine modules of the gas turbine powerplant. When whole engine cycle modelling was required, as was the case in Chapter 4, the author referred to Turbomatch [71].

The Turbodev compression module can handle most types of compressor geometries. Some of its capabilities are the support of the following.

- LPC/IPC and HPC modules
- Inter-compressor duct pressure losses
- Constant hub/casing and pitchline compressors
- Upstream compressor(s) inefficiency
- Varying stage loading along the compressor length
- Flow and blade computation at casing, hub and pitchline
- Inter and outlet compressor bleed

Furthermore, the computations incorporated within Turbodev are all based on the theory presented in the literature review of this dissertation. Also, the efficiency level predicted by this program is thought to be highly realistic and achievable using current engineering

practice. Moreover, an efficiency validation exercise was successfully concluded and showed very satisfactory results.

6.1.2 Work objectives review

It is believed that the overall work, as documented within this thesis, satisfies the work objectives outlined in Chapter 2.

1. The data tabulated within Chapter 4, together with Section 5.2.2, acknowledges the first objective outlined in the aforementioned chapter. The boundary conditions are explicitly well defined and justified.
2. The establishment of the compressor figure of merits, as stipulated by the second objective, is documented in Section 5.1. Moreover, the subsequent sections of Chapter 5 discuss, in a thorough manner, these objectives and the rational used for prioritising them.
3. Section 5.2 lists all the candidate compressor configurations, thus satisfying the third objective. A total of sixteen different designs were considered.
4. A new preliminary design tool, as reported in Section 5.2.1, and summarised above, has been developed to assess the initial candidate designs thus concluding Objective 4.
5. Finally, the last objective was acknowledged in Section 5.4. The chosen design was evaluated against all the initial parameters as outlined in Chapter 4.

6.1.3 Compressor comparitive design and conclusions

The aim of preliminary design in any engine development endeavour is to propose suitable component geometry based on an initial assessment amongst all the different alternatives. The compressor preliminary design documented within this dissertation follows a similar methodology and specifies a final compression layout from an initial of sixteen different propositions. The selection process was based on a set of different criteria, referred to as

Figure of Merits (FOMs), classified in accordance of importance. The chosen FOMs are listed below.

- Efficiency potential
- Turbine requirements
- Reliability and long life
- Compressor length and weight
- Off design considerations
- Operating range and performance retention
- Low cost of ownership

The selection process within this report was based on a two step process. The first, or preliminary assessment, identified the three most suitable designs amongst the initial sixteen contenders. The first two FOMs listed above were used as the sole criteria for this purpose. The three chosen designs consisted of a lightly loaded but efficient design, a highly loaded and a mid-level loading design. It was also noted that each of these imposed no significant performance penalty on the corresponding driving turbines, hence were found suitable to be more thoroughly studied in a second, or detailed, analysis.

Further work then concentrated only on the three latter designs, identified as configurations 10, 13 and 16. This approach towards identifying the preferred compressor layout was chosen because it is was deemed a good compromise between development time consumption and proper result realisation. It was noted in an earlier section that, by using this approach, the author could dedicate more time and energy on the three most promising contenders rather than having to conduct a full preliminary design analysis on all the sixteen contenders. Also, since a more thorough investigation was conducted on these three designs, than would have been possible if all the sixteen contenders were examined in detail, the results achieved from this approach are thought to be meaningful and possibly more realistic.

The detailed analysis suggested configuration 13, possessing a mid-level loading and efficiency promises to achieve the best overall performance amongst the three finalists. This configuration appears to provide a fine compromise between performance and mechanical requirements. Also, it is predicted that the proposed new engine shall provide a 13% reduction in sfc compared to current production engines. This magnitude, is suggested by

Trimble [72], as being the required "magic number" for launching a new propulsion system and is also similar to the improvement advertised by CFM for their new CFM Leap engine [73] when compared to the previous model. More so, such an improvement in fuel efficiency will certainly help towards achieving the ICAO 2050 benchmark for reducing carbon dioxide emissions [72].

The compressor stages of this configuration are moderately loaded, however even though some of stages appear to be over-stressed, the minimum predicted de Haller number is 0.62. This magnitude suggests the existence of stalled flow; however, this was deemed satisfactory for the intent of preliminary design. This is because, modern compressor designs may adopt three-dimensional blade characteristics, such as sweep and lean, which suppress stall and may tolerate higher diffusion limits than is traditionally accepted. The 0.7 de Haller limit was adopted from diffuser analogy, before the advent of modern technologies, hence this magnitude is considered more as a guideline than an actual constraint.

Furthermore, this configuration provides the shortest alternative amongst the three chosen designs. The overall compressor length of 1.25m is very reasonable for this type of engine and allows for the development of a stiff, two frame engine design with minimum spacing between the two supports. This characteristic reduces the tendency for tip rubs and thus prolongs engine life.

In addition to the above arguments, the off-design performance of this compressor appears to be respectable. It is predicted that the HPC will require four variable stages, including one inlet guide vane. Also, moderate use of bleed air is expected to be required to alleviate the drop in PR across this compressor when operating at low speed. However, the use of this bleed air should not be excessive, and considering that it is only required at relatively low speeds, the penalty associated with its use is acceptable.

Moreover, it has been shown that the HPC of this configuration can be easily adapted to suit a higher PR engine by installing a zero stage in front of the existing nine stages. This will make it attractive for a medium/long range aircraft such as the B757/A330, thus possibly, increasing its demand and hence commercial advantage. Also, the constant reaction design allows for constant camber stators, which may prove beneficial if an industrial version of this

compressor is eventually developed. This feature may reduce manufacturing costs but imposes a marginal efficiency and performance penalty.

In conclusion, the overall design process, documented herein, has been tackled in a pragmatic manner as much as possible. The use of bleed air for aircraft requirements and turbine cooling has been factored in accordance with the principles laid out in [7]. Also, the HPT power requirement considered the need for accessory and generator drive power; hence, the loading and efficiency predictions of the latter were more reliable. Finally, the use of moderate turbine inlet temperature and overall pressure ratio, allow room for further power growth and efficiency improvement if the need arises. All these factors combined, provide a realistic engine development experience and exposed the reader to all the constraints and merits an engine manufacturer is confronted with whilst developing a new, or possibly, modified engine component.

6.1.4 Future work

In spite of the fact that, by and large, the work objectives of this work have been achieved, further work is thought necessary to expand the knowledge of this subject within the public domain.

A more thorough examination of the compressor design figure of merits should yield more insight into the development constraints and concessions pertaining to short-haul operation. The similarity, or lack thereof, between this type of flight profile and long-haul operation, and the resulting influence on compressor design, may become more evident and will further expand the non-proprietary literature which is currently available on this matter.

Moreover, the use of Turbodev, for academic purposes, may become more useful and generic if further work is conducted to enhance the modules to make the system more versatile and competent. The turbine module in particular, is currently at a very early stage of development. This system may also be interlinked with Turbomatch, or any other whole engine modelling software, to make it more user-friendly and quick to use.

6.1.5 Work contribution

It is the author's belief that this work elucidated compromises imposed within any real life compressor design study. Important aspects related to compressor preliminary design, which are not normally available in the public domain, have been discussed and tackled using only limited non-proprietary knowledge available to the author. Aspects such as cost of ownership, reliability and performance retention have been addressed and a measure of their influence on any given design has been devised.

In conclusion, the material contained within this dissertation, combined with the developed turbomachinery preliminary design tool, achieve the aim of presenting a realistic compressor comparative design study as stipulated by the work objective.

Appendix

A.1
- Engine station numbering

A.2
- Lieblein's Diffusion Factor
- Loss correlations with Diffusion Factor

A.3
- Compressor C2/101_13 stage design

A.4
- ASME paper

A.1 Engine station numbering

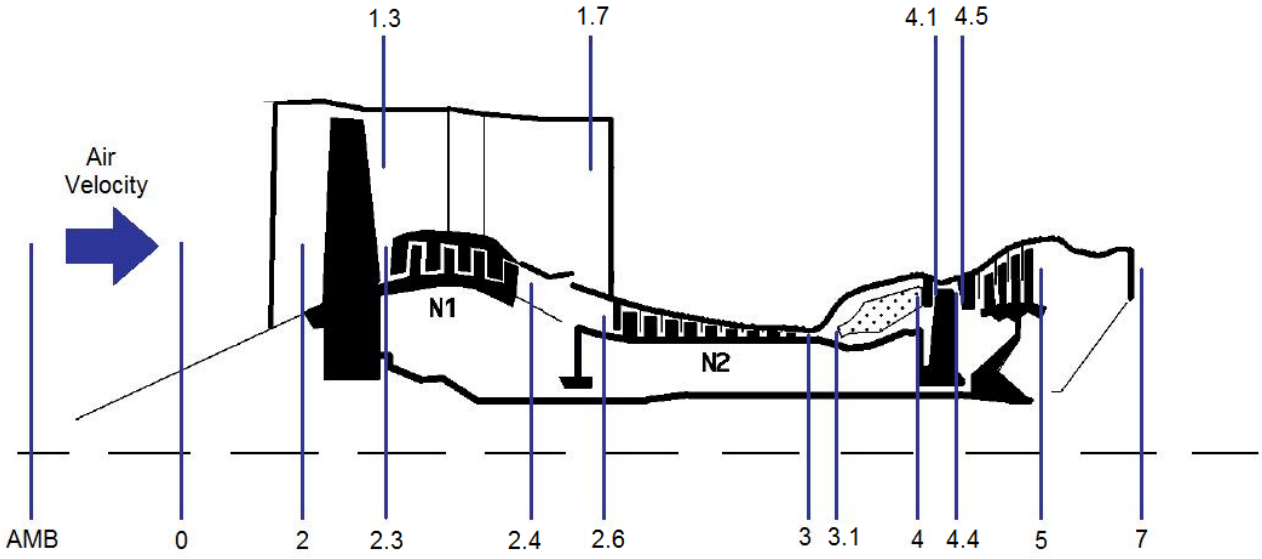

Figure A.1: Engine station numbering, modified from [59]

The engine station numbering utilised in this dissertation and Turbodev conforms to the ARP755A standard outlined in [74]. With reference to Figure A.1, the following is a list of the station numbering used throughout this report. Note that some of the station numbers are missing in the above diagram but are nevertheless mentioned below.

AMB	Ambient Conditions
0	Ram conditions in free stream
1	Engine intake leading edge
2	Fan front face
1.3	Fan exit bypass stream
2.3	Fan exit core stream
1.7	Bypass propelling nozzle inlet
2.4	First compressor exit
2.6	Second compressor front face
3	Last compressor exit face
3.1	Diffuser exit, combustor inlet

4	Combustor exit plane, first turbine nozzle guide vane leading edge
4.0.5	First turbine nozzle guide vane throat
4.1	Stator outlet temperature
4.4	First turbine exit
4.5	Second turbine nozzle guide vane leading edge
5	Last turbine exit face
7	Core propelling nozzle inlet

Table A.1: Engine station numbering; data obtained from [74]

A.2 Lieblein's Diffusion Factor

Lieblein investigated the loading limit for compressor cascades by initially considering a separation criterion for two dimensional, incompressible, turbulent boundary layer flow [50] as indicated in Equation A.1.

$$D = -\frac{\theta}{V}\frac{dW}{dx}Re^{n} \qquad \textit{(equation A.1)}$$

This criterion was then eventually developed into the familiar Diffusion Factor (DF).

$$DF = \left[1 - \frac{W_2}{W_1}\right] + \frac{\Delta W_\theta}{2\sigma W_1} \qquad \textit{(equation A.2)}$$

This suction surface DF is a function of two principal factors, the overall change in relative velocity through the blade row and a term proportional to the lift coefficient.

The assumptions for deriving the DF from the initial separation criterion were the following:

1. The flow was presupposed to be two-dimensional and incompressible since the original criterion also embodied these assumptions. In fact, this means that DF represents best the mid-passage (two-dimensional) flow and is not representative of the actual end-wall (three-dimensional) loading.

2. The ratio of $\frac{Distance\ of\ Vmax\ from\ blade\ LE}{Chord\ length}$ was assumed not to vary between different blade profiles at different loadings.

3. Boundary layer Reynolds's number was considered not to vary between different blade profile types and for any surface roughness, turbulence level, inlet Mach number and blade size.

4. W_2 at blade trailing edge was equal to mean W_2 from blade velocity diagram.

5. The velocity on the suction surface varied linearly from W_{max} to W_2. This assumption was substantiated by reports from the NACA Langley research laboratory which

indicated that it is the overall diffusion ($W_{MAX} - W_2$) that is the more significant factor and not the velocity gradient on the suction surface.

6. Average velocity between W_{max} and W_2 was equal to W_1.

7. A relationship between the velocity ratio ($^{W_{max}}/_{W_1}$) and a circulation parameter ($^{\Delta W_\theta}/_{\sigma W_1}$) was conceived in the form of, $\frac{Wmax}{W_1} - 1 = b\frac{\Delta W_\theta}{\sigma W_1} + d$, were d represents the suction surface velocity rise due to the affect of finite blade thickness. This expression was obtained from test results published in [44] using NACA65 blades with the following attributes:

   - The t_b/c was 0.1.
   - The testing was conducted at the optimum angle of attack according to Emery *at al.* which is basically that which gives a smooth pressure distribution on the suction surface. Cumpsty [25], has shown that both this optimum and Lieblein's optimum incidence are almost exactly the same and thus may be interchanged without much loss in accuracy.
   - The pressure distribution results were obtained from cascades and not from actual compressor configurations. However, Westphal *et al.* [75] concluded that the pressure distributions on the suction surface in actual compressor blades were similar to that observed in cascades.
   - The blades used in the tests had solidities which varied from 1.0 to 1.5.
   - The speed range used in the analysis was considered to be entirely incompressible. In fact, the Mach number was in the range of 0.1.

   Furthermore, Lieblein *et al.* assumed that the local pressure coefficient and the circulation parameter varied in the same manner with Mach number according to the Prandtl-Glauert relationship which is valid up to Mach numbers of around 0.75. This led to the conclusion that both b and d are relatively constant up to this speed.

   Finally, it was thought that the thickness and thickness distribution of commonly used compressor blades did not vary much from the test conditions hence the affect of 'd' on the given blade profile was also neglected.

8. The ratio of θ/c was considered to remain constant for all blade types and loadings.

The DF was in mainstream use by 1960s; however, because of the aforementioned assumptions, this parameter suffers from several limitations which are listed below.

1. It does not consider blade maximum thickness and the thickness distribution. It is known that lower thickness/chord (t_b/c) ratios yield less suction surface loadings. However, DF was formulated from blades which had a NACA65 profile and a t_b/c of 0.1. The change of suction surface loading with blade maximum thickness is however, thought to be small, especially for a low DF. At higher loadings, the affect of blade thickness increases but the error incurred by not including it is small compared to the other assumptions.

2. This parameter neglects inlet Mach number affects even though increasing the inlet Mach number, increases exponentially the blade loading for a given DF.

3. Aspect ratio is not considered since DF was conceived from a two-dimensional stalling parameter, representative only of the mid-passage loading.

4. DF was originally intended for use at the minimum loss incidence condition only. Lieblein, aware of this shortcoming, derived D_{eq} which considers both the minimum loss incidence condition and other positive incidences.

$$D_{eq} = \frac{W_{m1}}{W_{m2}} \frac{cos\beta_2}{cos\beta_1} \left[\frac{W_{MAX}}{W_1}\right] \qquad \textit{(equation A.3)}$$

W_{MAX}/W_1 was eventually correlated against NACA65 and C4 cascade test results conducted at Lieblein's design incidence.

$$\frac{W_{MAX}}{W_1} = 1.12 + 0.61 \frac{cos^2\beta_1}{\sigma} [tan\beta_1 - tan\beta_2] \qquad \textit{(equation A.4)}$$

Despite its merits, D_{eq} was mostly disregarded due to the fact that it is not well documented.

Originally, the DF was conceived because of the difficulty at the time in calculating the limiting suction surface velocity. Nowadays, this is more easily achieved with the use of CFD. Hence, a more meaningful loading parameter might be the local diffusion factor, D_{loc},

which was also suggested by Lieblein. D_{loc}, $\left(D_{loc} = \frac{W_{max} - W_2}{W_{max}}\right)$, more correctly quantifies the suction surface diffusion of a particular geometry.

A.2.1 Loss correlations with Diffusion Factor

Lieblein [51] also studied the affect of loss variation with DF. The loss considered by the author was derived from the total pressure deficit across the blade element. This pressure loss was assumed to include profile, trailing edge and wake mixing losses across the blade.

The loss versus loading data was obtained from a series of single stage rotor and stator experiments. The blades had a NACA65 profile with a t_b/c of between 0.05 and 0.1. Also, the aspect ratio in the experiments varied between 1.6 and 5.4.

Given that this data was obtained from two-dimensional cascade tests and single stage compressor stages, the limiting values of DF are mostly valid to the first stages of multi-stage compressors where the complex three-dimensional flow effects have the least impact. Also, no mention of the tip clearance magnitude was given in Lieblein's report; hence, caution needs to be exercised when applying the DF to blade sections near a blade tip as the reported results may be unrepresentative of modern compressor environments.

Furthermore, re-enforcing the fact that the DF only gives meaningful results at low Mach numbers, Lieblein also reported that his loading parameter should ideally only be used at subcritical Mach numbers. The critical Mach number, according to him, was that above which the losses increase substantially at a constant DF. The critical Mach number is reported to be around 0.7 for NACA65 blades with a t_b/c of 0.1.

Finally, Lieblein also studied the affect of Reynolds's number on loss at a set DF. The results indicate that the loss increases almost linearly with a reduction of Re. However, because the tests were carried out at a substantial Reynolds's number, the variation of this parameter in actual compressors should not cause significant error.

The results from these experiments are the DF limits listed in Table A.2.

Stator hub/mean/tip sections	0.6
Rotor hub/mean sections	0.6
Rotor tip	0.4

Table A.2: Diffusion limits; data obtained from [7]

A.3 Compressor C2/101_13 stage design

The information listed herein includes a detailed stage by stage mechanical design of the proposed compressor configuration. Most of the information has been obtained through the use of Turbodev.

LPC/booster

Mass flow	20kg/s	**PR**	3.8
Efficiency	90%	**Mean stage loading**	0.33
Length	0.43m	**Weight**	223kg
Annulus type	Constant hub line	**Number of stages**	4

Stage 1

Stage efficiency	0.89	**Stage temperature rise**	35.8°
		Rotor	**Stator**
Blade number		134	137
DF pitchline		0.49	0.49
σ pitchline		1.41	1.28
ξ		50°	50°
Blade inlet angle casing		62°	59°
Blade inlet angle pitchline		59°	60°
Blade inlet angle hub		54°	61°
Blade outlet angle casing		49°	39°
Blade outlet angle pitchline		41°	41°
Blade outlet angle hub		30°	43°

Stage 2

Stage efficiency	0.90	**Stage temperature rise**	35.2°
		Rotor	**Stator**
Blade number		123	127

DF pitchline	0.53	0.53
σ pitchline	1.14	1.05
ξ	51°	51°
Blade inlet angle casing	63°	60°
Blade inlet angle pitchline	61°	61°
Blade inlet angle hub	57°	62°
Blade outlet angle casing	47°	38°
Blade outlet angle pitchline	40°	40°
Blade outlet angle hub	30°	42°

Stage 3

Stage efficiency	0.90	**Stage temperature rise**	34.8°
		Rotor	**Stator**
Blade number		165	170
DF pitchline		0.52	0.53
σ pitchline		1.53	1.41
ξ		49°	50°
Blade inlet angle casing		61°	58°
Blade inlet angle pitchline		58°	59°
Blade inlet angle hub		54°	60°
Blade outlet angle casing		48°	39°
Blade outlet angle pitchline		40°	41°
Blade outlet angle hub		31°	42°

Stage 4

Stage efficiency	0.89	**Stage temperature rise**	41.2°
		Rotor	**Stator**
Blade number		27	37
DF pitchline		0.51	0.56
σ pitchline		1.13	1.48
ξ		62°	19°
Blade inlet angle casing		69°	46°
Blade inlet angle pitchline		69°	47°

Blade inlet angle hub	63°	47°
Blade outlet angle casing	58°	-9°
Blade outlet angle pitchline	56°	-8°
Blade outlet angle hub	54°	-8°

Table A.3: LPC/Booster blade design

Note

i. *All angles listed in this table are referenced to the axial direction, as depicted in Figure 3.11.*

HPC

Mass flow	20kg/s	**PR**	6.47
Efficiency	89%	**Mean stage loading**	0.32
Length	0.53m	**Weight**	293kg
Annulus type	Constant casing line	**Number of stages**	9

Stage 1

Stage efficiency	0.89	**Stage temperature rise**	37.2°
		Rotor	**Variable Stator**
Blade number		149	158
DF pitchline		0.53	0.54
σ pitchline		1.29	1.25
ξ		50°	50°
Blade inlet angle casing		63°	59°
Blade inlet angle pitchline		61°	61°
Blade inlet angle hub		57°	62°
Blade outlet angle casing		46°	38°
Blade outlet angle pitchline		39°	39°
Blade outlet angle hub		30°	40°

Stage 2

Stage efficiency	0.89	**Stage temperature rise**	37.5°

	Rotor	Variable Stator
Blade number	170	180
DF pitchline	0.53	0.53
σ pitchline	1.35	1.31
ξ	50°	50°
Blade inlet angle casing	62°	60°
Blade inlet angle pitchline	61°	61°
Blade inlet angle hub	57°	62°
Blade outlet angle casing	46°	38°
Blade outlet angle pitchline	39°	39°
Blade outlet angle hub	31°	41°

Stage 3

Stage efficiency	0.89	**Stage temperature rise**	37.8°

	Rotor	Variable Stator
Blade number	183	205
DF pitchline	0.53	0.52
σ pitchline	1.33	1.37
ξ	50°	50°
Blade inlet angle casing	62°	60°
Blade inlet angle pitchline	61°	61°
Blade inlet angle hub	57°	61°
Blade outlet angle casing	46°	38°
Blade outlet angle pitchline	40°	39°
Blade outlet angle hub	32°	41°

Stage 4

Stage efficiency	0.89	**Stage temperature rise**	38.0°

	Rotor	Stator
Blade number	196	185
DF pitchline	0.53	0.55
σ pitchline	1.31	1.14
ξ	50°	51°

Blade inlet angle casing	62°	61°
Blade inlet angle pitchline	61°	62°
Blade inlet angle hub	58°	63°
Blade outlet angle casing	45°	38°
Blade outlet angle pitchline	40°	39°
Blade outlet angle hub	33°	40°

Stage 5

Stage efficiency	0.89	**Stage temperature rise**	38.2°
		Rotor	**Stator**
Blade number		199	220
DF pitchline		0.54	0.53
σ pitchline		1.23	1.26
ξ		51°	50°
Blade inlet angle casing		63°	61°
Blade inlet angle pitchline		61°	61°
Blade inlet angle hub		59°	62°
Blade outlet angle casing		45°	38°
Blade outlet angle pitchline		40°	40°
Blade outlet angle hub		33°	41°

Stage 6

Stage efficiency	0.90	**Stage temperature rise**	38.5°
		Rotor	**Stator**
Blade number		212	200
DF pitchline		0.54	0.56
σ pitchline		1.22	1.07
ξ		51°	51°
Blade inlet angle casing		63°	62°
Blade inlet angle pitchline		62°	63°
Blade inlet angle hub		59°	63°
Blade outlet angle casing		45°	38°
Blade outlet angle pitchline		40°	39°

Blade outlet angle hub		34°	40°

Stage 7

Stage efficiency	0.89	**Stage temperature rise**	38.6°
		Rotor	**Stator**
Blade number		238	221
DF pitchline		0.53	0.55
σ pitchline		1.27	1.12
ξ		51°	51°
Blade inlet angle casing		62°	62°
Blade inlet angle pitchline		61°	62°
Blade inlet angle hub		59°	63°
Blade outlet angle casing		45°	39°
Blade outlet angle pitchline		40°	40°
Blade outlet angle hub		35°	41°

Stage 8

Stage efficiency	0.89	**Stage temperature rise**	38.7°
		Rotor	**Stator**
Blade number		214	220
DF pitchline		0.56	0.56
σ pitchline		1.08	1.06
ξ		51°	51°
Blade inlet angle casing		64°	61°
Blade inlet angle pitchline		62°	63°
Blade inlet angle hub		60°	63°
Blade outlet angle casing		44°	39°
Blade outlet angle pitchline		40°	40°
Blade outlet angle hub		35°	41°

Stage 9

Stage efficiency	0.87	**Stage temperature rise**	46.6°
		Rotor	**Stator**
Blade number		56	83

DF pitchline	0.50	0.55
σ pitchline	1.21	1.71
ξ	64°	19°
Blade inlet angle casing	70°	46°
Blade inlet angle pitchline	69°	47°
Blade inlet angle hub	64°	47°
Blade outlet angle casing	60°	-5°
Blade outlet angle pitchline	58°	-5°
Blade outlet angle hub	57°	-5°

Table A.4: HPC blade design

Notes

i. *All angles listed in this table are referenced to the axial direction, as depicted in Figure 3.11.*

ii. *The data provided for the variable stages assume position at the design point. Off-design stagger angle is not computed.*

iii. *A VIGV, preceding the first rotor row, is required; however the data for this blade row is not documented. The aim of the VIGV is to alter the incoming flow direction to make it suitable for the rotor leading edge.*

A.4 ASME paper

This appendix is a copy of the ASME paper which was submitted in relation to the work outlined within this dissertation.

Proceedings of ASME Turbo Expo 2013: Power for Land, Sea and Air
GT2013, June 3-7, San Antonio, Texas, USA

GT2013-95749

A COMPRESSOR PRELIMINARY DESIGN ASSESSMENT CONSIDERATIONS ON THE COMPRESSION SYSTEM PRELIMINARY DESIGN OF A SHORT HAUL AIRCRAFT PROPULSION SYSTEM

Dr. Pavlos A. Zachos, Giovanni Piscopo
Department of Power and Propulsion
Cranfield University
College Road, Cranfield, MK430AL, UK

ABSTRACT

The preliminary design of turbomachinery components is a strongly affected by the application process. This paper documents a compressor comparative design assessment which was conducted with the intent of proposing a new propulsion system for use on short haul aircraft, similar to the Embraer E-Jet. This study establishes and discusses the compressor figures of merit pertaining to short haul operation and their influence on the desired compression layout.

A computational tool to undertake compressor designs is developed and validated against the NASA E3 published compressor layout. With the aid of this software, a few alternative compressor layouts that meet the established criteria are suggested.

The best candidates are highlighted and further studied in terms of individual design parameters such as temperature rise distribution, number of stages and off-design performance. The figures of merit that dictate particular design choices are highlighted and commented. The most advanced candidate design is found to yield a very respectable performance compared to current production engines of the same class. This fact, coupled with the forecast need for such an engine give merit to this work which is aimed to be used as an academic understanding of the design challenges confronting the short-haul engine design process.

NOMENCLATURE

β_1	Relative inlet flow angle
β_2	Relative outlet flow angle
c	Blade chord
D_{eq}	Lieblein's Equivalent Diffusion Factor
DF	Diffusion Factor
Dm	Compressor mean diameter
FOM	Figure of Merit
h	Blade height
K1, K2	Constants
Lc	Compressor length
M	Mach number
M_1	Inlet Mach number
M_{crit}	Critical Mach number
N	Number of stages
η_B	Blade row efficiency
η_p	Compressor stage efficiency
PR	Pressure ratio
ΔP_{th}	Stage theoretical pressure rise
s	Blade pitch
sfc	specific fuel consumption
T_b	Blade thickness
TIT	Turbine inlet temperature
V_1	Absolute flow velocity into blade row
V_2	Absolute flow velocity out of blade row
W_1	Relative flow velocity into blade row
W_2	Relative flow velocity out of blade row
$\overline{w}$	Loss coefficient
Wc	Compressor weight
σ	Blade solidity
Ψ_{mean}	Compressor mean stage loading
Λ	Stage reaction
ρ	Density

INTRODUCTION

The primary objective of this study was to investigate the short haul engine requirements and their effect on compressor design. This paper presents a summary of this work and is intended to provide the reader a general grasp of short haul compressor requirements and illustrate a design methodology that may be easily implemented and which may prove useful as an educational aid.

The great majority of academic engine development studies consider long haul operation where the importance of achieving a high level of propulsive efficiency predominates. Needless to say that this is a very important criterion in any engine development program; however, this emphasis shifts when dealing with short haul requirements. The latter type of activity necessitates frequent but short engine cycles and a significant amount of off-design operating time.

The gas turbine engine performs best at a predetermined operating point, such as cruise or top of climb thrust setting. All other operating conditions, or thrust requirements are satisfied at a somewhat lower performance. This latter mode of operation is called off-design.

To achieve this aim, a list of compressor design figures of merit (FOMs) was outlined and a preliminary turbomachinery design tool developed. This tool is specifically catered for preliminary design and was used throughout this work to help define the optimum compressor layout.

This paper discusses the compressor FOMs specifically catered for a short haul engine. Furthermore, the outcome of a comparative design assessment is discussed and a finalised compressor layout is suggested, which is believed to yield a significant performance improvement compared to other engines within this class.

COMPRESSOR DESIGN FIGURES OF MERIT

In order to help define and prioritize the performance attributes which were deemed important for this type of commercial operation a theoretical aircraft flight profile was conceived. This profile was chosen to be quite similar to that adapted for the CFM56-5 [6], which is also a short haul engine, albeit this has a higher thrust rating than that considered for this study.

The aircraft to which this engine is hypothesized to be matched is the Embraer E-190. This platform requires engines within the 20klbf thrust category and coincidentally, the aircraft manufacturer is considering re-winging this aircraft to be able to accept more modern and efficient engines than those currently available [70]. The authors also conducted a market analysis study which concluded that potentially there exists a market for in excess of 30,000 new engines, within this thrust category, up to 2030 [10]. All these arguments combined indicate that a commercially viable engine catered for this mission profile may be developed.

In addition to the efficiency potential, one of the more important aspects which determine the success of any commercial engine is the reliability the design inherently has. High reliability also generally implies a long life between overhaul. This aspect of engine performance is especially important for short haul aircraft since these tend to operate to less equipped regional airports which may not have an approved maintenance organization. Thus, if any malfunction were to occur which is considered a 'No-Go' by the flight manual, it will disrupt the entire schedule since the aircraft would have to be grounded for a significant amount of time. It is thus readily apparent that each and every aspect of the engine should be designed towards high reliability and ease of repair.

Reliability concerns are mostly within the mechanical domain of the engine development process. Also, this criterion is often ascertained with the means of reliability indices which may be specific to an individual manufacturer and are naturally also influenced by the geometrical layout of the components. To overcome these limitations the authors sought to ascertain the aptitude of compressor reliability from a purely aerodynamic point of view. This approach can be justified given that this study is concerned only with preliminary design wherein the mechanical properties of the different components are normally too early to analyze.

With regards to turbomachinery, the primary cause of failure, from an aerodynamic point of view, is caused by vibration. Vibration within compressors is normally induced by flutter. Flutter is blade excitation at the natural frequency which may eventually lead to failure. This may be induced by any source of flow instability. It is thought that the most common cause of aerodynamic instability within compressors is caused by stalled flow. This phenomenon creates wake vortices at the trailing edge of the blades or near the endwall boundaries which may excite any downstream object standing within their path.

The authors thus assumed that a general relationship, which may be used within preliminary design and that gauges the aptitude of the compressor towards aerodynamic stability can be similar to that used to measure the blade and endwall loadings. A good criterion for measuring endwall stall is the deHaller number. This, as explained by Cumpsty [25] is thought to be a simple, but effective, measure of endwall loading and thus flow separation. Furthermore, the Diffusion Factor (DF) can be used to represent the blade suction surface loading. Thus, combining these two, one can grasp the level of compressor aerodynamic instability at a preliminary stage during development.

It must however be emphasized that, this approach towards gauging the mechanical integrity of any design is very simplistic in nature. In industry each and every component's natural frequency is monitored and any conflicts with adjacent components properly assessed using Campbell Diagrams. This approach is obviously more robust, but is thought too complex and detailed for the present study.

Other important FOMs, in addition to those outlined above, are the compressor weight and length. The latter can be, rather easily determined, by adding all the respective axial chord lengths and allowing for suitable blade spacing. Walsh *et al.* [7] suggest that a good estimate for the minimum spacing is 20% of the upstream blade chord. This magnitude also considers blade excitation, or vibration tendencies. Hence, preserving the required amount of blade spacing will also help mitigate any aerodynamic instabilities which may arise within the compressor. A shorter compressor implies a shorter and stiffer engine coupled with a more simplified bearing and support structure. Engines of this size are normally supported by a bearing assembly at the front and rear of the HP shaft. This, as depicted in Figure 1, allows for a compact two frame system which supports the entire rotor assembly [6].

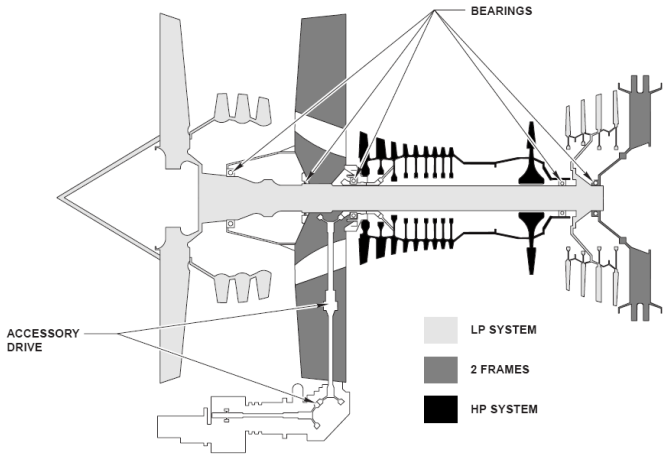

Figure 1: Engine rotor and frame assembly, sourced [13]

Furthermore, the importance of a short LPC is considered more critical than that corresponding to a HPC because the former is usually cantilevered from the front bearing support and is thus more prone to radial displacements and hence aerofoil rubs.

For the intent of weight prediction, the authors utilized a modified Sagerser correlation [67]. This correlation was originally developed in the 1970s to predict the components' weight of VTOL engines of the time. However, this report also suggests corrections that may be used to alter the results to better suit conventional gas turbines. Moreover, the authors of this current work further modified the results from this correlation to better approximate modern engines. The correction was derived from a Gerend *et al.* [68] report which suggests that the components' weight should have decreased by 30% in last four decades due to design improvements and more modern material fabrication techniques. The modified weight prediction correlation used within this study is as follows.

$$W_c = 17(\overline{D_m})^{2.2}(N)^{1.2}\left[1+\frac{L_c/\overline{D_{m,1}}}{0.2+0.081N}\right] \qquad (1)$$

In addition to the above requirements, it is also thought beneficial to keep the compressor pressure ratio (PR) as low as possible. This helps in preserving the operating range between choke and stall and also improves the off design performance. A large operating range is beneficial because this can better tolerate minor surge line degradations which tend to occur over time. The surge line tends to degrade over time due to dirt or blade damage incurred from foreign or possibly even internal objects. The most common cause of blade damage in aero engines is due to bird strikes. Furthermore, some magnitude in blade damage is usually tolerated to improve the engine's dispatch capability. This issue is very important for short haul engines, which tend to accumulate more takeoffs and landings, compared to longer-haul engines.

Furthermore, because of the shape of the efficiency contours on a typical compressor characteristic, a flatter constant speed line, such as the case with a large operating range, causes a smaller efficiency penalty during working line transients. This implies that, if the working line migrates from the original design intent, such as for example due to engine degradation [19] or operating altitude variations [17], the compressor efficiency should remain relatively unchanged.

A small component pressure rise also helps alleviate off design complexities. Engine monitoring and control is nowadays very complex and its development represents a considerable expense on the part of the manufacturer. If the off design performance is simplified, the development of the control system will also be greatly eased and surely less costly. The authors chose to limit the PR of an individual compressor to 9, even though modern compressors can handle considerably more than this magnitude. This limitation was imposed by the nature of the aircraft mission profile which necessitates a considerable amount of operating time at off design. Also, short haul engines do not require such a large PR since, as expected, this will require additional stages which increase the overall engine weight and length. The importance of the latter two criteria tends to be more pronounced compared to longer haul engines, were the efficiency potential is much more paramount. All these factors combined contribute towards a more reliable engine possessing respectable on-line performance retention.

One final FOM worth considering, even during preliminary design, is the cost of ownership the engine will have on the

customer. Powerplant related costs can be split up into initial purchase price, recurring maintenance costs and fuel expenditure. Maintenance costs can be reduced by designing an inherently reliable engine with good performance retention throughout its service life. Also, fuel costs depend not only on the efficiency of the gas turbine, but also on the total engine weight. A slightly more efficient but significantly heavier engine may result in increased fuel usage for a given flight profile. This fact is even more pronounced on short haul engines which tend to operate only a small portion of the entire flight at the design operating point. Thus, it is expected that the weight and length considerations need to be evaluated coherently with the efficiency potential of the engine, especially for short or medium haul engines.

Lastly, the initial purchase price is very complex to determine during preliminary design. This depends on a multitude of factors such as the geographic location of the manufacturer, any special arrangements between the latter and the customers, such as guaranteed maintenance agreements and also development related costs. The latter, however, can be reduced by minimizing the risk of encountering program complexities and cost overruns. The development cost can be further reduced by splitting this cost between different yet related products. The former issue has been tackled briefly before whilst discussing the control issues the off design performance may dictate. Moreover, minimizing the development risk which inherently exists within any development program depends to a large extent on the organization and experience of the manufacturer. Designing a component with realistic targets will surely help towards achieving this aim. The primary cause of compressor related program overruns is usually owed to an over-ambitious stage loading [36]. Finally, if the component can be designed in a way that it can be easily adapted to another application, the development costs can be shared between the two or more projects hence leading to a reduction of the initial purchase price.

Figure 2: Compressor FOMs

TURBOMACHINERY PRELIMINARY DESIGN TOOL

A new preliminary design tool was sought for this project due to the limited non-proprietary software which is readily available. A software, encompassing broadly similar qualities to those required for this work is T-AXI [60] which is developed by Turner *et al.*. Nevertheless, T-AXI is primarily intended for teaching practice, hence the results are rather theoretical in nature and not suited for preliminary design. Also, since T-AXI develops its own component geometry, it does not allow the user to specify any specific turbomachinery layout, which was a very important requirement for this present work.

The new software is named Turbodev and was programmed using Microsoft Excel. Turbodev is designed with several interlinked modules which, if properly utilized, may calculate detailed compressor geometrical and aerodynamic design properties coupled with some preliminary turbine analysis. It should be noted that the compression module is much more detailed and complex than the corresponding turbine counterpart. The latter's use within this work was restricted as a generic aid for the quick validation or otherwise of a given turbine design for the required compression geometry. The following paragraphs will provide a brief description of the algorithmic sequence incorporated within the compression module.

Turbodev allows the user to specify a multitude of different compression requirements such us required PR, number of stages, bleed requirements, stage loading distribution etc. Also, this system is thought to cater for all known designs since different types of booster and fan stages can be simulated together with any form of inter-compressor duct.

Once the required data has been inputted, the program assumes an initial efficiency of 88% and generates a preliminary annulus layout and a more refined mean stage loading, ψ_{mean}. This is calculated using the results from the previous computations. A second, more refined efficiency guess is predicted using a relationship of ψ_{mean} versus η as depicted below.

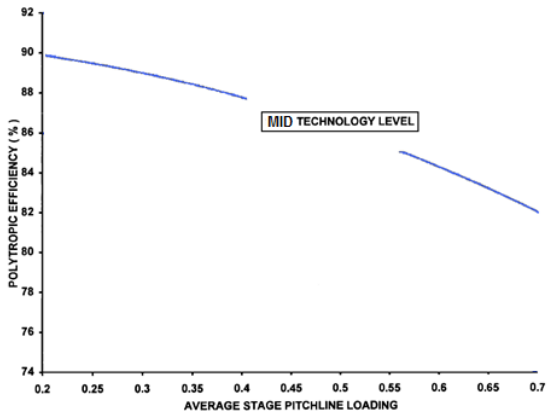

Figure 3: ψ_{mean} versus η, data obtained from [7]

A second, more refined, annulus geometry is then generated. Also, during this iteration, Turbodev attempts to predict the stage by stage aerodynamic and geometrical characteristics. The computed blade heights assume that both the rotor and stator chords are equal in all the stages and that the spacing between each blade row is equal to 20% of the upstream blade chord. This is thought to be a realistic estimate based on the arguments discussed above. Moreover, the blade vortex is assumed to conform to a constant reaction design. An appropriate DF is chosen to help define the blade shape. During this iteration, the blade incidence and deviation are calculated using modified Lieblien's empirical correlations as suggested by Aungier [36]. These correlations assume the use of modern controlled diffusion blades with reduced separation and higher suction surface loading tolerance. Furthermore, the hub reaction is constrained to a minimum of 0.3 [36] to avoid excessive flow diffusion in the stator row. The pitchline reaction is set to 0.5 unless otherwise constrained by the hub reaction.

Once the blade and flow aerodynamic geometry are calculated, the stage loss is predicted according to the principles outlined by Aungier [36].

$$\bar{w}_{subsonic} = \frac{2\sigma}{cos\beta_2}\left(\frac{W_2}{W_1}\right)^2 \left\{K_1\left[K_2 + 3.1(D_{eq}-1)^2 + 0.4(D_{eq}-1)^8\right]\right\}$$

$$K_1 = 0.0073,\ K_2 = 1 + \left(\frac{s}{h}\right)cos\beta_2 \qquad (2)$$

Aungier, assumes that $\bar{w}_{subsonic}$ does not change significantly when the inlet Mach number is lower than the critical value, M_{crit}. M_{crit} is the inlet Mach value at which the flow on the suction surface first attains a sonic value, W_{sonic}. This magnitude of M_{crit} depends appreciably on the blade geometry; however, from data provided in [25] and [19], it is further supposed that this is 0.8 for controlled diffusion blades having a 0.05 t_b/c. When the inlet Mach number, M_1, exceeds M_{crit}, $\bar{w}_{subsonic}$ is corrected for transonic induced losses. Finally, for simplicity, the authors assume that $\frac{W_{sonic}}{W_1} \propto \frac{M_{sonic}}{M_1}$.

$$\bar{w}_{transonic} = \bar{w}_{subsonic}\left[1 + \left\{\left(\frac{M_1}{0.8} - 1\right)\left(\frac{1}{M_1}\right)\right\}^2\right] \qquad (3)$$

Moreover, Saravanamuttoo *et al.* [19] outline a procedure whereby the stage isentropic efficiency may be deduced once the loss coefficients have been finalised. Also, because of the relatively low stage pressure ratio, it may be assumed that the stage isentropic and polytropic efficiencies are equal in magnitude.

$$\eta_p = \Lambda\eta_{Brotor} + (1-\Lambda)\eta_{Bstator}$$

$$\eta_B = 1 - \frac{\bar{w}}{\Delta P_{th}\Big/ 1/2\,\rho V_1^{\,2}}$$

$$\frac{\Delta P_{th}}{1/2\rho V_1^{\,2}} = 1 - \frac{cos^2\beta_1}{cos^2\beta_2} \qquad (4)$$

Turbodev then sequences through a final iteration, using the same logic used previously to obtain a third, more precise, efficiency and contour estimate.

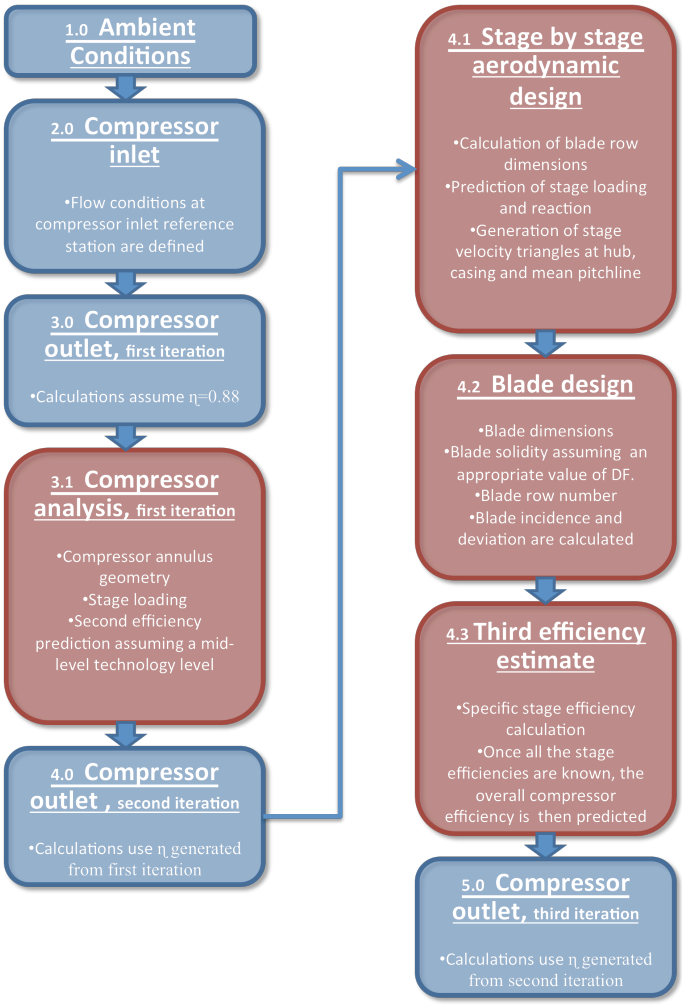

Figure 4: Turbodev compression module iteration sequence

TURBODEV EVALUATION

Due to the fact that Turbodev is a new turbomachinery analysis tool, it was deemed necessary to validate the results of this system against published data. The well documented NASA Energy Efficient Engine (EEE) ten-stage HPC was chosen to validate the efficiency prediction accuracy of the developed system [64], [61].

For the intent of validating Turbodev, it was thought best to mirror the EEE compressor geometry exactly as documented in the aforementioned literature. Thus, a more realistic efficiency prediction can be generated which is directly

related to the published data. This EEE compressor data was obtained from the NASA Detailed Report [64]. Also, since the compressor design intents of the EEE and the current engine are different, the turbomachinery geometry which would be generated by Turbodev will most certainly not conform to the actual compressor. Furthermore, considering the fact that the EEE compressor is derived from a detailed parametric design and includes an unusual annulus shape, which cannot be modeled by Turbodev, the current approach, to validating Turbodev was thought to be the most opportune.

Turbodev predicted an overall efficiency potential of 90.0% for the EEE configuration. The EEE Performance report [61], outlines a measured adiabatic efficiency, at the design point, of 82%. However, Cline *et al.* suggest that this magnitude should be corrected upwards by 2.6% to account for instrumentation induced losses and deterioration from previous high speed stalls. The resulting 84.6% adiabatic efficiency corresponds to a polytropic efficiency of 89.5%. This shows very satisfactory agreement with the predicted value. The error is only 0.6%.

To summarize, even though this testing is by no means an extensive evaluation of Turbodev's capabilities, it reinforces the fact that the aerodynamic computations implemented within this system are sound and the results should be satisfactory for the intents of preliminary design.

MERITS OF TUBODEV AS AN EDUCATIONAL TOOL

Even though Turbodev is a competent compression preliminary development tool, its use is primarily intended as an educational tool. This code can accept a wide variety of compressor geometries and is ideally suited as an aid for students who wish to endeavour within the design field.

It is structured in such a way to be easy to implement on a wide variety of platforms and can readily provide a realistic performance assessment of the chosen geometry. Through the use of this tool one can grasp a better understanding of the constraints that confront any component design process.

The use of this tool will be exemplified with a simulated compressor comparative design process intended for use on a short haul aircraft. A summary of this work is documented in the following sections of this paper. The interested reader may refer to [92] for a more thorough documentation of this design exercise.

COMPRESSOR BOUNDARY CONDITIONS

In order to perform this work an initial set of compressor boundary conditions was outlined. In general, since this engine is meant as a replacement for the GE CF34-10E5, the physical constraints of the new engine were matched to dimensions of this existing powerplant.

Also, a conservative PR and turbine inlet temperature (TIT) of 32.5 and 1650^{o}K were chosen. A low PR was deemed desirable because this diminishes the engine size and complexity, albeit at a small efficiency penalty. Moreover, a low TIT is beneficial, especially for a new short haul engine, since this diminishes the risk associated with the engine development program and also lowers the bleed requirements from the compressor. This further simplifies the engine manufacture and also allows for possible further growth of this baseline model.

Furthermore, the fan at the front of this engine was treated as a 'black box' with set parameters and performance level. The hub PR was fixed at 1.32. Thus, a cruise PR of 24.6 was required from this compressor.

The bleed requirements for this engine were modelled on the suggestions of Walsh *et al.* [7] for a 150 passenger capacity aircraft and for the TIT specified above. Finally, the minimum acceptable compressor efficiency which was required was 88%. This performance was necessary to achieve a cruise specific fuel consumption (sfc) of 1.82×10^{-5}(kg/s)/N.

For a detailed list of compressor boundary conditions, refer to [92].

FINAL COMPRESSOR DESIGN FOR A SHORT HAUL 20KLBF AERO ENGINE

The design analysis conducted for this study was a comparative assessment of several initial design layout proposals. Each and every one was initially assessed for efficiency potential and turbine suitability. The latter consisted of a preliminary assessment of whether the design imposed any negative constraints on the driving turbine. This study was thought beneficial because any potentially sound compressor layout may impose additional turbine stages or loading compared to the others. Thus, even though the compressor may appear to perform satisfactory as a stand-alone module, the turbine may end up being excessively heavy or inefficient.

This preliminary assessment produced three candidate designs which appeared to be respectable proposals for the required task. A summary of these designs is outlined below.

Configuration	**LPC/Booster *(no. of stages)***	**HPC *(no. of stage***	**LPC efficiency predictio**	**HPC efficiency predictio**

		s)	n	n
C2/101_10	5	10	0.89	0.90
C2/101_13	4	9	0.88	0.89
C2/10_16	3	9	0.88	0.88

This preliminary assessment was followed by a more detailed analysis, whereby the three chosen designs were examined in detail using the FOMs outlined in the previous section of this report. Turbodev was used extensively since it can generate accurate predictive weight, length and stage diffusion estimates from the user defined data. The weight and length computations follow the arguments discussed above and further pre-suppose a 0.3m inter-compressor duct. This duct is designed to yield uniform flow at the HPC face and may be used to extract bleed flow for aircraft or engine requirements.

This study resulted in configuration C2101_13 being chosen as the preferred design since it possesses a good balance between aerodynamic and mechanical performance and efficiency. The stages of this design are moderately loaded but the overall design promises to have a good operating range between choke and stall. The following table outlines a more detailed summary of this design. It is worth noting that the estimate number of variable stages follows the recommendation listed in [7]. This recommendation was found to be a simple, but rather accurate prediction of the complexity of the variable geometry required for this class of engine.

C2101_13 LPC, 4 stages				
Mean stage loading	**Compressor PR**	**No. of Variable stages**	**Weight *(kg)***	**Length *(m)***
0.33	3.8	0	221	0.42
C2101_13 HPC, 9 stages				
Mean stage loading	**Compressor PR**	**No. of Variable stages**	**Weight *(kg)***	**Length *(m)***
0.32	6.47	4	295	0.53

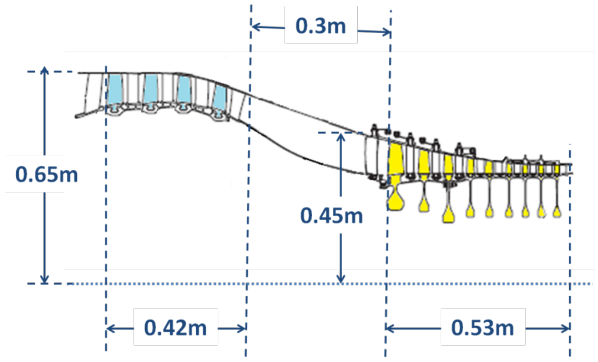

Figure 5: C2101_13 compressor layout and dimensions

Furthermore, Figure 6 depicts the stage loading distribution for this compressor. The recommended maximum loading, which is also depicted, is an indicative value for which a polytropic efficiency of 0.89 is realistically achievable. Exceeding this value may necessitate a more thorough and expensive detailed design to achieve the required efficiency.

In addition to the above arguments, this compressor is expected to yield quasi constant camber blades which may lower manufacturing costs if an industrial version of this compressor is eventually produced. Moreover, the LPC and the first four stages of the HPC can be manufactured from titanium based alloys due to the moderate stage temperature rises. This will further lower costs, thus making the module more profitable.

Finally, it transpires that, configuration number 13 offers significant potential of adapting the HPC of this design to suit an engine of higher PR, possibly for a longer range aircraft, requiring better thermal efficiency. This, if realizable, may significantly lower the initial purchase price for the customer since the development cost of this compressor will be shared by many more units. It was noted that if a zero stage is added in front of this compressor, the new design would be capable of delivering a 7.8 PR at a very satisfactory 90% efficiency. This compressor will then be suited for an engine requiring a PR of around 40 which is thought beneficial for a medium to long range aircraft such as the B767 or A330.

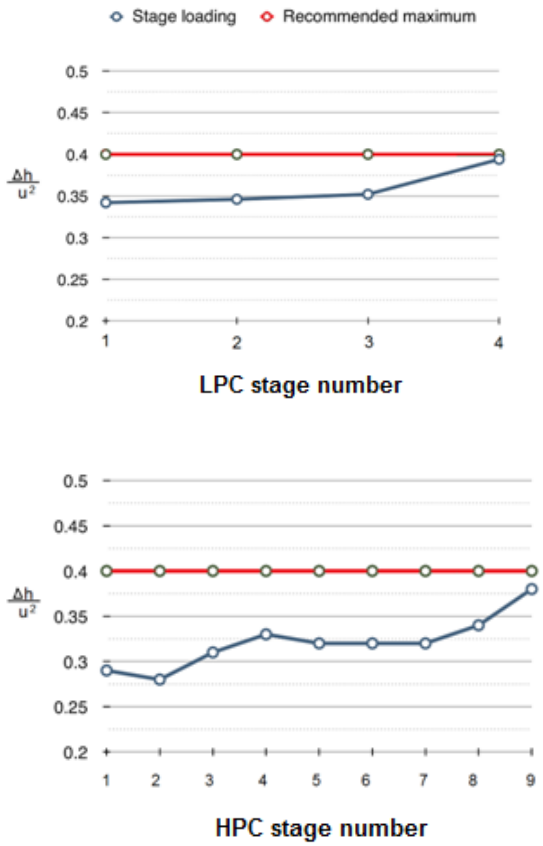

Figure 6: C2101_13 compressor stage loading distribution

CONCLUSIONS

This paper summarized a compressor comparative design assessment aimed for a short haul, regional jet. The FOMs pertaining to this type of compressor have been outlined and discussed. The subjects delved upon within the paper were:

- compressor efficiency
- turbomachinery reliability
- compressor weight and length
- off-design performance
- performance retention
- commercial viability.

Furthermore, a new preliminary design tool has been developed and verified to yield realistic information, suitable for use during preliminary design. However, the authors note that, even though the use and adaptability of this system can be easily expanded through future upgrades, the current development is appropriate mostly for academic purposes and as such should only be used in this capacity.

Finally, a new compressor design and layout was suggested, which is expected to yield a significant performance improvement compared to currently in-development engines within this thrust class.

[1] *The Jet Engine*, 5th ed: Rolls Royce plc., ISBN: 0 902121 2 35, 2005.
[2] B. Gunston, *The Development Of Jet And Turbine Aero Engines*, 4th ed: PSL, ISBN: 0 7509 4477 3, 2006.
[3] E. Roux, *Turbofan and Turbojet Engines Database Handbook*, 1st ed: Editions Elodie Roux, ISBN: 978-2-9529380-1-3, 2007.
[4] J. E. Green, "Greener by Design - the technological challenge," *The Aeronautical Journal*, vol. 106, pp. 57-113, 2002.
[5] N. Cumpsty, *Jet Propulsion*, 2nd ed: Cambridge University Press, ISBN: 978-0-521-54144-2, 2007.
[6] *Jet Engines And Propulsion Systems For Engineers*, GE Training and Educational Development Department and the University of Cincinnati 1989.
[7] P. P. Walsh and P. Fletcher, *Gas Turbine Performance*, 2nd ed: Blackwell Publishing, ISBN: 0-632-06434-X, 2004.
[8] B. Gunston, *World Encyclopaedia Of Aero Engines From The Pioneers To The Present Day*, 5th ed: Sutton Publishing, ISBN: 0-7509-4479-X, 2005.
[9] *Powering the Whispering Giant, the Trent 900 Engine*: Rolls Royce plc., ISBN: N/A, 2008.
[10] *Market Outlook 2007, Forecast 2007-2026*, Rolls Royce plc. 2007.
[11] L. H. Smith, "Axial Compressor Aerodesign Evolution at General Electric," *Journal of Turbomachinery*, vol. 124, pp. 321-330, 2002.
[12] M. P. Boyce, *Gas Turbine Engineering Handbook*, 3rd ed: Gulf Professional Publishing, ISBN: 0750678461, 2006.
[13] *CFM56-5A Training Manual*: CFM International, 2000.
[14] O. Domercq and J. F. Escuret, "Tip clearance effect on high-pressure compressor stage matching," *Proc. IMechE*, vol. 221, pp. 759-767, 2007.
[15] D. A. Jackson, *Performance Of Gas Turbine Components*, in *Gas Turbine Design & Performance course*. Cranfield University, 2011.
[16] *Oxford Aviation Training JAA, Airline Transport Pilot's Licence Theoretical Manual*, vol. 4, 2nd ed, ISBN: 0-88487-285-8, 2001.
[17] M. G. Philpot, "Practical Considerations In Designing The Engine Cycle," *AGARD Lecture Series LS-183, Paper 2*, 1992.
[18] J. Ostrower, "Brand New," *Flight International, 22nd March*, 2011.
[19] H. I. H. Saravanamuttoo, G. F. C. Rogers, and H. Cohen, *Gas Turbine Theory*, 5th ed: Pearson Prentice Hall, ISBN: 0-13-015847-X, 2001.
[20] D. J. Pickerell, "Rolls Royce RB211-535 Powerplant," *Journal Of Aircraft*, vol. 20, pp. 15-20, 1983.
[21] "Engine For Change," *Flight International*, pp. 39-41, 1993.
[22] L. M. Larosiliere, J. R. Wood, M. D. Hathway, A. J. Medd, and T. Q. Dang, *Aerodynamic Design Study of Advanced Multistage Axial Compressor*, NASA & US Army Research Laboratory ARL-TR-2859, 2002.
[23] A. H. Lefebvre, *Gas Turbine Combustion*, 2nd ed: Taylor & Francis Publishing, ISBN: 1-56032-673-5, 1999.
[24] J. Kurzke, "Fundamental Differences Between Conventional And Geared Turbofans," presented at Proceedings of ASME Turbo Expo, Power for Land, Sea and Air, GT2009, Orlando, Florida, 2009.
[25] N. A. Cumpsty, *Compressor Aerodynamics*: Krieger Publishing Company, ISBN: 1-57524-247-8, 2004.

[26] H. Tubbs, *Aerodynamic development of the high pressure compressor for the IAE V2500 aero engine*, C423/023, 1991.
[27] Eastop and McConkey, *Applied Thermodynamics for Engineering Technologists*, 5th ed: Pearson Prentice Hall, ISBN: 0-582-09193-4, 1993.
[28] M. T. Gresh, *Compressor Performance, Aerodynamics for the User*: Butterworth-Heinemann, ISBN: 978-0-7506-7342-6, 2001.
[29] E. M. Goodger and S. T. Ogaji, *Fuels & Combustion in Heat Engines*: Cranfield University Press, ISBN: 978-1-907413-00-1, 2011.
[30] Rogers and Mayhew, *Engineering Thermodynamics, Work & Heat Transfer*, 4th ed: Pearson Prentice Hall, ISBN: 0-582-04566-5, 1992.
[31] W. J. Calvert and R. B. Glinder, "Transonic Fan and Compressor Design," *Journal Of Mechanical Engineering Science*, vol. 213, pp. 419-436, 1999.
[32] NASA, *Aerodynamic Design Of Axial-Flow Compressors*, N65-23345, 1965.
[33] S. J. Gallimore, "Axial Flow Compressor Design," *IMechE*, vol. 213 Part C, pp. 417-449, 1999.
[34] B. J. Abu-Ghannam and R. Shaw, "Natural Transition of boundary layers-the effects of turbulence, pressure gradient and flow history," *Journal Of Mechanical Engineering Science*, vol. 22, 1980.
[35] J. D. Denton, "Loss Mechanisms in Turbomachines," *Journal of Turbomachinery*, vol. 115, pp. 621-656, 1993.
[36] R. H. Aungier, *Axial-Flow Compressors, A Strategy for Aerodynamic Design and Analysis*: Professional Engineering Publishing, ISBN: 0-7918-0192-6, 2003.
[37] C. C. Koch and L. H. Smith, "Loss sources and magnitudes in axial-flow compressors.," *Trans ASME Journal of Engineering for Power*, vol. 103, pp. 411-424, 1976.
[38] A. R. Howell, "Fluid dynamics of axial compressors," *Proc. IMechE*, vol. 153, pp. 441-482, 1945.
[39] J. L. Kerrebrock, "Flow in Transonic Compressors," *American Institute of Aeronautics and Astronautics*, vol. 19, pp. 4-19, 1981.
[40] I. J. Day and N. A. Cumpsty, "The measurement and interpretation of flow within rotating stall cells in axial compressors," *Journal of Mechanical Engineering Science*, vol. 20, pp. 107-114, 1978.
[41] C. Hah and J. Loellbach, "Development of Hub Corner Stall and Its Influence on the Performance of Axial Compressor Blade Rows," *Journal of Turbomachinery*, vol. 121, pp. 67-77, 1999.
[42] A. S. Gamage, *Compressor Rotating Stall Analysis*, in *School of Engineering*: University of Cranfield, 2007.
[43] D. C. Wisler, C. C. Koch, and L. H. Smith, *Preliminary Design Study of Advanced Multistage Axial Flow Core Compressors*, NASA CR-135133, 1977.
[44] J. C. Emery, L. J. Herrig, and J. R. Erwin, *Systematic Two-Dimensional Cascade Tests of NACA65-Series Compressor Blades at Low Speeds*, NACA RM L51G31, 1951.
[45] A. D. S. Carter, R. C. Turner, D. W. Sparkes, and R. A. Burrows, *The Design and Testing of an Axial-Flow Compressor having Different Blade Profiles in Each Stage*, Aeronautical Research Council R&M No. 3183, 1960.
[46] C. C. Koch, "Stalling pressure rise capability of axial flow compressor stages," *Trans ASME Journal of Engineering for Power*, vol. 103, pp. 645-656, 1981.

[47] R. N. Brown, *Compressors Selection And Sizing*: Gulf Professional Publishing, ISBN: 0-88415-164-6, 1997.
[48] A. D. S. Carter, *The Low Speed Performance of Related Aerofoils in Cascades*, Aeronautical Research Council Report No. R.55, 1950.
[49] J. P. Gostelow, "Design and performance evaluation of four transonic compressor rotors," *Trans ASME Journal of Engineering for Power*, vol. 93, pp. 33-41, 1971.
[50] A. R. Howell, *The Present Basis of Axial Flow Compressor Design*, Aeronautical Research Council R&M 2095, 1942.
[51] S. Lieblein, F. C. Schwenk, and R. L. Broderick, *Diffusion Factor for Estimating Losses and Limiting Blade Loadings in Axial-Flow-Compressor Blade Elements*, NACA RM E53D01, 1953.
[52] S. J. Andrews and H. Ogden, *A Detailed Experimental Comparison of Axial Compressor Blades Designed for Free Vortex Flow and Equivalent Untwisted and Twisted Constant Section Blades*, Aeronautical Research Council R&M No. 2928, 1956.
[53] W. L. Stewart, *Analysis of two-dimensional compressible flow characteristics downstream of turbomachine blade rows in terms of basic boundary layer characteristics*, NACA TN 3515, 1955.
[54] B. Lakshminarayana, "Methods of predicting the tip clearance effect in axial flow turbomachinery," *Trans ASME Journal of Basic Engineering*, vol. 92, pp. 467-482, 1970.
[55] S. C. Kacker and U. Okapuu, "A Mean Line Prediction Method for Axial Flow Turbine Efficiency," *Journal of Engineering for Power*, vol. 104, pp. 111-119, 1982.
[56] R. H. Aungier, *Turbine Aerodynamics, Axial-Flow and Radial-Inflow Turbine Design and Analysis*: ASME Press, ISBN: 0-7918-0241-8, 2006.
[57] D. G. Ainley, *Internal Air-Cooling for Turbine Blades. A General Design Survey*, Aeronautical Research Council R&M No. 3013, 1957.
[58] ISO, *Standard Atmosphere, ISO 2533*, International Organisation for Standardisation, Geneva 1975.
[59] *Airbus A320 CFM Flight Crew Operating Manual*, vol. 1, 2009.
[60] M. G. Turner, A. Merchant, and D. Bruna, "A Turbomachinery Design Tool for Teaching Design Concepts for Axial-Flow Fans, Compressors, and Turbines," *Journal of Turbomachinery*, vol. 133, pp. 1-12, 2011.
[61] S. J. Cline, W. Fesler, H. S. Liu, R. C. Lovell, and S. J. Shaffer, *Energy Efficient Engine High Pressure Compressor Component Performance Report*, NASA CR-168245, 1983.
[62] D. G. Cherry, C. H. Gay, and D. T. Lenahan, *Low Pressure Turbine Test Hardware Detailed Design Report*, NASA CR-167956, 1982.
[63] P. R. Hollowny, G. L. Knight, C. C. Koch, and S. J. Shaffer, *Energy Efficient Engine High Pressure Compressor Detail Design Report*, NASA CR-165558, 1982.
[64] P. R. Holloway, G. L. Knight, C. C. Koch, and S. J. Shaffer, *Energy Efficient Engine High Pressure Compressor Detail Design Report*, NASA CR-165558, 1982.
[65] M. J. Bridgeman, D. G. Cherry, and J. Pedersen, *NASA/GE Energy Efficient Engine Low Pressure Turbine Scaled Test Vehicle Performance Report*, NASA CR-168290, 1983.
[66] A. A. Mikolajczak, R. A. Arnoldi, L. E. Snyder, and Stargardter, "Advances in Fan and Compressor Blade Flutter Analysis and Prediction," *Journal of Aircraft 12*, 1975.

[67] D. A. Sagerser, S. Lieblein, and R. P. Krebs, *Empirical Expressions For Estimating Length And Weight Of Axial-Flow Components Of VTOL Powerplants*, NASA Lewis Research Center NASA TM X-2406, 1971.
[68] R. P. Gerend and J. P. Roundhill, *Correlation Of Gas Turbine Engine Weights And Dimensions*, The Boeing Company 70-669, 1970.
[69] A. Stone, "Effects of Stage Characteristics and Matching on Axial-Flow-Compressor Performance," *Transactions of the ASME*, vol. 80, pp. 1273-1293, 1958.
[70] A. Doyle, *Embraer Explores Common E-Jet Wing*, in *Flight International*, 12 June 2012.
[71] W. L. Macmillan, *Development of a Module Type Computer Program for the Calculation of Gas Turbine Off Design Performance*, in *Power and Propulsion*, vol. Ph.D.: Cranfield University, 1974.
[72] S. Trimble, *Civil Future Engines. Radical Shifts in Power*, in *Flight International*, 3rd July 2012.
[73] *CFM Leap Engine advertisement*. Flight International 30th October, 2012.
[74] SAE, *Gas Turbine Engine Performance Station Identification and Nomenclature*, Society of Automotive Engineers, Warrandale, Pennsylvania 1974.
[75] R. W. Westphal and R. W. Godwin, *Comparison of NACA 65-Series Compressor-Blade Pressure Distributions and Performance in a Rotor and in a Cascade*, NACA RM L51H20, 1951.
[76] R. A. Zimbrick and J. L. Colehour, "An Investigation of Very High Bypass Ratio Engines for Subsonic Transports," presented at Propulsion Specialist Conference, Boston, 1988.
[77] A. J. Wennerstrom, "Highly Loaded Axial Flow Compressors: History and Current Developments," *Journal of Turbomachinery*, vol. 112, pp. 567-578, 1990.
[78] A. J. Wennerstrom, "Low Aspect Ratio Axial Flow Compressors: Why and What It Means," *Journal of Turbomachinery*, vol. 111, pp. 357-365, 1989.
[79] A. R. Wadia, P. N. Szucs, and D. W. Crall, "Inner Workings of Aerodynamic Sweep," *Journal of Turbomachinery*, vol. 120, pp. 671-682, 1998.
[80] A. H. Thiam, R. W. Whittlesey, C. E. Wark, and D. R. Williams, *Corner Separation and the onset of stall in an axial compressor*, Illinois Institute of Technology 2008.
[81] J. D. Stevenson and H. I. H. Saravanamuttoo, "Simulating Indirect Thrust Measurement Methods for High-Bypass Turbofans," *Transactions of the ASME*, vol. 117, pp. 38-46, 1995.
[82] J. P. Smed, F. A. Pisz, J. A. Kain, N. Yamaguchi, and S. Umemura, "501F Compressor Development Program," *Journal of Turbomachinery*, vol. 114, pp. 271-276, 1992.
[83] H. I. H. Saravanamuttoo, "Component Performance Requirements," *AGARD Lecture Series LS-183, Paper 4*, 1992.
[84] S. M. H. Rizvi, *Design Of High Bypass Ratio Turbofan For A Civil Aircraft*, in *School Of Engineering*: Cranfield University, 2007.
[85] C. J. Rahnke, "The Variable-Geometry Power Turbine," *Transactions of the Society of Automotive Engineers*, vol. 78, pp. 213-223, 1969.
[86] V. Y. Nezym, "Development of New Casing Treatment Configuration," *JSME International Journal*, vol. 47, pp. 804-812, 2004.
[87] S. Miller, "Advanced Materials Mean Advanced Engines," *Materials World*, vol. 4, pp. 446-449, 1996.

[88] H. P. Kau, "Compressor Matching and Designing for Tip Clearance," presented at RTO AVT Lecture Series on Integrated Multidisciplinary Design of High Pressure Multistage Compression Systems, Lyon, France, 1998.
[89] I. H. Johnston and L. R. Knight, *Tests on a Single-stage Turbine Comparing the Performance of Twisted with Untwisted Rotor Blades*, Aeronautical Research Council R&M No. 2927, 1956.
[90] V. Iyengar, *A First Principles Based Methodology For Design Of Axial Compressor Configurations*, in *School of Aerospace Engineering*: Georgia Institute of Technology, 2007.
[91] A. M. T. Islam and S. A. Sjolander, *Deviation In Axial Turbines At Subsonic Conditions*, The American Society of Mechanical Engineers 99-GT-26, 1999.
[92] G. Piscopo, *Preliminary aerothermal design of axial compressors*, in *School of Engineering*, vol. MSc.: Cranfield University, 2013.
[93] J. H. Horlock, "The Determination of End-Wall Blockage in Axial Compressors: A Comparison Between Various Approaches," *Transactions of the ASME*, vol. 122, pp. 218-224, 2000.
[94] V. Gummer, U. Wenger, and H. P. Kau, "Using Sweep and Dihedral to Control Three-Dimensional Flow in Transonic Stators of Axial Compressors," *Journal of Turbomachinery*, vol. 123, pp. 40-48, 2001.
[95] C. C. Gates, *A Computational Study Of Axial Compressor Rotor Casing Treatments And Stator Land Seals*, in *Mechanical Engineering*: Virginia Commonwealth University, 2002.
[96] C. Fu, L. Shaobin, S. Jiexian, and W. Zhangqi, "Experimental Study of Bowed-twisted Stators in an Axial Transonic Fan Stage," *Chinese Journal of Aeronautics*, vol. 22, pp. 364-370, 2009.
[97] S. Friedrichs, *Endwall Film-Cooling in Axial Flow Turbines*, in *Engineering Department*: Cambridge University, 1997.
[98] D. Elliott, *The Potential Benefits of Advanced Casing Treatment for Noise Attenuation in Ultra-High Bypass Ratio Turbofan Engines*, Glenn Research Center, NASA 2007.
[99] J. F. Coplin, "The accelerating pace of advancing aero engine technology," *Aerospace*, vol. 11, pp. 17-23, 1984.
[100] M. Choi, J. H. Baek, S. H. Oh, and D. J. Ki, *Role of the Hub-Corner-Seperation on the Rotating Stall*, AIAA 2006-4462, 2006.
[101] CFM, "*Flight Ops Support* " *Audio-Visual Presentation*, 10th September 2005.
[102] D. G. Ainley and G. C. R. Mathieson, *A Method of Performance Estimation for Axial-Flow Turbines*, Aeronautical Research Council R&M No. 2974, 1957.
[103] D. G. Ainley and G. C. R. Mathieson, *An Examination of the Flow and Pressure Losses in Blade Rows of Axial-Flow Turbines*, Aeronautical Research Council R&M No. 2891, 1955.
[104] *Airbus A340 RR Flight Crew Operating Manual*, vol. 1, 2009.
[105] "Aero Engines The Propulsion Spectrum," *Flight International*, pp. 381-412, 1959.